Dipartimento di Biopatologia e Biotecnologie Mediche e Forensi

Ministero dell'Istruzione, dell' Università e della Ricerca

UNIVERSITÀ DEGLI STUDI DI PALERMO
L'Univercittà

Dottorato di ricerca in Immunofarmacologia XXI ciclo

Exosomes released by K562 chronic myeloid leukemia cells promote endothelial cell tubular differentiation through uptake and cell-to-cell transfer

Tesi di Dottorato del
Dott. Marco Mineo

Tutor
Ch.mo Prof. R. Alessandro

Coordinatore
Ch.mo Prof. Francesco Dieli

2007/2009

CONTENTS

ACKNOWLEDGEMENTS

I would like to acknowledge the people who supported me and helped me to make this thesis possible. First of all I would like to express my sincere gratitude to my supervisor Prof. Riccardo Alessandro. He provided me with a lot of helpful suggestions, with very important advice and with his patient encouragement. I appreciated all his efforts to make my Ph.D. experience productive and stimulating. I also wish to express my deepest gratitude to Dr. Elise C. Kohn who allowed me to carry out a part of my research in her laboratory at the National Cancer Institute/NIH of Bethesda (USA). Her joy and enthusiasm for the research, our exciting scientific discussion and her support made my experience at NIH unforgettable. I'm also thankful to her for her help in reviewing my thesis. I would like to thank Prof. Giacomo De Leo for his sage advice that helped me to never give up during the difficult periods. I wish to thank Dr. Anna Flugy, Dr. Simona Fontana and all the members of Prof. Alessandro's Lab who contributed to improve my knowledge and technical skills. This group has been a source of friendship as well as I found there good advice and cooperation. In addition I would like to acknowledge the debt I owe to Dr. Kohn's group to support me during my stay at NIH. The friendly environment and their help were very important for me. Thanks to Dr. Victoria Virador for her help in carry out the electron microscopy analysis and to Dr. Giovanna Casagrande for her help in the creation of the figure that is inside the paragraph concerning the discussion. I am grateful to my parents who supported and encouraged me during all the steps of my studies. Last, and most importantly, I wish to thank my wife, Angela, and my son, Gabriele, because without their support it would have been much harder to finish my Ph.D. I know I can always rely on their encouragement whatever I'll do in my future. Their unflagging love makes every day of my life better.

CHRONIC MYELOID LEUKEMIA

Chronic myeloid leukemia (CML) results from an increased and unregulated proliferation of myeloid cells in the bone marrow. CML typically evolves in three distinct clinical stages: chronic phase, accelerated phase and blast crisis (1). The chronic phase lasts several years and is characterized by accumulation of myeloid precursors and mature cells in the bone marrow, peripheral blood and extramedullary sites. The accelerated phase lasts on average four to six months and is characterized by an increase in the frequency of early progenitor cells rather than differentiated cells. The blast crisis can last only a few months and is characterized by the rapid expansion of myeloid differentiation-arrested blast cells and has a poor prognosis (2).

The cause of CML is a characteristic reciprocal translocation between chromosome 9 and 22, t(9;22)(q34;q11), which results in the Philadelphia chromosome (Ph) (3, 4). This translocation generates the bcr/abl fusion gene, translated into a constitutively active protein kinase BCR/ABL (5).

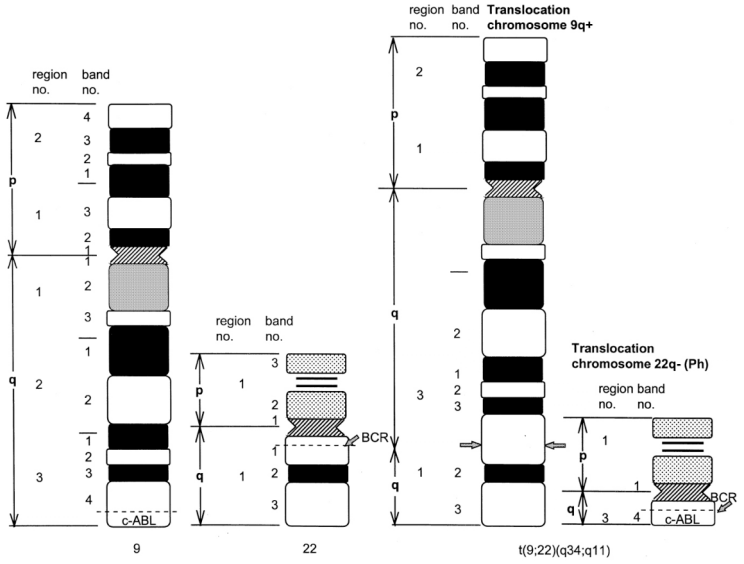

Figure 1. Schematic representation of the translocation that creates the Philadelphia chromosome (6). The abl and the bcr genes localize on the long arms of chromosome 9 and 22, respectively. The translocation (9;22)(q34;q11) creates a shorter chromosome 22 called Philadelphia-chromosome, in which the bcr/abl fusion gene is generated.

Although the presence of a Ph-chromosome always parallels the presence of a bcr/abl rearrangement, there is variability in the type of rearrangement between bcr and abl at the molecular level. As a consequence, bcr/abl hybrid genes can generate different types of fusion transcripts and proteins, which show a preferential but not exclusive association with different leukemia phenotypes (7, 8). All bcr/abl fusion genes contain a 5' portion derived from bcr sequences and a 3' portion that includes the entire abl gene sequence with the exclusion of the first 26 codons, corresponding to the alternative 5' exons, that normally generate two variant protein products denoted as type Ia and Ib (9). The constitutively activation of BCR/ABL is due to the fact that BCR acts by causing dimerization of the BCR/ABL proteins and in this way promotes a transphosphorylation process (10).

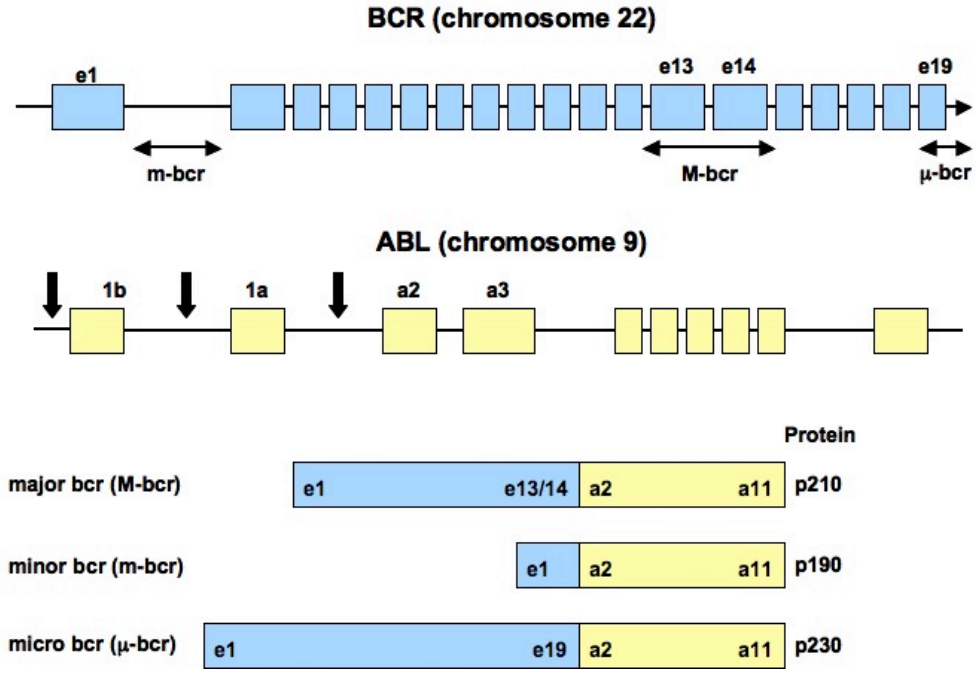

Figure 2. Schematic representation of the various breakpoints in the abl and bcl genes and the three different proteins encoded by the bcr/abl fusion gene *(From: www.cincinnatichildrens.org/svc/alpha/m/molecular-genetics/bcr-testing.htm).* The bcr and abl genes are shown at the top and the RNA transcripts and corresponding proteins below. The arrows show the possible sites of breakage in the bcr and abl genes.

There are three separate zones where breakpoints occur in bcr gene on chromosome 22, one of these is the central region called M-BCR (major breakpoint cluster region), which contains five exons corresponding to bcr exons 10 to 14 (11, 12). Breaks in the M-BCR nearly always occur in the intron between exon e13 and e14 or in the intron between exon e14 and e15. In the first case exon 13 is joined to abl exon 2 (e13a2 junction), whereas in the second, bcr exon 14 is spliced to abl exon 2 (e14a2 junction) (13). The two chimeric mRNAs differ by the presence of the bcr exon 14 sequences (75 bp), and the corresponding p210 proteins differ by 25 amino acids.

The second breakpoint location in the bcr gene occurs between exons e1 and e2 in an area designated the m-BCR (minor breakpoint cluster region) and form a bcr/abl transcribed in an e1a2 mRNA encoding a p190 BCR/ABL protein (14, 15). This is found in 70% of patients with Ph positive acute lymphoblastic leukemia (ALL). Both *in vivo* and *in vitro* studies suggest that p190 is characterized by a higher transforming activity than p210, and this may explain why p190 is preferentially associated with an acute leukemia phenotype (16).

A third breakpoint location is in the μ-BCR (micro breakpoint cluster region) and result in an e19a2 mRNA (17). This transcript contains the same portion of abl sequence as the other more common types of bcr/abl transcripts, but includes almost all the bcr coding sequences and result in a fusion protein of 230 kDa in molecular weight (p230). This type of bcr/abl rearrangement has been often associated with a very mild form of CML, denominated Ph-positive neutrophilic CML (18).

The function of the ABL and BCR proteins

Both bcr and abl are expressed in cells of various tissues. The abl gene encodes a 145-kDa protein belonging to the family of the non-receptor tyrosine kinases (TK). ABL protein may be found both at the cytoplasmic and nuclear level (19). In order to understand the possible function of ABL, it is important to consider the

different domains present in the ABL protein, which represent the basis for its interaction with other proteins.

The N-terminal ABL protein contains SH3 and SH2 domains (SRC homology region 3 and 2), that are the docking sites of proteins that contain, respectively, proline-rich sequences interacting with an SH3 region and phosphotyrosine residues interacting with an SH2 region of partner proteins (20). It is through these domains that ABL, like its oncogenic counterpart BCR/ABL, is capable of activating the transduction of mitogenic signals (21). The C-terminal end of the ABL protein contains a domain of interaction with F-actin (22), through which the ABL protein plays a role in the physiology of the cytoskeleton. The ABL protein is the only non-receptor tyrosine kinase to possess a DNA binding domain in the C-terminal region (23). It also contains specific sequences that allow the nuclear localization of the protein (NLS) and its nuclear extrusion (NES) (24).

ABL has been implicated as both a negative and a positive regulator of cell growth, depending on its phosphorylation state, level of expression, and cellular localization (cytoplasmic or nuclear). Several studies suggest a positive role of ABL in cell cycle regulation. In quiescent cells, nuclear ABL is kept in an inactive state by binding to the retinoblastoma protein (pRB) (25). Phosphorylation of pRB by cyclin D-Cdk4/6 disrupts this complex and result in activation of ABL in S-phase, during which ABL is able to stimulate the transcriptional activity of factors such as CREB and E2F-1 and to promote the activity of RNA polymerase II (26). ABL plays a key role at cytoplasmic level in the signalling pathways regulating growth factor-induced proliferation. It has been implicated in the TK signaling cascade involving the platelet-derived growth factor receptor (PDGFR) and downstream signaling through non-receptor TKs (SRC/ABL) important for mitogenesis and growth factor-induced Myc expression (27). Phospholipase C (PLC)-γ1 is required for the activation of ABL by PDGFR. PLC-γ1 and ABL form a complex that is enhanced by PDGF stimulation, but after activation, ABL phosphorylates PLC-γ1 and, in turn, negatively modulates its function (28, 29).

In contrast to the previously described positive role in stimulating proliferation, overexpression of wild-type ABL in fibroblasts has been shown to be able to

induce cell cycle arrest in the G1 phase (30). The growth inhibitory effect of ABL requires nuclear localization of ABL and its TK activity (31). ABL is able to induce apoptosis in response to genotoxic stress such as ionizing radiation, which is known to activate ABL. Cell lacking ABL can activate cell cycle check points and DNA repair, but show defects in apoptosis. This ABL function is dependent on the presence of wild-type p53, Rb, and p73 proteins (32).

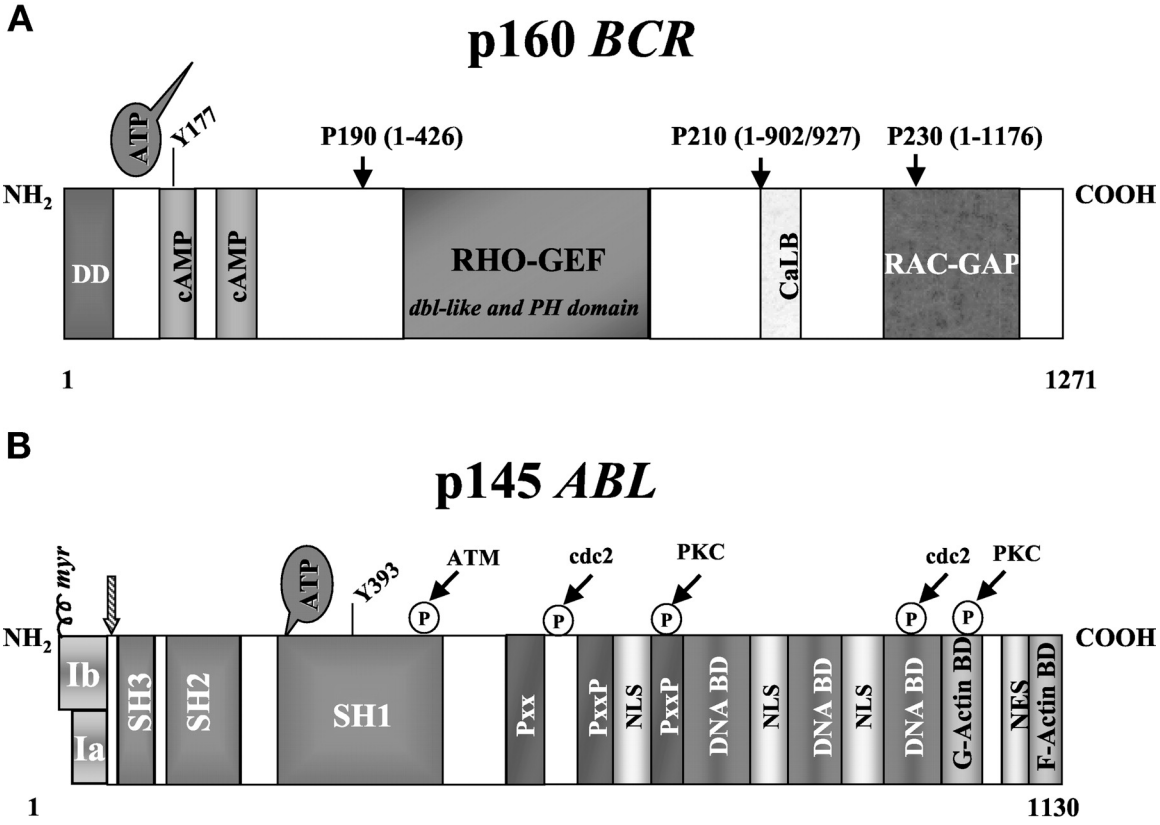

Figure 3. Schematic representation of the functional domains of BCR and ABL proteins. A) Functional domains of the BCR protein. At the NH2-terminal end the BCR protein presents the dimerization domain (DD) and tyrosine 177, an important autophosphorylation site. The center of the protein has a Rho guanidine exchange factor domain. CalB is a lipid-binding domain, and RAC-GAP mediates GTP/GDP exchange on Rac proteins. Arrows indicate the breakpoints in the various types of Bcr-Abl fusion proteins. B) Functional domains of ABL protein. In the ABL protein the 5' alternative exons and the Src homology domains (SH1-3) form most of the NH2-terminal region. The SH1 domain carries the tyrosine kinase function, whereas the SH2 domain interacts with phosphotyrosines on other proteins. The center of Abl consists of proline-rich regions (PxxP) that are important for interaction with SH3 domains of other proteins. At the COOH terminal region, nuclear localization signals (NLS), DNA-binding function (DNA-BD), a nuclear export signal (NES), and actin-binding motifs are found. Shown are also major phosphorylation sites for ATM, cdc2, and protein kinase C (PKC) as well as tyrosine 393, a major autophosphorylation site that regulates kinase activity (33).

The bcr gene product is a 160-kDa cytoplasmic protein with several functional domains (34). The N-terminal 426 amino acids of BCR, encoded by the first exon, are retained in all BCR/ABL fusion protein isoforms. This region contains a serine-threonine kinase domain, whose only known substrates are BCR and Bap-1, and two serine/threonine-rich regions that bind SH2 domains of other protein, including ABL, p190 BCR/ABL, and p210 BCR/ABL (35). The proximal SH2-binding domain appears to be important for the transformation of murine fibroblasts by BCR/ABL (36). The two key motifs of the first BCR exon are tyrosine 177 and the coiled-coil domain contained in amino acids 1 to 63, that appears to be important for the dimerization of BCR/ABL, which is crucial for the ABL kinase activity (10, 37). Whereas, phophorylated tyrosine 177 forms a binding site for growth factor receptor-binding protein (GRB-2) (37). In cells with a bcr/abl fusion gene, the BCR/ABL oncoprotein, unlike the normal ABL, has enhanced tyrosine kinase activity (38) and is predominantly localized in the cytoplasm (39). The tyrosine kinase activity is essential for cell transformation (16) and the cytoplasmic localization of BCR/ABL allows the assembly of phosphorylated substrates in multiprotein complexes that transmit mitogenic and antiapoptotic signals (40).

Effects of BCR/ABL on proliferation and survival of CML cells

BCR/ABL activates numerous signal transduction pathways responsible for growth factor independent proliferation and reduced susceptibility to apoptosis of these cells. The RAS pathway becomes constitutively activated by alternative mechanisms involving the interaction of BCR/ABL with the GRB-2/Gab2 complex, via the GRB-2-binding site in the BCR portion of BCR/ABL, and the recruitment/phosphorylation of the SHC adaptor protein (41, 42). The interaction of BCR/ABL with GRB-2/Gab2 and the phosphorylation of SHC lead to enhanced activity of the guanosine diphosphate/guanosine triphosphate (GDP/GTP) exchange factor SOS, which promotes accumulation of the GTP-bound form of RAS. The importance of RAS-dependent signaling for the phenotype of

BCR/ABL-expressing cells is supported by the observation that down-regulation of this pathway by antisense strategies, expression of dominant-negative molecules, or chemical inhibitors suppresses proliferation and sensitize cells to apoptotic stimuli (43-45).

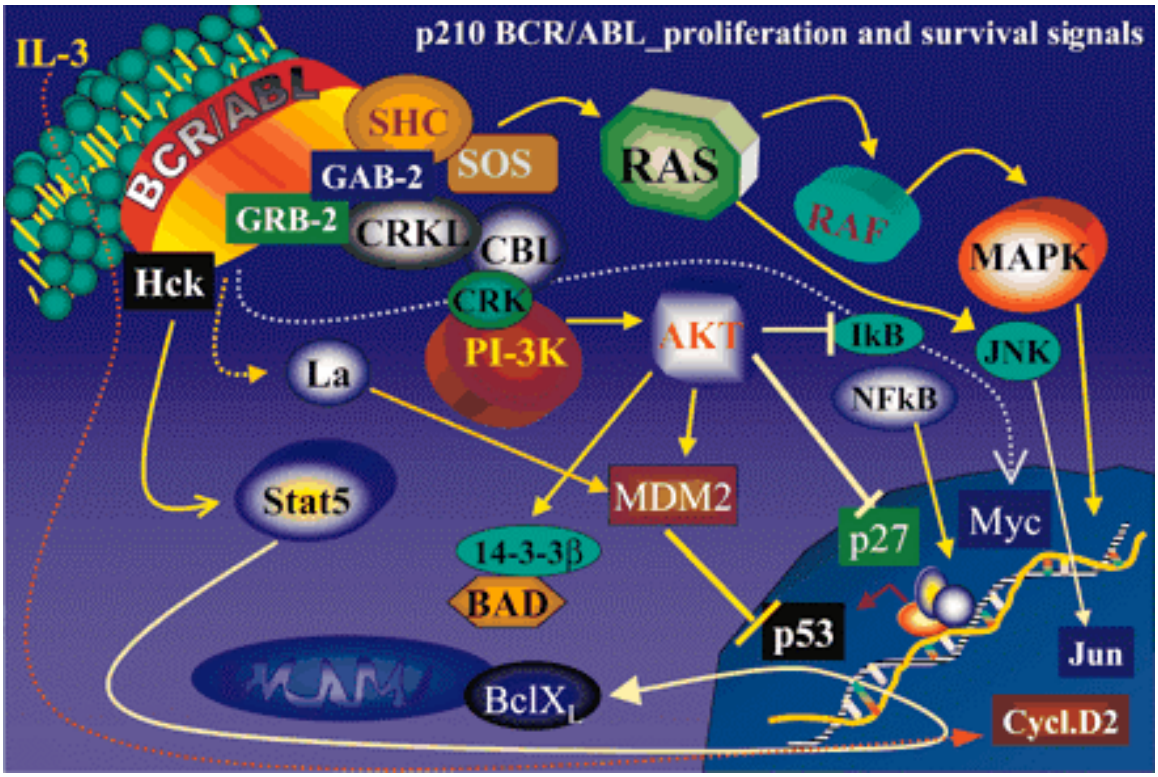

Figure 4. Signaling pathways activated by BCR/ABL fusion protein involved in proliferation and survival of CML cells (46).

The phosphatidylinositol-3 kinase (PI-3K) is another important pathway activated by BCR/ABL (47, 48). BCR/ABL interacts indirectly with the p85 regulatory subunit of PI-3K (49) via various docking proteins including GRB-2/Gab2 and c-cbl (50). Activation of the PI-3K pathway triggers an Akt-dependent cascade that has critical role in BCR/ABL transformation (51) by regulating the subcellular localization or activity of several targets such as BAD, MDM2, IκB-kinase-α, and members of Forkhead family of transcription factors (e.g. FKHRL1) (52). Phosphorylation of BAD suppresses its pro-apoptotic activity because, when

phosphorylated, BAD is sequestered in the cytoplasm in a complex with 14-3-3β (53). In BCR/ABL-expressing cells, BAD is cytoplasmic and heavily phosphorylated (54). Phosphorylation of MDM2 enhances its nuclear-to-cytoplasm export, potentially inducing a more efficient degradation of p53 (55, 56). Phosphorylation of IκB-kinase-α enhances its activity toward IκB, its substrate (57). Upon phosphorylation, IκB kinase is subjected to ubiquitination and proteasome-dependent degradation, allowing the translocation of p65 nuclear factor κB (NF-κB) into the nucleus where it functions as a transcription factor (58). Thus, the net effect of IκB-kinase-α phosphorylation is enhanced NF-κB activity, which has been associated with BCR/ABL-dependent transformation of primary mouse marrow cells (59). Phosphorylation of the FKHRL1 prevents its translocation into the nucleus and its transactivation of genes promoting apoptosis or inhibiting cell cycle progression (60, 61).

Another antiapoptotic pathway activated by BCR/ABL is that one dependent on signal transducer and activator of transcription 5 (STAT5) (62-65). STAT5 is activated by BCR/ABL via the Src family hematopoietic cell kinase (HcK) (66). On interaction with the SH3 and SH2 domains of BCR/ABL, this kinase is activated and phosphorylates tyrosine 699 of STAT5B, leading to its translocation to the nucleus where it functions as a transcription factor (66). The role of STAT5 in BCR/ABL leukemogenesis is likely to depend on transcriptional activation of its target genes. A STAT5 target potentially involved in BCR/ABL leukemogenesis is the anti-apoptotic protein Bcl-X_L (67), which could have a role in the reduced susceptibility to apoptosis in BCR/ABL-expressing cells.

Effect of BCR/ABL on CML cells adhesion to bone marrow stroma

Normal hematopoiesis in the bone marrow is regulated by cell-cell, cell-matrix, cell-growth factor interactions. A cascade of specific signals is required to initiate and control proliferation and differentiation of hematopoietic cells. Under normal conditions, a balance exists between self-renewal of pluripotent stem cells, maturation of cells to be released from the bone marrow, and cell death. CML

cells have a defective capacity to adhere to the bone marrow stroma. This may due to the fact that BCR/ABL may form multiprotein complexes with adhesion proteins such as paxillin and that is able to bind to F-actin, suggesting a direct action on cytoskeleton function (68, 69). Part of the adhesion defect of Ph-positive hematopoiesis is mediated through abnormalities of phosphatidyl-inositol (PI)-linked surface receptors, that are involved in the reduced adhesion capacity of CML progenitor to the bone marrow stromal compartment (70). In particular, lymphocyte-associated-antigen 3 (LFA 3) has been associated with abrogation of immune-mediated control of CML progenitor cells (71). The only know function of LFA 3 is to act as the binding ligand for the T cell surface protein CD2. CD2/LFA 3 adhesive interaction between a subset of human T cells and CD34+ hematopoietic progenitors plays a role in controlling the size of the actively cycling stem cell pool. Deficient expression of LFA 3 may allow Ph-positive cells escape this immune mediated growth regulation.

Target therapy in CML

Imatinib mesylate (Gleevec, Novartis) was the first active BCR/ABL tyrosine kinase inhibitor (TKI). It has been demonstrated to have significant activity in treatment of all phases of CML (16, 72). Protein kinases such as ABL have evolved highly specialized mechanisms for transitioning between active and inactive states. Imatinib binds to the activation loop of ABL kinase outside of a highly conserved ATP binding site and traps the kinase in an inactive conformation (73). In doing so, imatinib inhibits activity of the kinase and induces a complete cytogenetic response in more than 80% of patients with CML in chronic phase (74).

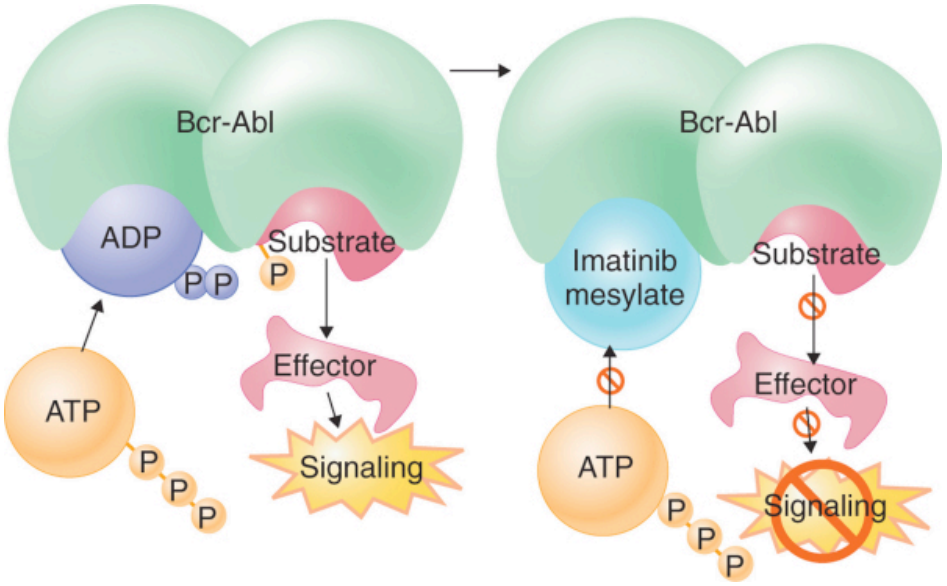

Figure 5. Mechanism of action of imatinib.
(From: www.mdconsult.com/das/book/body/225459465-3/0/1492/I4-u1.0-B978-1-4160-2805-5..50200-7--f4.fig). The constitutively active BCR/ABL tyrosine kinase functions by transferring phosphate from ATP to tyrosine residues on various substrates. By occupying the ATP binding pocket of the ABL kinase domain, imatinib prevents substrate phosphorylation and downstream activation of signals, thus inhibiting the leukemogenic effects of BCR/ABL on CML cells.

Even if imatinib is effective in the majority of patients with CML, some patients in the chronic phase and a substantial portion of patients in advanced phases are resistant or intolerant to imatinib (75-77). One cause of resistance is the development of point mutations within the kinase domain of BCR/ABL altering imatinib binding. The frequency of BCR/ABL mutations in imatinib-resistant patients ranges from 40-90% depending on the CML phase (78-82). More than 50 distinct point mutations encoding single amino acids substitutions in the kinase domain of the bcr/abl gene have been detected in patients with imatinib-resistant CML. At the protein level, these point mutations result in distorted configurations of the ABL kinase-imatinib interface. The result is that ABL is unable to adopt the inactive conformation to which imatinib binds (78, 83, 84). The impaired interaction between imatinib and ABL kinase as a consequence of mutations within the ABL kinase is best exemplified by the T315I mutation, which has frequently been detected in patients with imatinib-resistant CML (85). The threonine residue at position 315 is located near the ABL catalytic domain in the

center of the imatinib binding site, which controls access to a hydrophobic region of the enzymatic active site.

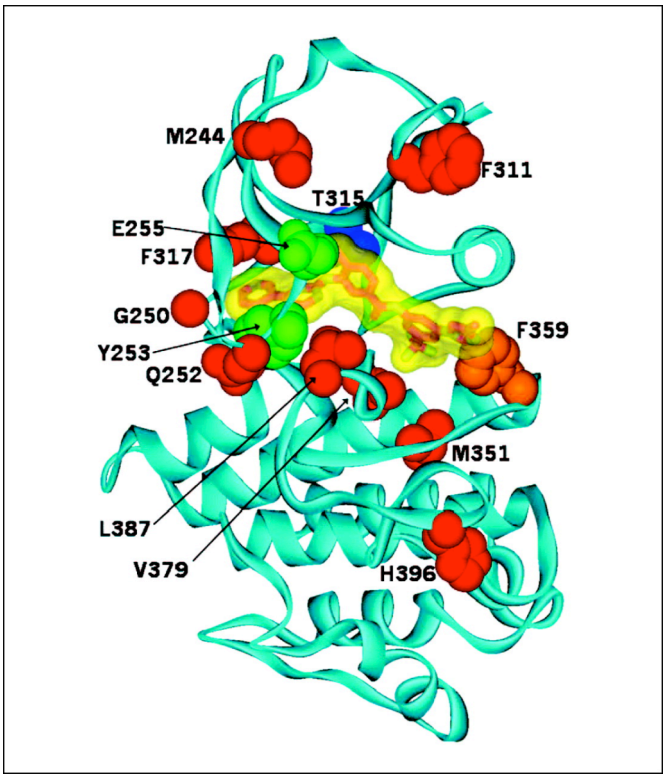

Figure 6. Locations of residues on Abl kinase corresponding to imatinib-resistant mutant forms of Bcr-Abl detected in patients (86).

Other mechanisms of imatinib resistance may include: increased expression of BCR/ABL through genomic amplification (87), overexpression of Lyn or other Src-family tyrosine kinases (88, 89), or overexpression of drug efflux proteins such as P-glycoprotein, that may decrease the intracellular concentration of imatinib in CML cells (90). The need for new strategies to treat imatinib-resistant CML has stimulated considerable efforts to develop novel BCR/ABL inhibitors.

Dasatinib (BMS-354825) is a multikinase inhibitor with potent activity against BCR/ABL (IC_{50} <1 nM) and SFKs (IC_{50} of 0.2-1.1 nM) (91). It has been approved by the U.S. Food and Drug Administration (FDA) for the treatment of patients with CML following failure of or intolerance to imatinib therapy. Dasatinib is able to bind ABL with a greater affinity than imatinib, due at least in part to its ability to

recognize multiple states of the enzyme (85, 91-93). It is active against imatinib-resistant mutant BCR/ABL oncoproteins tested to date, except for T315I (85, 86).

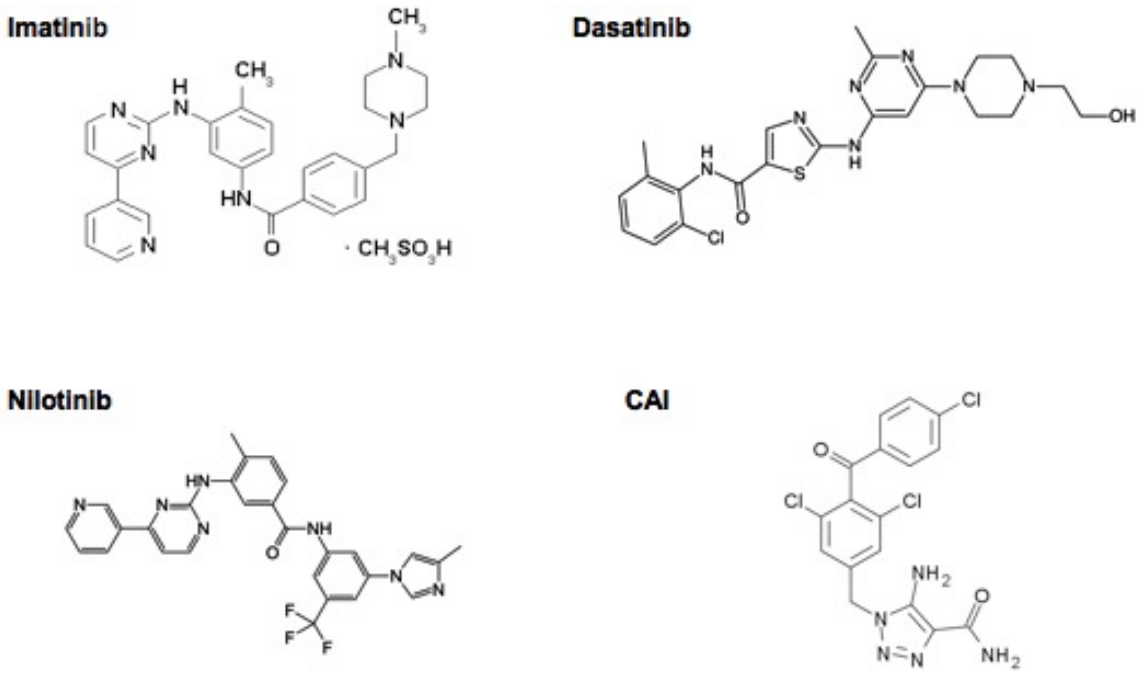

Figure 7. Imatinib chemical structure compared with other inhibitors able to block BCR/ABL function.

Nilotinib (AMN107) is a phenylaminopyrimidine derivate that was rationally designed to bind to BCR/ABL with a better topographic fit than imatinib, resulting in greater potency and less likelihood of resistance mutations (94). Nilotinib is approximately 20-30-fold more potent than imatinib against BCR/ABL expressing cell lines, but approximately 16-fold less potent than dasatinib (86, 94). *In vitro*, nilotinib inhibited 32 of 33 BCR/ABL mutants (not T315I), although nilotinib has a 20-25-fold lower potency against some BCR/ABL P-loop mutations, such as Y253H, E255K and E255V (86, 95). Other than T315I, nilotinib-resistant BCR/ABL mutations commonly affected residues within the P-loop (Y253H, E225K and A225V).

A potential limitation of these compounds, particularly of dasatinib, is that their increased potency may be associated with untoward off-target toxicities, which probably relate to their inhibitory activity against a broader range of protein kinases than imatinib. For instance, dasatinib, in addition to inhibiting SFKs, is also a potent inhibitor of the KIT, PDGFR and ephrin receptor (EPHA2) tyrosine kinases, which are directly implicated in hematopoiesis, control of tissue interstitial-fluid pressure and angiogenesis (96).

Carboxyamidotriazole (**CAI**) is an inhibitor of voltage-independent channel mediated calcium influx (97, 98) originally described by our group. CAI is able to induce growth inhibition and apoptosis in several tumors (98-100). CAI also has anti-angiogenetic activity *in vivo*, and is able to inhibit the proliferation of human umbilical vein endothelial cells (HUVECs) *in vitro* (101). It has been recently shown that CAI induces apoptosis in imatinib-resistant CML cells. CAI inhibits BCR/ABL-dependent and –independent signaling pathways and reduce phosphorilation of cellular proteins including STAT5 and CrkL (102).

EXOSOMES

Cell-to-cell communication is required to coordinate different cell types within tissues. Cells may communicate by the release of soluble factors (103), adhesion molecule-mediated cell-to-cell interaction, or by tunneling nanotubes that establish conduits between cells, allowing the transfer of surface molecules and cytoplasmic components (104). Recent studies have shown that cells may also communicate by the release of microvesicles (MVs). Two distinct classes of vesicles have been described: shedding vesicles and exosomes (105).

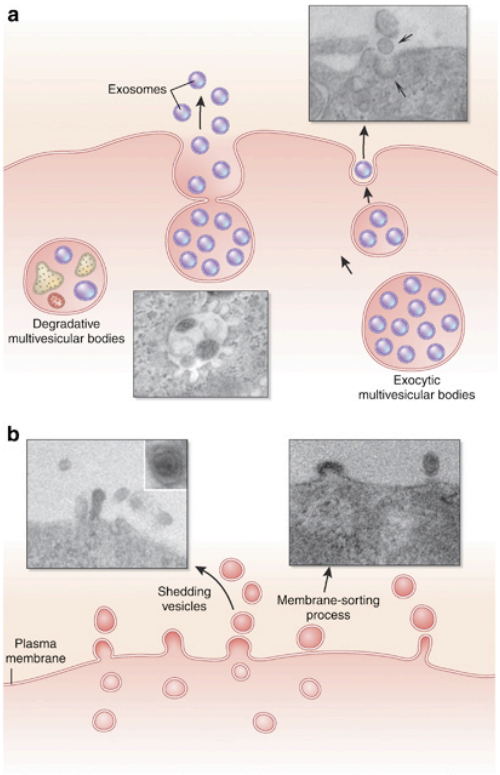

Figure 8. Schematic representation of exosome and shedding vesicles formation. (**a**) Release of exosomes. Exosomes accumulate within multivesicular bodies as a result of endosome compartmentalization. Exosomes are released by fusion of multivesicular bodies with the plasma membrane. (Upper inset) The representative transmission electron microscopy (TEM) shows exocytosis of exosomes from the surface of a mesenchymal stem cell. (Lower inset) A representative TEM shows a multivesicular body within a mesenchymal stem cell. (**b**) Production of shedding vesicles from the cell surface. Shedding vesicles are sorted out from cytoplasm by budding of cell plasma membrane in response to cell stimulation. (Left micrograph) The TEM panel shows vesicles shed from the surface of an endothelial progenitor cell. (Right micrograph) The TEM panel shows an aspect of cell membrane budding in an endothelial progenitor cell during microvesicle formation (106).

Shedding vesicles are MVs with a size ranging from 100 nm to 1 μm. Formation of shedding vesicles takes place from the budding of small cytoplasmic protrusions followed by detachment from the cell surface. This process is dependent on calcium influx, calpain, and cytoskeleton reorganization (107). Exosomes are the smallest vesicles: they have an endocytic origin and are release by most cells in culture (108). However, typical exosomes are sometimes generally referred to as MVs (109-111), or were initially described as plasma membrane vesicles (112) and then later characterized as exosomes (113).

Exosome composition

Exosomes are vesicles with a diameter ranging between 30 and 100 nm (105), and with a characteristic cup-shaped morphology. They sediment in sucrose gradients in ranges from 1.13 to 1.19 g/ml (108). The protein content of exosomes has been extensively analyzed from various cell types and body fluids by mass spectrometry, Western blotting, fluorescence-activated cell sorting and immuno-electron microscopy (114). Exosome protein composition varies depending on the cell type of origin and a unique tissue/cell type signature for exosomes was revealed (115). There is also a conserved set of proteins in exosomes as a class, independent of their cellular origin. Most of these proteins are used as markers to characterize the purified vesicles as exosomes (Table 1). Multivescicular body (MVB) biogenesis molecules such as Alix, Tsg101, and clathrin are highly associated with exosomes (114). Exosomes also contain heat shock proteins, such as the constitutive isoforms of HSC70 and HSP90. These ubiquitous proteins are involved in antigen presentation, as they can bind antigenic peptides and participate in loading peptides onto MHC molecules (116). Another class of cytosolic proteins commonly seen in exosomes includes the Rabs, the largest family of small GTPase, which regulate exosome docking and membrane fusion (117, 118). In addition to Rabs, exosomes are rich in annexins, which aid in membrane trafficking and fusion events (119). Finally, one of the

most abundant protein families that is found in exosomes comprises the tetraspanins (120).

Table 1. Characteristic protein markers of exosomes (121)

Protein	MW (KDa)	Cell types with exosomes containing the protein[a]	Enrichment in exosomes	Remarks
Alix	96	DC, M, U	Medium	MVB marker
Annexin II	38	DC, M, IEC, MC Mov, U	Low	
B7-2	80	DC, B, Mast	High	Not all cells express B7-2
Calnexin	96		Absent in exosomes	Endoplasmic Reticulum marker
CD9	25	DC, IEC, U, P	High	
CD63, CD81	50-60	Human: DC, B, IEC	High	
Clathrin	192	DC, IEC, B, HEK	Medium	
Flotillin-1	48	DC, Mov, U, Ret	Medium	Associated with Lipid rafts
Gi2-α	40	DC, Mov, U, B, Ret	Medium	
Grp 94(or gp96)	96		Absent in exosomes	Endoplasmic reticulum marker
Hsc 70	70	DC, M, MC, Mov, U B, Ret, Mast	Low	
ICAM-1	90	Mature DC, B	Variable, Depending on the cell type	
Lamp-1 or 2	90	DC, B	Low	Enrichment of lamp-1 or lamp-2 on exosomes depends on the cell type
MFG-E8	70+ 60	DC, IEC, Mov	Very high (not detectable in cell lysates)	Not all cells express MFG-E8
MHC I	47	DC, IEC, MC, U, B T, HEK	Medium	
MHC II	30 (α Chain)	DC, IEC, B, T, Mast	High	Not all cells express MHC II
Transferrin receptor	90	DC, Mov, Ret	Variable, depending on the cell type	
Tgs 101	44	DC, Mov, U	Medium	MVB marker

[a] Abbreviations for cell types: B, B cells; DC, dendritic cells; HEK, human embryonic kidney cells; IEC, intestinal epithelial cells; Mast, mast cells; M, melanoma cells; MC, mesothelioma cells; Mov, immortalized Schwann cells; MVB, multivesicular bodies; P, platelets; Ret, reticulocytes; T, T cells; U, urine

Several members of this family (including CD9, CD63, CD81 and CD82) are highly enriched in exosomes from virtually any cell type. Tetraspanins interact with many protein partners, including integrins and MHC molecules, which indicates that they are involved in the organization of large molecular complexes and membrane subdomains.

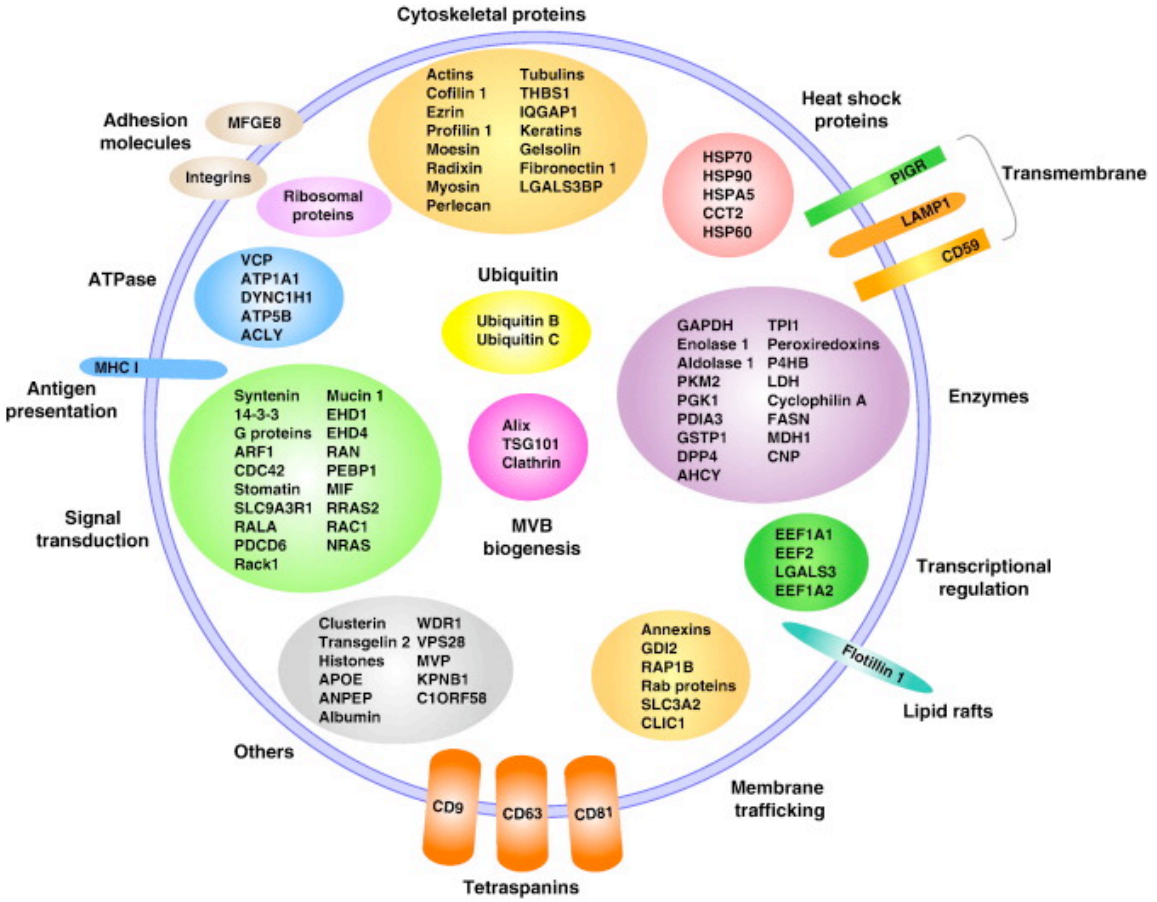

Figure 9. A graphical representation of the protein composition of exosomes(114).

Limited data are available describing the lipid composition of exosomes. The general composition of reticulocyte-derived exosomes is similar to that of the plasma membrane of the producing cell (122). The presence of lyso-bis-phosphatidic acid, a lipid that is enriched in late endocytic compartment, has been reported in B-cell-derived exosomes (123). Phosphatidylserine (PS), a lipid that is present normally at the cytosolic side of the plasma membrane, is also

present, but at low levels, at the surface of exosomes that are derived from platelets and dendritic cells (DCs) (105). Finally, internal vesicles of late endosomes and exosomes of EBV-transformed B cells are rich in cholesterol, as are the plasma-membrane microdomains known as 'lipid-rafts' (124).

Biogenesis and release of exosomes

Exosomes originate from the inward budding of the endosomal membrane leading to the formation of the MVBs. They are then released into the extracellular milieu by fusion of the MVBs with the plasma membrane. Accumulating evidence suggests that some components of the molecular machinery involved in sorting proteins toward the degradative pathway drive membrane invagination in early endosomes, thereby generating the MVBs. Central players in this processes are the endosomal sorting complexes required for transport (ESCRT) (125, 126).

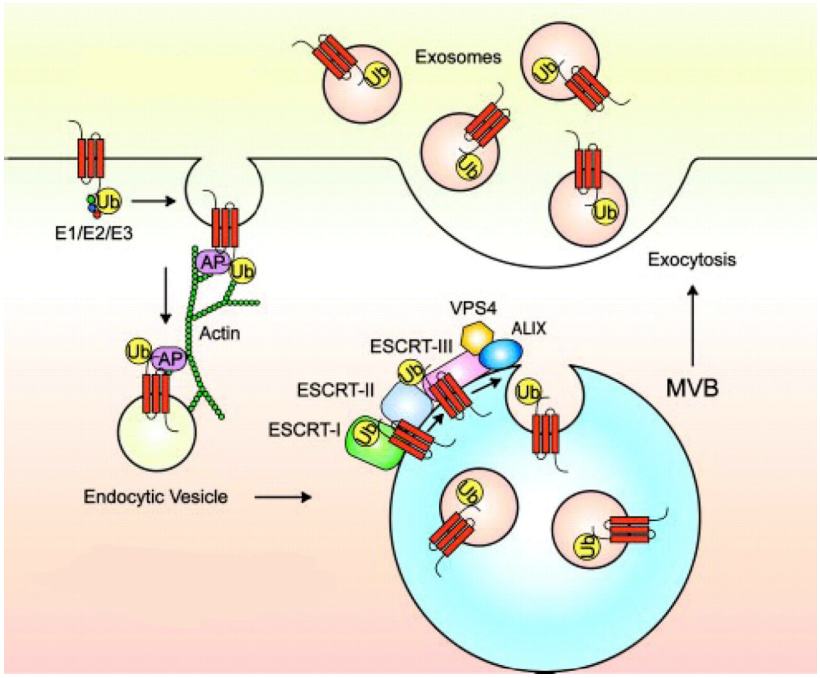

Figure 10. Process of exosome formation and release. Ub, ubiquitin; AP, adaptor protein; ESCRT, endosomal sorting complex required for transport; ALIX, ALG-2 interacting protein X (127).

ESCRT complexes deform the endosomal-limiting membrane by specific protein-protein and protein-lipid interactions, thereby orchestrating inward budding of vesicles. ESCRT-0, ESCRT-I and ESCRT-II have ubiquitin-interacting modules that are essential for cargo recognition and sorting. Ubiquitinated cargo first binds to HRS (hepatocyte growth factor-regulated kinase substrate, a component of ESCRT-0) on flat clathrin coats on the endosomal membrane (126). Next, ESCRT-I and ESCRT-II are recruited to the membrane, where they cluster the ubiquitinated trans-membrane proteins and package them into budding exosomes (128). ESCRT-III recruits de-ubiquitinating enzymes to remove ubiquitin from cargo proteins before their incorporation into the exosomes, and it also recruits Vps4, an ATPase that catalyze the disassembly of all ESCRTs from membrane. Another class E Vps protein, Alix (apoptosis-linked gene 2 (ALG-2)-interacting protein X), acts as a linker between different ESCRT complexes and might also play a part of intraluminal vesicle generation (129).

The coordinated recruitment and utilization of ESCRT machinery after ubiquitination is a well-established model of MVB biogenesis and cargo sorting. However, recent studies have provided evidence that some exosomal proteins are released in an ESCRT-independent manner (130, 131). One of these pathways requires the lipid, ceramide (130, 132, 133). Ceramide has many structural properties that may facilitate vesicle biogenesis. Ceramides are known to induce lateral phase separation and domain formation in model membranes (134). In addition, the cone-shaped structure of ceramide may induce spontaneous negative curvature in the membrane bilayer promoting membrane invagination. Proteins, such as tetraspanins, may partition into these domains. It is also possible that tetraspanins are part of the sorting system, as they are known to form oligomers by interacting with other tetraspanins and also with a variety of trans-membrane and cytosolic proteins (120). There is increasing evidence that the clustering of exosomal cargo is an important sorting determinant. For example, antibody-induced crosslinking of the transferrin receptor in reticulocytes (135), MHC-II in lymphocytes (136) or CD43 in Jurkat T cells (131), enhances their secretion in association with exosomes. Furthermore,

the addition of multiple homo-oligomerization domains to an acylated reporter protein increases its exosomal release (131). The oligomerization of exosomal components may lead to recruitment and stabilization of exosomal membrane domains. If these grow beyond a critical size, domain-induced budding may be triggered and vesicles formed after fission has occurred at the domain boundaries (137). There are some examples of proteins that may use such a pathway. The melanosomal protein (Pmel17) is sorted to the intraluminal vesicles of multivesicular endosomes by a luminal domain-dependent and ESCRT-independent pathway (138). Furthermore, the exosomal release of CD63, CD82 and the proteolipid protein (PLP) was not affected after inhibition of class E Vps proteins (130, 131). The function of the ESCRT machinery to recruit cargo and to deform membrane does not seem to be required in this pathway.

Exosomes are released both constitutively and in a regulated manner. The molecular machinery involved in the exocytic fusion of MVBs to release exosomes is still under investigation. One hypothesis is that the regulated release of exosomes uses similar mechanisms to those involved in the fusion of secretory lysosome with the plasma membrane (139). Calcium ionophores, which trigger lysosomal exocytosis (140), stimulate exosome release in many cell types, including epithelial cells and the CML cell line K562 (141-145). Additionally, a rise in calcium concentration enhances exosome secretion in Rab11 overexpressing cells (117). Rab11 inhibits membrane recycling from the recycling compartment and drives membrane proteins to MVBs. Moreover, Rab11 facilitate homotypic fusion of MVBs (117). Cellular stress has also been shown to stimulate exosome secretion. DNA damage, for instance, activates the tumor suppressor p53, which induces the release of exosomes, presumably as a mechanism of tumor surveillance or to affect gene expression in adjacent cells (146). Finally, other two Rab proteins, Rab27a and Rab27b, have been shown to be involved in docking and fusion of MVBs to the plasma membrane, allowing the final release of the exosomes in the extracellular space (118).

Interaction of MV with target cells

Upon release from their cell of origin, it seems that MVs do not interact with just any cell they come into contact with but, rather, only with cells that they recognize specifically. For example, the vesicles shed from platelets interact with macrophages and endothelial cells, but not with neutrophils (147). Those from neutrophils interact with platelets, macrophages and dendritic cells (148-150). Also important is the nature of the interaction with the target cell. In some cases, it is restricted to the surface and mediated, at least in part, by receptor binding (151). In this case, MVs may act as signaling complexes by direct stimulation of target cells. MVs derived from platelets, for instance, have an important role in coagulation as their phosphatidylserine-enriched membranes provide a surface for assembly of clotting factors (152, 153). The coagulation defects seen in Scott syndrome, a rare congenital bleeding disorder, depend on defective scrambling of membrane phospholipids with an impaired formation of MVs (153). After activation, platelets shed MVs coated with tissue factor that may interact with macrophages, neutrophils, and other platelets by ligation with molecules expressed on the surface of these cells such as P-selectin (154). On the other hand, MVs released from neutrophils express activated leukocyte integrin alpha M beta2 (Mac-1) that is able to induce platelet activation (155).

MVs may also act by transferring receptors between cells. The transferring of receptors is supported by the observation that bystander B cells rapidly acquire antigen receptors from activated B cells by a membrane transfer (156). This allows an amplified expansion of the antigen-binding B cells with the ability to present a specific antigen to CD4 T cell. A number of other receptors have been found to be transferred from one to another cell type. For instance, MVs can transfer the adhesion molecule CD41 from platelets to endothelial cells (157) or tumor cells (158), conferring pro-adhesive properties to them. MV-mediated transfer of Fas ligand from tumor cells induces apoptosis of activated T cells favoring tumor immune escape (159). Another recent report showed that tumor MVs can transfer an oncogenic form of EGF receptor (EGFR) to cells expressing

a wild-type receptor, which then leads to aberrant intracellular signaling by the oncogenic receptor and subsequent transformation of the recipient cells (160).

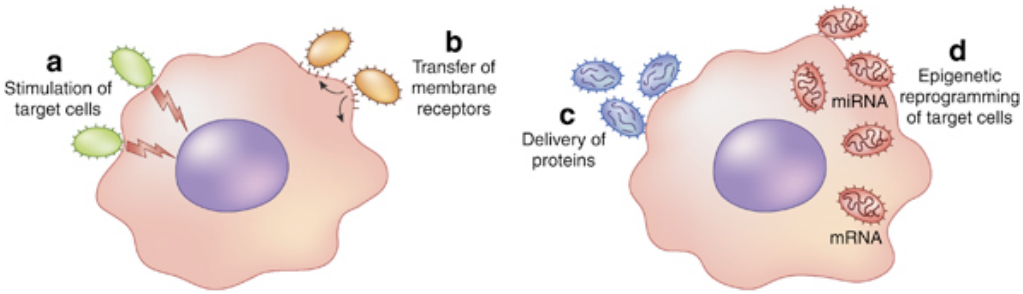

Figure 11. Schematic representation of mechanisms involved in microvesicle (MV)-mediated cell-to-cell communication. (a) MVs may act as a 'signaling complex' through surface-expressed ligands that directly stimulate the target cells. (b) MVs may transfer receptors between cells. (c) MVs may deliver functional proteins or infectious particles to target cells. (d) MVs may transfer genetic information via mRNA, microRNA (miRNA), or transcription factors from one cell to another (106).

MVs are also able to deliver proteins within the target cells. An example of this mechanism is the recent reported MV-mediated transfer of a cell death message via encapsulated caspase-1 (161). It has been found that endotoxin-stimulated monocytes induce the cell death of vascular smooth muscle cells by releasing MVs containing caspase-1. This trans-cellular apoptosis induction pathway depends on the function of the delivered caspase-1 within the target cells. It has also been suggested that MVs may contribute to dissemination of certain infective agents, such as human immunodeficiency virus and prions (162, 163).
Very interesting is the ability of MVs to deliver mRNAs, which can ultimately contribute to the molecular phenotype of target cells. It has been recently shown that mRNA incorporated in MVs from glioblastoma cell lines can be delivered to normal endothelial cells and generate functional proteins (164). The MVs can also contain microRNAs (miRNAs) that are known to control gene expression by regulating mRNA turnover (165). Many vesicles transferring mRNAs were shown to be released from progenitors of differentiated cells and also from tumor cells (152, 166, 167).

Role of exosome in antigen presentation

The finding that secreted MVs carry both antigenic material and peptide-MHC complexes generated interest on a possible role of MVs in triggering immune responses. MVs released by live cells are a possible source of exogenous antigens for antigen presenting cells (APC). Exosomes purified from cultured tumor cell lines (168) or from ascites of patients with tumors (169) contain tumor antigens and can induce the activation of antigen-specific T cells *in vitro* in the presence of recipient dendritic cells (DCs). In addition to whole or partially processed antigens, secreted vesicles also display preformed peptide-MHC complexes on their surface that can, in certain circumstances, be directly presented to T cells. Several groups have reported that DC-derived exosomes could induce the activation $CD8^+$ T cell clones, either alone (170-172) or when incubated with DCs that express allogenic MHC class I molecules (173, 174), which indicates that preformed peptide-MHC class I complexes from exosomes are functional. APC-derived exosomes also contain large amounts of MHC class II molecules (175, 176) because they originate from late endocytic compartments, in which MHC class II molecules reside. APC-derived exosomes can directly activate cognate T cell clones or lines (171, 175), or pre-activated $CD4^+$ T cells (136), but they need to be captured by recipient DCs to activate naïve $CD4^+$ T cells (136, 177, 178).

Role of exosomes in inflammation

Inflammation is sustained by the interaction of various cell types, either directly and/or through mediation by cytokines and other soluble factors (179). MVs released by various cell type are known to participate as well. Their role can vary depending on the stage of the process. At an early stage, the vesicles shed by neutrophils stimulate the release of anti-inflammatory factors such as TGFβ1 and interleukin-10 from macrophages with reduction of TNFα and interleukin-8 (151, 180). At later time points, however, MVs can become pro-inflammatory,

mediating the transfer of chemokine receptors, such as CCR4 and CCR5, and stimulating the release of other mediators, such as interleukin-6 and the monocyte chemotactic protein 1 (MCP1), which induce and strengthen inflammatory responses (181). MVs seem also play an important role in the pathogenesis of various inflammatory diseases, as indicated by their high levels in the foci of inflammation. For example, abundant vesicles shed from fibroblast seem to stimulate production of metalloproteinases and secretion of cytokines in arthritis (181).

Role of MV in tumor progression

The tumor microenvironment of many tumors is highly enriched in MVs released not only by the tumor cells but also by macrophages and neutrophils infiltrating the host parenchima. The increased number of circulating MVs in patients with gastric cancer is correlated with poor prognosis (182). MVs can carry active metalloproteinases that may contribute to stromal remodeling and favor tumor cell migration and metastasis (183-186). Matrix digestion favors angiogenesis, which is of key importance for tumor growth (187). Moreover, pro-angiogenic cytokines or mRNAs present inside MVs also stimulate angiogenesis (164). Another mechanism by which MVs can reinforce tumor cell growth is by triggering a Fas-dependent apoptosis of activated lymphocytes (188). In addition, tumor-derived MVs promote expansion and resistance to apoptosis of human regulatory T cells (T_{reg}) and upregulate their suppressor function (189). Interaction of tumor MVs with T_{reg} may affects peripheral tolerance by tumors and supports immune evasion of human cancers. Finally, accumulation of drugs, such as doxorubicin and other anti-cancer agents in the membrane of MVs decrease their cellular levels and can contribute to the process of drug resistance (190).

ANGIOGENESIS

Angiogenesis is the formation of new blood vessels from pre-existing vasculature. Pro-angiogenic molecules can initiate this process, and anti-angiogenic molecules can stop it. These molecules with opposite function are continuously acting in concert to maintain a quiescent vasculature (191). Various signals can trigger a switch that tips this balance in favor of angiogenesis. These include metabolic stress, mechanical stress, immune/inflammatory response, and genetic mutations (192, 193).

One of the stimuli that can initiate angiogenesis is the production of proteases in stimulated endothelial cells. These proteases degrade the subendothelial basement membrane (194). As a consequence, endothelial cells have an opening through which to migrate into local tissue, where they proliferate and differentiate to form a new vessel. The endothelial cells produce specific growth factors, such as platelet-derived growth factor (PDGF) and transforming growth factor-β (TGF-β), to attract supporting cells, called pericytes (195). A new highly specific basement membrane is subsequently produced, containing collagen IV, laminin, perlecan, nidogen, and fibronectin (196). At the end of this process, vessels surrounded by membrane and pericytes are mature. Several cytokines have been show to be involved in regulation of angiogenic processes. Among these, members of the vascular endothelial growth factor (VEGF) and fibroblast growth factor (FGF) family have a predominant role.

VEGF and VEGF receptor function during angiogenesis

The VEGF ligand family includes six related proteins: VEGF-A, placental growth factor (PlGF), VEGF-B, VEGF-C, VEGF-D, VEGF-E (197-201). VEGF-A, PlGF, VEGF-B and VEGF-E appear to exert their effects preferentially on vascular endothelial cells. VEGF-C and -D, on the other hand, act on lymphatic endothelial cells. Structurally, VEGFs are homodimers composed of polypeptide chains, which in their overall organization and spacing of cysteine residues are

related to PDGF. The original human VEGF (VEGF-A) exists in several isoforms, VEGF 121, 165, 189, and 206, which differ in heparin-binding ability (197, 202-204). The VEGF-A_{165} isoform appears to be the biologically active form in physiological as well as pathological angiogenesis. Hypoxia is an important factor in induction of VEGF-A expression (205, 206). In fact, several different elements for binding of hypoxia-inducible transcription factors (HIFs) have been identified in the VEGF promoter (207).

The VEGFs bind to three cell surface-expressed receptors, that are structurally related. VEGFR-1 and -2 are expressed preferentially on vascular endothelial cells (208). During embryogenesis, VEGFR-3 is expressed on vascular and lymphatic endothelial cells, but later, expression of this receptor is confined to lymphatic endothelium (209). The extracellular domains of these receptors contain seven immunoglobulin-like loops; they have a single transmembrane spanning domain, and their intracellular domain contain the tyrosine kinase activity. The binding of the ligand induces dimerization of the VEGFR receptors, which leads to the activation of the kinase (210).

A number of phosphorylation sites have been described in VEGFR-1 and -2, which appear to interact with signal transduction molecules that have been assigned more or less critical roles in the establishment of the VEGF-induced endothelial cell response (211-214). Proliferation of endothelial cells involves the Ras/MAPK pathway. However, at least in certain endothelial cells, downstream components in the Ras/MAPK pathway are activated even in the absence of active Ras (215). This may occur through activation of phospholipase Cγ (PLCγ) that leads to activation of protein kinase C family members, which in turn may phosphorylate and activate serine kinases downstream of Ras (216). The serine/threonine kinase p38 has been suggested to have an essential role in migration of endothelial cells towards VEGF (217). Other signal transduction molecules activated downstream of VEGFR are PI3K, that has been implicated in cell migration, proliferation and survival, and endothelial nitric oxide synthase (eNOS) that induces angiogenesis and increase vascular permeability (218).

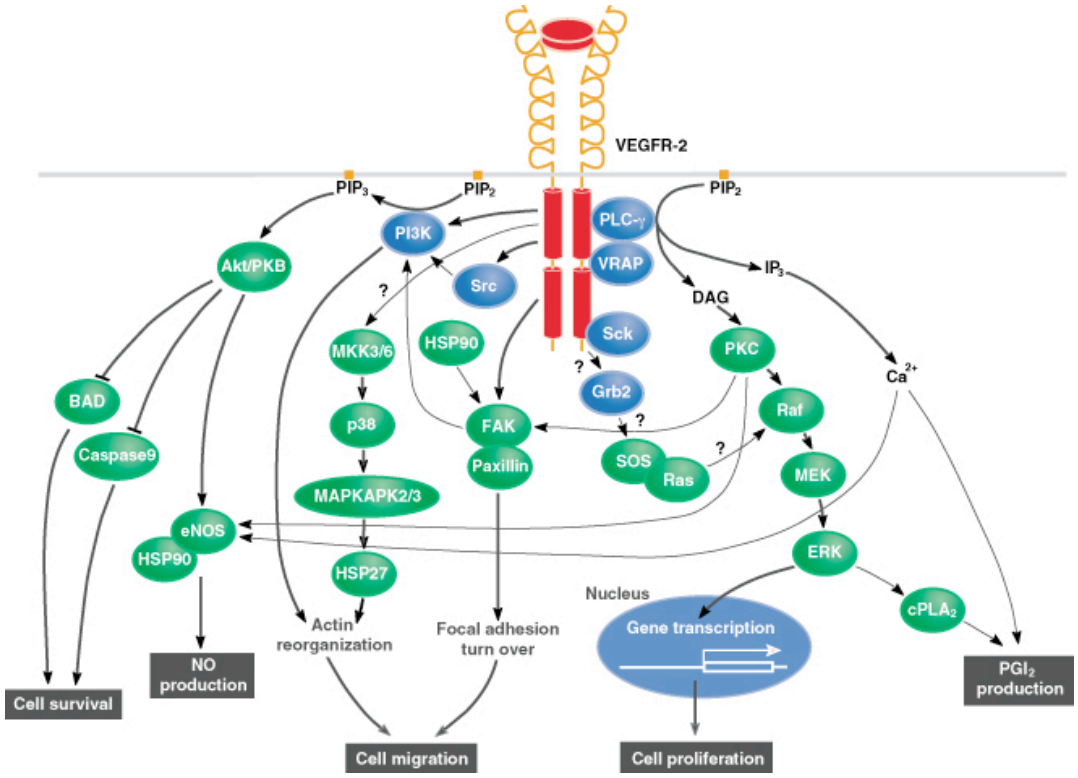

Figure 12. Schematic illustration of VEGFR-2 signaling. After receptor dimerization, several SH2 domain-containing signal transduction molecules (blue) are activated either directly by receptor binding, such us PLCγ, VRAP, and Sck, or by indirect mechanisms, such as Src and PI3K. A number of downstream signal transduction molecules (green) are thereby activated and mediate different pathways leading to cellular functions such as cell proliferation, migration, and survival. Activation of PKC plays a crucial role in VEGF-A mitogenic signaling via Raf-MEK-ERK pathway. Cell survival signal is mainly mediated through PI3K-mediated activation of Akt/PKB. Activation of PI3K, FAK, and p38 MAPK is also implicated in cell migration signaling. Bold arrows, positive stimulation; bold lines, inhibition; fine arrows, interactions not well established. MAPKAPK2/3, MAPK-activating protein kinase-2 and -3 (218).

FGF and FGF receptor function during angiogenesis

There are about twenty-four members of the FGF family (219). All members contain heparin/heparan sulfate-binding domains and for at least for some FGFs, heparin/heparan sulfate is critical for their biological effect (220). Of the different FGF family members, FGF-1 (acidic FGF) and FGF-2 (basic FGF) are preferentially implicated in angiogenesis (221). Four related FGF receptor tyrosine kinases have been described, which through alternative splicing appear in numerous variants (222). It appears that several FGFs bind more than one

FGF receptor type with high affinity. FGF receptor-1 (FGFR-1) has been shown to be expressed on endothelial cells *in vivo* and *in vitro* (223-225). For potent activation of receptors by FGF, the ligand has to be presented via heparan sulfate or heparin. This presentation may involve the creation of a ternary complex involving FGF, heparin/heparan sulfate, and the receptor (226, 227). Activation of FGFR-1 lead to autophosphorylation of at least seven tyrosine residues (228, 229), which allows more or less stable interaction with several different signal transduction molecules. FGF-induced cellular proliferation involves several different parallel pathways, initiated via the adaptor molecules Shc, FRS2, and Crk. These may converge on the Ras patway. PLCγ and the cytoplasmatic tyrosine kinase Src are also known to affect signal transduction in the Ras pathway (229). Moreover, Src has been implicated in FGF-induced cell migration and differentiation (229).

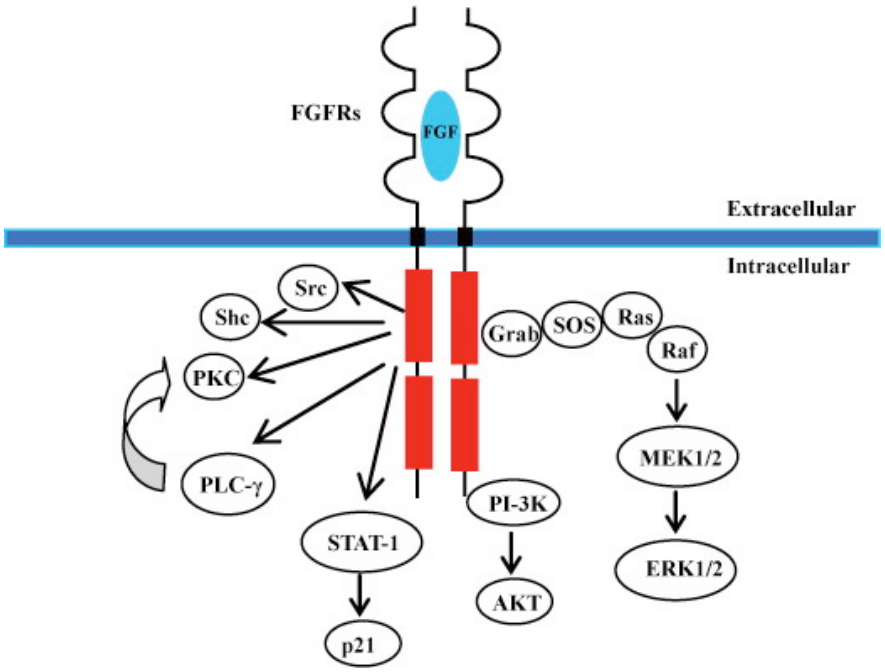

Figure 13. Structure of FGFRs and the major signaling pathways of FGF signal. FGFRs contain an extracellular ligand-binding domain, a transmembrane region and a highly conserved intracellular signaling domain. Activated FGFRs (red rectangles) stimulate multiple pathways such as PLC-γ, Ras-MAP kinase and PI-3 Kinase/AKT pathway. In some cells, FGF signaling also phosphorylates the Shc and Src protein. Additionally, activation of FGFR3 can stimulate STAT1-p21 pathway in chondrocytes (230).

Tumor angiogenesis

Angiogenesis is a key element in the pathophysiology of tumor growth and metastasis (231). Once a tumor grows beyond approximately 100-200 μm in diameter, passive diffusion is no longer able to support malignant cell survival and division, and neovascularization becomes essential (232). Hypoxia induces vessel growth by signaling through HIFs. These factors induce the production of pro-angiogenic compounds such as VEGF, FGF angiopoietin (Ang)-1, and various cytokines (233). This destroys the normal balance between pro-angiogenic and anti-angiogenic factors leading to the 'angiogenic switch'.

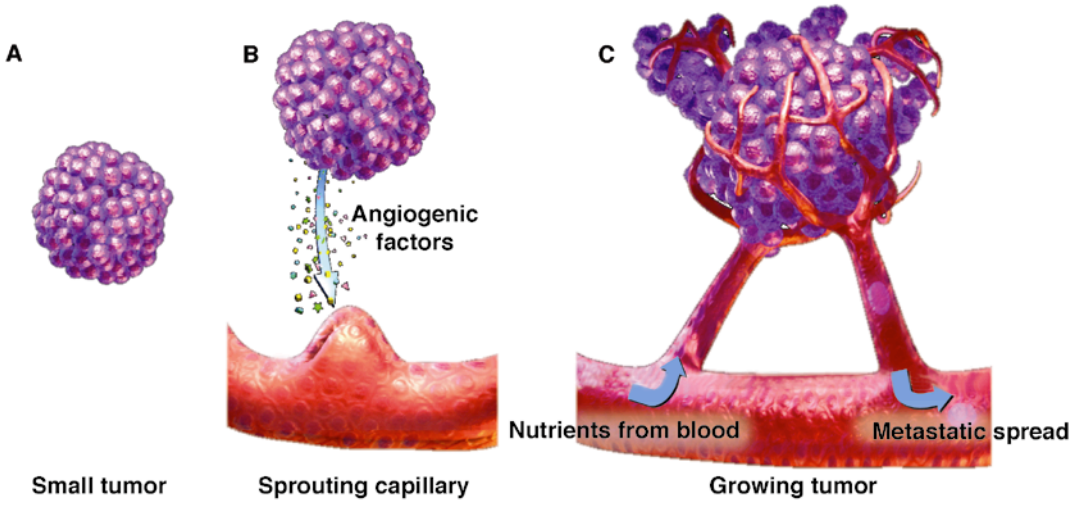

Figure 14. The development of new vessels in tumor angiogenesis. (*From : Siemann DW., Vascular targeting agents. Horizons in Cancer Therapeutics: From Bench to Bedside. 2002;3(2):4-15)*

Tumor vessels are structurally and functionally abnormal. In contrast to normal vessels, tumor vasculature is highly disorganized; vessels are tortuous and dilated, with uneven diameter, excessive branching and shunts. This may be due to an imbalance in angiogenic regulators, such as VEGF and angiopoietins. Consequently, tumor blood flow is chaotic and variable (234), and leads to hypoxic and acidic regions in tumors (235). These conditions lower therapeutic

effectiveness, modulate the production of angiogenic stimulators and inhibitors, and select for cancer cells that are more malignant and metastatic. In addition, hypoxia may select for clonal expansion of cells that have lost their apoptotic response to hypoxia (236).

Tumor vessels ultrastructure is also abnormal. Their vessel walls have numerous openings, widened interendothelial junctions, and a discontinuous or absent besement membrane. In addition, tumor-associated endothelial cells are abnormal in shape, growing on top of each other and projecting into the lumen. These defects make tumor vessels leaky (237-239). Cytokines and angiogenic molecules secreted by cancer and immune cells can modulate the expression of cellular adhesion molecules and other surface markers on the tumor endothelium. For example, VEGF and tumor necrosis factor-α (TNF-α) up-regulate, and bFGF and TGF-β1 down-regulate adhesion molecules (240). Chaotic blood supply coupled with non-uniform expression of adhesion molecules may explain why leukocyte-endothelium interaction is low in tumors and why activated lymphocytes adhere non-uniformly to tumor vessels.

In vitro models of angiogenesis: the use of Matrigel

Matrigel is a soluble and sterile extract of basement membrane proteins from the Engelbreth-Holm-Swarm (EHS) tumor that forms a 3D gel at 37°C and support cell morphogenesis, differentiation, and tumor growth (241). *In vivo*, endothelial cells are in contact on their basal surface with a thin basal membrane matrix. This matrix forms a continuous sleeve around the endothelial cells, and maintains the tube-like structures of the blood vessels (242, 243). The biological function of this basement membrane matrix was demonstrated when Kubota et al. plated endothelial cells on a reconstituted basement membrane matrix and found that they rapidly attached, aligned, and formed capillary-like tubules (244). The process is rapid, taking 2-3 hr for immortalized endothelial cells, and 6-20 hr for primary endothelial cells to complete the process. The vessels that are formed contain a lumen and tight cell-cell contacts. The cells are polarized with

the nuclei located towards the basement membrane matrix. Furthermore, the capillary-like structures take up acetylated low-density lipoprotein (LDL), which is a marker of differentiation for these cells. Such LDL uptake is not observed when these cells are cultured in monolayer on either plastic or collagen I substrates (244).

The normal basement membrane contains many proteins that vary in both amount and type, depending on the tissue of origin and function of the vessel. The major components of the vascular basement membrane are laminins 8 and 10, collagen IV, and nidogens/entactins 1 and 2. Many isoforms of these and other molecules are also found in different basement membrane matrices and further contribute to complexity. For example, there are six isoforms of collagen IV chains resulting in 56 possible combinations of trimers. Collagens VIII, XV, and XVIII, heparan sulfate proteoglycans, growth factors (FGF, TGF, PDGF, and VEGF), matrix metalloproteinase proenzymes (MMPs), BM40/SPARC/osteonectin, fibulins 1 and 2, thrombospondins 1 and 2, and fibronectin, are also reported in basement membrane matrices (245-247).

The complexity and dynamic nature of the endothelial basement membrane contributes to its various functions. Collagen IV is a scaffolding protein involved in the basement membrane's structural integrity and promotes cell adhesion and migration (242). Heparan sulfate proteoglycans link collagen and laminin networks, bind soluble components such as growth factors, and regulate the filtration activity of the basement membrane matrix (248). Laminins are considered the major biologically active components of the basement membrane, in part because they are the largest proteins in the basement membrane at over one million Daltons (249, 250). Laminins organize and establish the basement membrane matrix and promote endothelial cell adhesion, migration, and differentiation. Fibulins bind to many matrix molecules to promote basement membrane stability, adhesion and migration (251).

Vascular tube formation on basement membrane has been widely used as screen for angiogenic and anti-angiogenic factors (252, 253). As a first screen assay, it has many advantages. It is rapid, quantitative, and can be done in high

throughput mode to screen large numbers of chemicals. Reduced growth factor-basement membrane can be prepared. This material is advantageous for testing factors that promote angiogenesis because tube formation in absence of added angiogenic factors is greatly reduced over complete basement membrane matrix. Moreover, organization of endothelial cells on basement membrane encompasses all steps in the angiogenic process: adhesion, migration, protease activity, alignment, and tube formation. Since the assay reflects these multiple events, it has many advantages over other *in vitro* assays, such as independent cell attachment, proliferation, migration, and invasion. These other assays measure individual events in the angiogenic process. Endothelial cell migration or invasion assays are useful but more difficult to perform, and, for a first screen, it is possible that they would not measure the activity of a factor that may regulate only tube formation (254, 255). Other *in vitro* tube forming assays, such as tube formation on collagen I gels, are not in wide use because they require longer time periods, their cells do not all form tubes (making quantification difficult), and the tubes might not be properly polarized (256).

The formation of endothelial tubules on basement membrane allows investigators not only to study factors that regulate this process, but also to define genes and signaling pathways that cannot be studied easily *in vivo* (101, 257). In this way, it serves as a model for the molecular dissection of tube formation. Because it is functional for multiple uses, this will continue to be widely used to study the angiogenesis both in physiologic that pathological processes.

AIMS

Exosomes are small membrane vesicles of endocytic origin secreted by both normal and tumor cells (108). An increasing body of evidence indicates that they play a pivotal role in cell-to-cell communication. Indeed, they may directly stimulate target cells by receptor-mediated interaction or may transfer bioactive molecules including membrane receptors, proteins, mRNAs, and miRNAs (106). Recent studies have shown that exosomes may also be enriched in angiogenic proteins (164).

Angiogenesis has a major role in growth, dissemination and metastasis in solid tumors (258-260). More recently, angiogenesis has been described as important in the behavior of hematopoietic tumors, including CML progression. There is a significant increase in the number of vessels in the bone marrow of patients with CML (261). Moreover, the detection of angiogenic factor receptors in leukemia cell lines (262) suggests that angiogenic factors may have a direct effect on marrow vascularity as well as on leukemic cells.

Imatinib mesylate, a specific inhibitor of BCR/ABL protein tyrosin kinase activity, has been recently developed as the treatment of choice for CML (96). Treatment with imatinib decreases the VEGF plasma concentration in patients with CML (263). And, imatinib treatment *in vivo* of nude mice xenografted with K562 CML cells resulted in a significant reduction in tumor size and microvessel density compared with untreated tumors (264). In this context, we hypothesized that during CML progression there is a close interaction between exosome secretion, angiogenesis and tumor cell behaviour.

Hypothesis: Exosomes released by K562 CML cells drive pro-angiogenic endothelial cells behaviour.

Specific aims: (A) to evaluate the effect of exosomes released by K562 CML cells in stimulating human vascular endothelial cells (HUVECs) differentiation into tubular structures; (B) to dissect K562 CML exosome internalization, intracellular exosome movement, and cell-cell communication during HUVEC tube formation;

(C) to evaluate the role of small molecule BCR/ABL kinase inhibitors on exosome effects on HUVEC differentiation.

MATERIALS AND METHODS

Cell cultures and reagents

The human erythroid leukemia cell line K562 was provided by Dr R. Childs (Hematology Branch, NHLBI/NIH, Bethesda, MD) and was cultured in DMEM (Gemini Bio-Products, Sacramento, CA) supplemented with 10% FBS, 2mM L-glutamine, 100 IU/ml penicillin and 100 µg/ml streptomycin. Human umbilical vein endothelial cells (HUVEC) were purchased from Invitrogen (Carlsbad, CA) and were cultured in Medium 200 supplemented with 2% low serum growth supplement (LSGS), 100 IU/ml penicillin and 100 µg/ml streptomycin. Imatinib mesylate (IM) was provided by Dr. R. Bertieri (Novartis, Milan, Italy) and was prepared as a 10 mM stock solution in sterile phosphate buffered saline (PBS) and stored at -20°C until use. Dasatinib (Selleck Chemicals LLC, Houston, TX) was prepared as a 50 mg/ml stock solution in dimethyl sulfoxide (DMSO) and stored at 4°C until use.

Isolation of exosomes

Exosome-free medium (EFM) was obtained by ultracentrifugation at 100,000 x g of DMEM containing 20% FBS for 16 hr at 4°C, to remove bovine microvescicles. Ultracentrifuged medium was then diluted 1:1 with DMEM without FBS to obtain a final concentration of 10% FBS. K562 cells were cultured in EFM and the conditioned medium (CM) from 12 x 10^7 cells (160 ml) was collected after 24 h for exosome purification. Exosomes were isolated by differential centrifugation as previously described (175) with the following modifications (Fig 1M). Briefly, CM was centrifuged progressively at 300 x g for 10 min, 2000 x g for 10 min, then filtered through a 0.22 µm filter sterilization device (Steriflip; Millipore, Billerica, MA) to eliminate cell debris and larger vesicles. The CM was then centrifuged at 100,000 x g for 2 h using a Type 70 Ti rotor in a Optima L-90K ultracentrifuge (Beckman Coulter, Brea, CA). All the centrifugation steps were performed at 4°C.

The exosome pellet was washed in PBS to eliminate contaminating proteins, and ultracentrifuged again under the same conditions. The final pellet was resuspended in PBS and exosome protein content measured by BCA assay (Pierce, Rockford, IL).

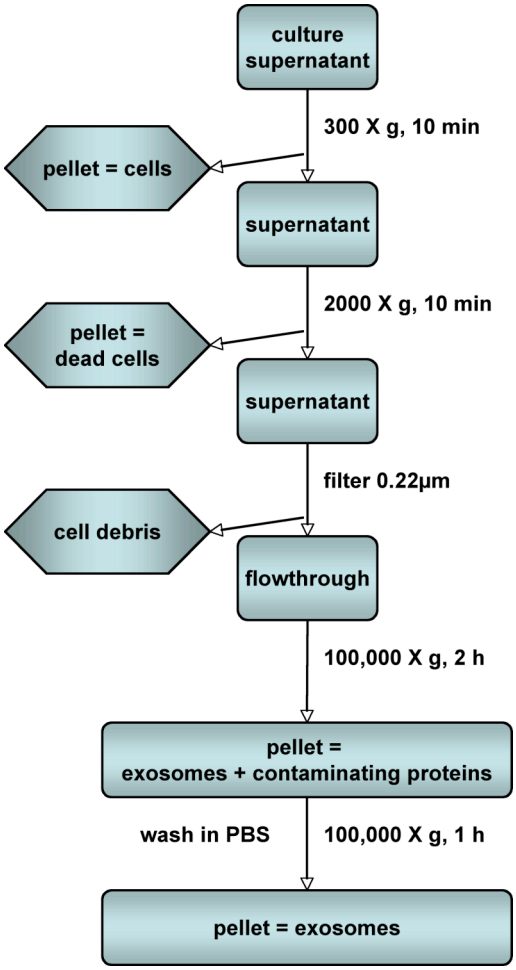

Figure 15: Flow chart for the exosome isolation procedure. The speed and length of each centrifugation are indicated to the right of the arrows. After the first two centrifugations, pellets are discarded and supernatant kept for the next step. After the two 100,000 X g centrifugations, pellets (consisting of exosomes) are kept and supernatant discarded.

Electron microscopy

An aliquot of exosome suspension was loaded into a carbon-coated electron microscopy (EM) grid. The sample was fixed with 2% glutaraldehyde and 2% paraformaldehyde in sodium cacodylate buffer for 2 min. After two washes in distilled H_2O, the sample was overlaid with 2% methylamine tungstate for 45 seconds and allowed to air dry. EM samples were observed in a Zeiss transmission electron microscopy (TEM) 912.

Acetylcholinesterase activity assay

A total of 40 μg of exosomes in 100 μl of PBS were resuspended in a solution of 1.25 mM acetylthiocholine and 0.1 mM 5,5'-dithiobis(2-nitrobenzoic acid) in a final volume of 1 ml. Incubation was carried out in cuvettes at 37°C, and the change in absorbance at 405 nm was followed at different time points (0, 5, 15, 30, 60 and 120 min).

XTT cell viability assay

K562 cells were seeded at 12,000/well in a final volume of 100 μl in 96-well flat-bottom microtiter plates with increasing concentrations of IM or dasatinib. Plates were incubated at 37°C in a 5% CO_2 incubator for the indicated time periods. At the end of incubation, 100 μl of XTT solution mix (sodium 3'-[1-(phenylaminocarbonyl)-3,4-tetrazolium]-bis (4-methoxy-6-nitro) benzene sulfonic acid hydrate) (Roche Applied Science, Indianapolis, IN) was added to each well, and plates were incubated at 37°C for 4 h. Absorbance was measured at 450 nm against a reference wavelength at 650 nm using a microplate ELISA reader. Calculation of XTT viability was done using the following formula:

$$\frac{(A450 - A650)_{\text{test cells}}}{(A450 - A650)_{\text{control cells}}} \times 100 = \text{percent viable}$$

Protein extraction

K562 cells were washed three times in PBS by centrifugation at 200 x g for 5 min at 4°C. The pellet was lysed in modified RIPA buffer (50 mM Tris pH 7.5, 150 mM NaCl, 4 mM EDTA, 10 mM Na pyrophosphate, 2 mM Na_2VO_4, 1% NP-40, 0.1% Na-deoxycholate, 10 µg/ml aprotinin, 10 µg/ml leupeptin, 1 mM PMSF) on ice for 1.5 h. The cell lysates were then centrifuged at 14,000 x g at 4°C for 15 min to remove DNA and particulate cell debris. The supernatant was recovered and stored at -80°C; before storage, protein concentration was determined using the BCA assay.

Protein quantification (BCA assay)

Protein quantification was performed using a colorimetric BCA protein assay kit (Pierce, Rockford, IL). In a 96-well flat-bottom microtiter plate, 10 µl of sample diluted 1:10 were added to 200 µl of working reagent. To prepare the working reagent, 50 parts of reagent A (containing sodium bicinchoninate, sodium carbonate, sodium bicarbonate and sodium tartrate in 0.1M sodium hydroxide) were mixed to 1 part of reagent B (containing 4% cupric sulfate in distilled water). Absorbance was measured at 562 nm and protein concentration calculated using a standard curve of bovine serum albumin (BSA). Standard curves were routinely linear with linear regression coefficients of 0.99X. Final concentration was calculated from the linear regression equation.

Western blot analysis

Cell lysates or exosomes were heated at 95°C in SDS sample buffer (0.125 M Tris-HCl pH 6.8, 4% SDS, 100 mM DTT, 0.004% bromophenol blue, 20% glycerol) for 5 min. Then 20 µg aliquots of proteins were loaded onto tris-glycine SDS-PAGE gels. Electrophoresis gels were subjected to 125V for approximately 90 min in running buffer (25 mM Tris, 0.2 M glycine, 0.1% SDS). Separated

proteins were then transferred to nitrocellulose membranes in transfer buffer (25 mM Tris, 0.2 M glycine, 20% methanol) at 170 mA for about 1 hr. The membranes were blocked for 1 h in PBS-0.1% Tween 20 containing 5% non fat dry milk, and then incubated over night at 4°C with primary antibody in PBS-0.1% Tween 20 containing 5% BSA. Specific antibodies used included: anti-CD63 (Abcam, Cambridge, MA), and anti-CD81 and anti-Tsg101 (Santa Cruz Biotechnology, Santa Cruz, CA). After three washes, membranes were incubated at room temperature with horseradish peroxidase-linked goat anti-mouse secondary antibody for 1 hr (Santa Cruz Biotechnology, Santa Cruz, CA). Bands were detected via enhanced chemiluminescence (Super Signal, Pierce, Rockford, IL) with Kodak film. Representative Western blot images are from triplicate experiments.

Endothelial tube formation assay

Subconfluent HUVECs were harvested and resuspended in limiting medium (Medium 200 with 0.2% LSGS) containing the indicated concentration of exosomes. This suspension was seeded (70,000 cells per well) on a growth factor reduced Matrigel- coated 24 well plate (BD Bioscience, San Jose, CA) and incubated for 6h at 37°C. As described in some experiments HUVECs were incubated with 10 μg/ml of exosomes and treated with increasing concentrations of imatinib (0.1, 1, 5 and 10 μM), or dasatinib (0.1, 1, 10 and 100 nM), or vehicle (DMSO) for 6h. Tube formation was examined under an inverted microscope and photographed using a 40X objective. Total tube length was measured using the NIS elements program (Nikon Instruments Inc., Melville, NY). Results are the mean of triplicate experiments

Labeling of exosomes

Exosomes from K562 cells were labeled using PKH26 (red) or PKH67 (green), membrane-binding fluourescence labels (Sigma-Aldrich, Allentown, PA).

Exosomes were resuspended in 500 μl of Diluent C from the kit, then mixed rapidly with 500 μl of freshly prepared PKH solution (final concentration during labeling step: 2 x 10^{-6} M) and incubated for exactly 3 min to ensure homogeneous staining. The labeling step was stopped by addition of an equal volume of FBS for 1 min, followed by an equal volume of complete DMEM medium. Stained exosomes were washed three times in PBS and ultracentrifuged. The collected exosomes were resuspended in 200 μl of PBS, and concentrated to 100 μl using an Amicon Ultra Concentrator with a 50kDa MW cut-off. The flow-through (100 μl) was used as control to determine the effects of free fluorescent dye present in the PBS used for suspension of the exosomes.

Internalization of PKH-labeled exosomes and immunofluorescence

HUVECs seeded on Matrigel-coated chamber slides were incubated at 37°C with labeled exosomes at a concentration of 1 μg exosomes per 10,000 cells. Uptake of exosomes was stopped by aspiration of medium and gentle washing three times with PBS, followed by fixation in 4% paraformaldehyde for 10 min at room temperature (RT). The cells were permeabilized for 5 min with 0.1% Triton-X 100 in PBS, blocked with 5% BSA in PBS and incubated with phalloidin AlexaFluor 488 (Invitrogen, Carlsbad, CA) for 20 min. Some slides were incubated with mouse monoclonal anti-α-tubulin (Sigma-Aldrich, Allentown, PA) overnight after which they were exposed for 1h at RT to secondary anti-mouse AlexaFluor 488 (Invitrogen, Carlsbad, CA) followed by incubation with phalloidin AlexaFluor 647 (Invitrogen, Carlsbad, CA) for 20 min. Chamber slides were mounted using DAPI Vectashield medium (Vector Labs, Burlingame, CA). Confocal images were sequentially acquired with Zeiss AIM software on a Zeiss LSM 510 Confocal system (Carl Zeiss Inc, Thornwood, NY) with a Zeiss Axiovert 100M inverted microscope and UV laser tuned to 364 nm, a 25 mW Argon visible laser tuned to 488 nm, and a 1 mW HeNe laser tuned to 543 nm. A 40X Plan-Neofluar 1.3 NA oil immersion objective was used. Emission signals after sequential excitation of

DAPI, AlexaFluor 488, and AlexaFluor 568 by the 364 nm, 488 nm, or 543 nm laser lines were collected with a BP 385-470 filter, BP 505-530 or LP 560 filter respectively, using individual photomultipliers. Z-stacks consisted of 16 to 54 slices at 0.5 or 1 μm intervals and these stacks were used with Bitplane's Imaris software (v6.0; Zurich, Switzerland) for surface rendering. In some cases, a cutting plane was used to expose internal surface or outer surface were made semi-transparent.

Exosome transfer assay

Two labeled populations of HUVECs were generated after incubation of the cells in standard culture monolayer for 3 h with PKH26- or PKH67-labeled exosomes. Following incubation, cells were harvested; the two labeled cell populations were mixed 1:1 and the cells seeded on Matrigel-coated chamber slides for a 4 h incubation. After the incubation, cells were fixed, mounted and examined by confocal microscopy as described above for the presence of double stained cells.

Src and FAK activation assessment

Subconfluent HUVECs were harvested and resuspended in basal medium containing a concentration of 10 μg/ml of exosomes. This suspension was seeded (70,000 cells per well) on a growth factor reduced Matrigel- coated slide chamber. The cells were allowed to adhere for 30 min in presence of dasatinib (10 nM), imatinib (1 μM), or vehicle (DMSO). After the incubation cells were washed in PBS and immunofluorescence was performed as described above. Cells were incubated with the anti-phospho-Src (Tyr416; Cell Signaling Technology, Beverly, MA), and anti-phospho-FAK (Tyr861; Millipore, Billerica, MA) over night, after which they were exposed for 1h at RT to secondary anti-mouse AlexaFluor 568 (Invitrogen, Carlsbad, CA).

Statistical analysis

Data are expressed as mean±SEM of at least triplicate experiments. Statistical analyses were performed using the unpaired two-tailed Student's *t*-test. Differences were considered statistically significant at $P < 0.05$.

RESULTS

Exosome isolation protocol optimization

Exosomes are small vesicles that originate from the inward budding of the endosomal membrane forming MVBs. They are then released in the extracellular milieu by fusion of MVBs with the plasma membrane (108). Exosomes have been successfully isolated from cell supernatant and body fluids. The original protocol used for exosome isolation involved several centrifugation and ultracentrifugation steps (175). Over the years, several modifications to this protocol have been made. However, optimization of the exosome isolation protocol was still required to obtain clean exosome preparations.

Most of the cells need the presence of serum to grow in vitro. Serum generally used for cell culture is unprocessed except for heat inactivation; thus, it would be expected to be contaminated by exosomes of the host from which the serum is drawn. These exosomes, if not depleted from serum, will contaminate the conditioned medium and therefore bias the experiment. To eliminate serum exosomes, serum or medium containing 20% serum was ultracentrifuged for different times, and the concentration of contaminating protein, representative of contaminating exosomes, was measured by BCA (Figure 16A). It was found that ultracentrifugation for 16 h yielded pellets containing more contaminating protein than ultracentrifugation for 1 h, the time recommended for exosome isolation (121). Moreover, it was observed that dilution of serum in medium increased the amount of contaminating material spun down compared to the undiluted serum. It was concluded that ultracentrifugation of medium containing 20% serum for 16 h is the optimal way to obtain an exosome-producing medium clear from contaminating exosomes.

Cell culture supernatant obtained after incubation of cells in exosome-producing (precleared) serum-containing medium can contain several types of vesicles. Therefore, it was important to ensure that the isolated vesicles were exosomes.

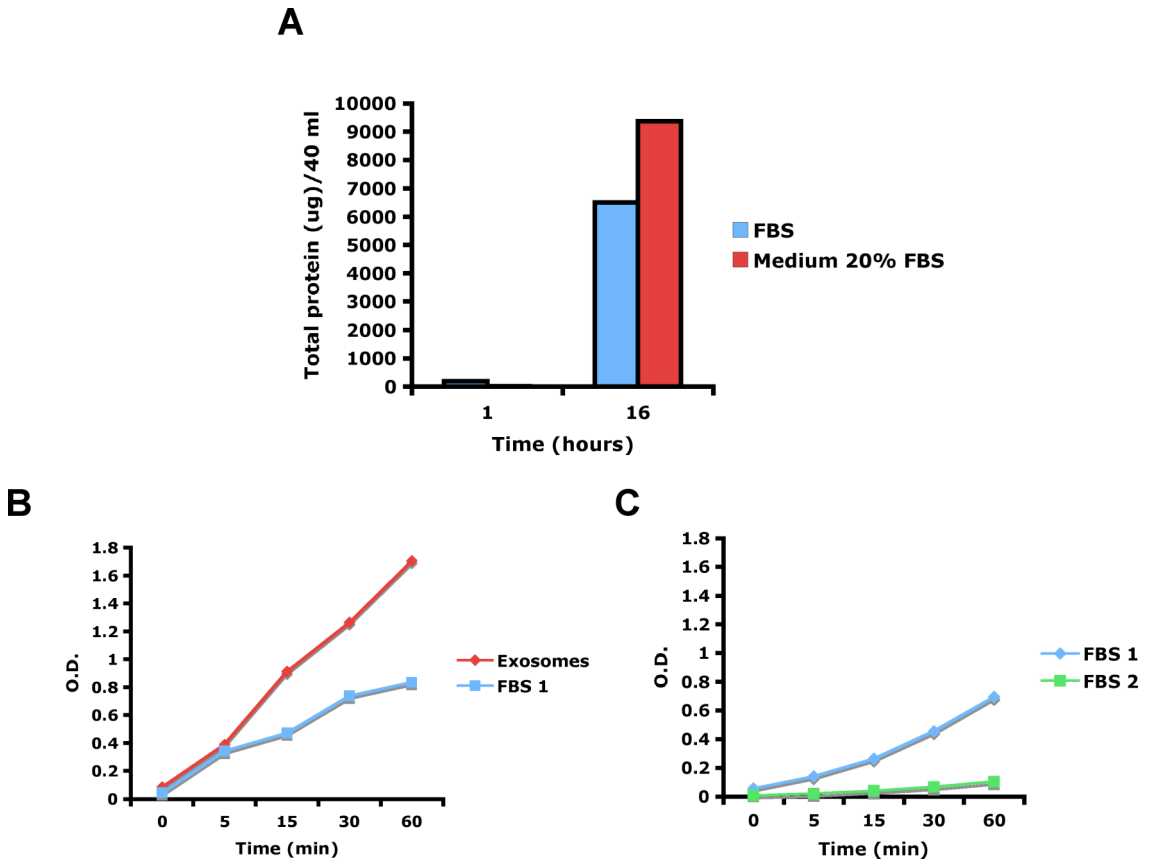

Figure 16. Elimination of contaminating exosomes from serum and evaluation of exosome AChE activity. A) Fetal bovine serum (FBS) or medium supplemented with 20% FBS were ultracentrifuged at 100,000 x g, 4°C at different times and total amount of protein in the pellet was quantified by BCA. B) Exosomes isolated from K562 cells were analyzed for the AChE activity. FBS was used as control. C) Analysis of AChE activity in serums from different companies.

Intermediate ultracentrifugation steps were replaced with filtration using a 0.22 μm filter. This filtration step allowed to eliminate larger vesicles and enrich the preparation for exosomes. There are different methods to characterize and assess the purity of the isolated exosomes. Since exosomes are reported be enriched in acetylcholinesterase (AChE), one such method applies quantification of AChE activity using a spectrophotometric assay. An exosome preparation was analyzed by AChE assay, using as control the serum (Figure 16B). It was found that exosomes displayed a high AChE activity. However, the serum also displayed AChE activity. To determine if the AChE activity generally is found in commercially available serum, AChE activity in sera from an additional company was tested (Figure 16C). AChE activity was found in both sera tested, but the

FBS 1 had very high activity compared to the FBS 2, in which the activity was low. These experiments allowed to verify that while the AChE assay is described as a good method to characterize vesicles as exosomes, it was not specific and could be misleading. Hence, other methods of validation are needed to be sure that the preparation consists of exosomes.

Characterization of K562 exosomes

The results of the K562 exosome purification procedure were further validated in two ways: electron microscopy and selective protein expression. Figure 17A shows an example of exosome preparation analyzed by transmission electron microscopy. The arrow points to the characteristic cup-shaped morphology and the sizing bar indicates that the vesicles in the preparation have the characteristic diameter range of 40 to 100nm.

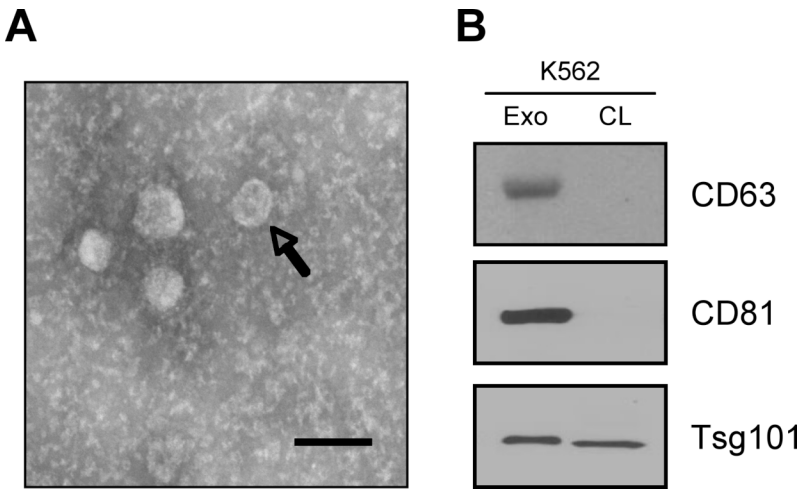

Figure 17: Characterization of exosomes released by K562 cells. A) Exosomes isolated from medium conditioned by K562 cells analyzed by transmission electron microscopy. Arrow: cup-shaped exosome. Scale bar 150 nm. B) Exosome characterization by immunoblot. Equal amounts of total exosomal proteins (Exo) and K562 cell lysate (CL) were analyzed for the expression of CD63, CD81, and Tsg101.

Next, the exosome pellet obtained after ultracentrifugation of the CML cell supernatant was analyzed by Western blot. CD63, CD81 and Tsg101 are known exosomal markers (121). Figure 17B shows the expression of these markers in

exosomes purified from K562 cells compared to equal amount of the K562 cell lysate. CD63 and CD81 are absent in lysate but found in abundance in the exosomal preparation. Tsg101 appeared equally present in both, suggesting enrichment in the exosomal compartment. It is therefore possible to conclude that the K562 cells release true exosomal vesicles into their conditioned medium.

Exosomes induce vascular tube formation in vitro

Angiogenesis has been demonstrated in the bone marrow of CML patients (261). We hypothesized that exosomes from K562 CML cells would induce tubular differentiation of HUVECs in culture. The effect of exosomes was examined by an endothelial tube formation assay. HUVECs were plated on Matrigel in low growth factor medium (see Materials and Methods) in presence of increasing concentrations of K562 exosomes and incubated for 6 hours to allow tubes to form.

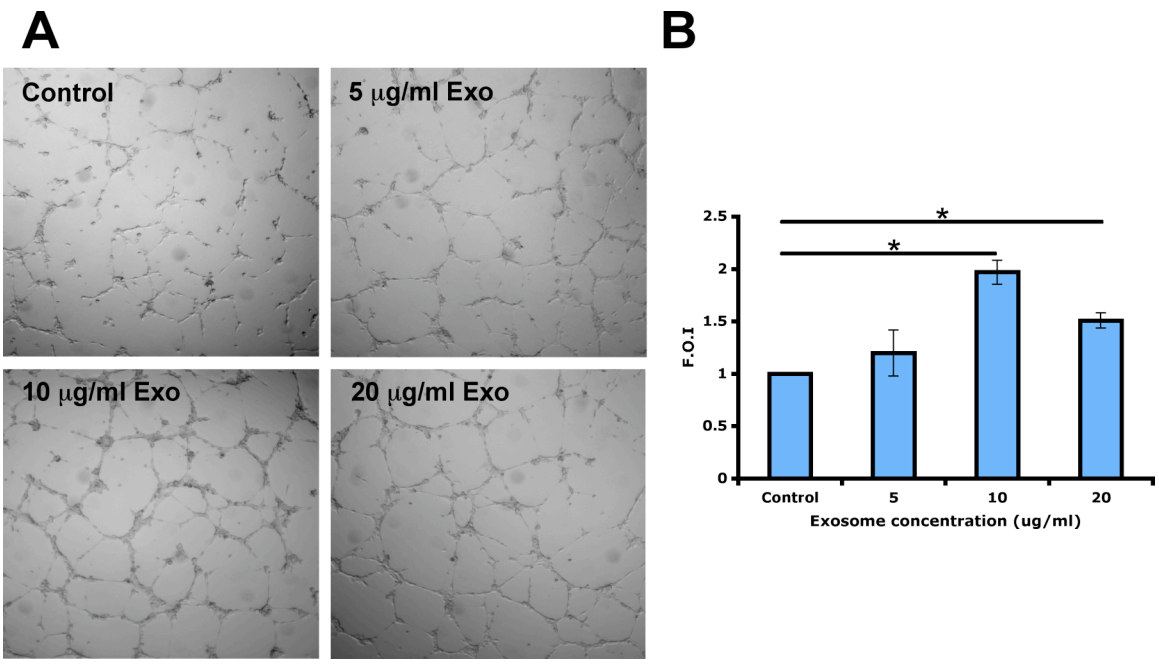

Figure 18: Dose-dependent stimulation of vascular tube formation by K562 exosomes. A) Exosomes promote tube formation by HUVECs on Matrigel B) Quantitative analysis of the total tube length (* $p < 0.01$ vs control).

Compared to the control, exosomes induced tube formation in a dose-dependent manner (Figure 18A). Addition of 5 μg/ml exosomes stimulated a morphologic change in HUVECs without significantly increasing the tube network formation as measured by cumulative tube length (Figure 18B). Increasing the dose to 10 μg/ml resulted in almost 100% increase in tube formation with respect to endothelial cells grown in low serum control medium. Quantitative analysis showed that exosomes induced a significant ($P<0.01$) increase in the total tube length at the dose of 10 μg/ml (Figure 18B). HUVECs exposed to a higher single dose of exosomes showed a reduced cumulative tube length and poor cellular organization compared to the 10 μg/ml dose.

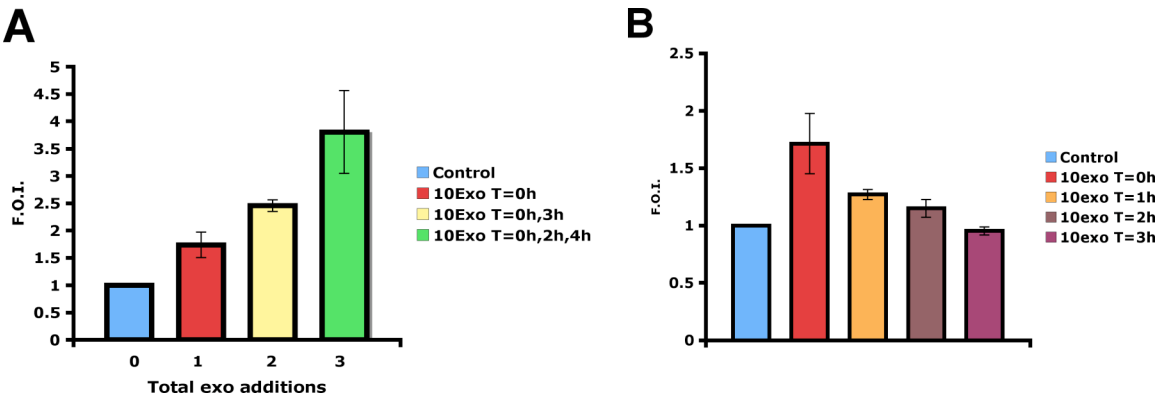

Figure 19. Tube formation induction related to the timing of exosome addition. Quantitative analysis of the total tube length in HUVECs plated on Matrigel and treated with increasing doses of exosomes given in sequential 10 μg/ml doses (A), or treated with a 10 μg/ml dose with increased delay of exosome addition (B).

To determine whether reduction of tube formation was due to a toxic effect of the exosome dose, HUVECs were exposed to 2 or 3 repetitive additions of 10 μg/ml doses of exosomes over a 3-4 hour period. As shown in Figure 19A, exposure to 20 μg/ml exosomes given in two 10 μg/ml doses (0 and 3 h) induced greater formation of tubes compared to a single 10 μg/ml dose given at time 0 h. Three additions of 10 μg/ml of exosomes (0, 2 and 4 h), a total of 30 μg/ml, further increased tube formation compared to the one or two time addition. This would suggest that the toxicity of 20 μg/ml dose (Figure 19B) might be due to the bolus effect rather than the total exposure over time. Next, it was examined whether

the timing of exosome addition was important for tubular differentiation. As previously demonstrated, addition of 10 μg/ml of exosomes at the initiation of tube formation induced an almost two-fold increase in cumulative tube length (Figure 19, red bars). The orange bar in Figure 19B shows that delaying exosome addition by 1 h resulted in an approximately 50% loss of net tube formation. Greater loss in exosome response was observed with increased delay of introduction of exosomes (Figure 19 brown bar). Stimulation was completely lost by the addition of exosomes after 3 h (Figure 19 purple bar). This suggest that there is an optimal exosome quantity for stimulation of tubular differentiation and the response was also time-dependent, with delay resulting in a reduced or lost response.

Exosomes are internalized by endothelial cells during tube formation

We posited that exosomes must be internalized in order to effect their function. Exosome internalization and intracellular localization during tube formation were examined in HUVECs on Matrigel. Exosomes were stained with PKH26, a membrane fluorescent dye. HUVECs were then incubated with PKH26-labeled exosomes and uptake was evaluated at different time points (Figure 20). At early stages of tube formation, cells were spread on Matrigel and exosome uptake was detectable (Figure 20A). Localization was mainly perinuclear (Figure 20A, arrows) suggesting that internalization occurs following the endocytic pathway as previous described for cells growing in monolayer. Cells start organizing into tubes after 1 h, and exosome localization remains chiefly perinuclear during this early time of differentiation (Figure 20B, arrows). Tube formation is not completed after 2 h but exosome localization starts to change. Predominant localization remains perinuclear, especially in cells that are not differentiating. However, exosomes begin to move to the cell periphery and into the arm of extending cells (Figure 20C, arrow). Tubes are mostly formed by 4h and it was observed an increase in the total amount of exosomes internalized (Figure 20D). Furthermore, exosomes diffused more broadly within the cytoplasm and a large quantity of

exosomes was localized in the cell periphery. In particular, exosomes were found in nanotubular structures connecting neighbor cells (Figure 20D, arrow). No red fluorescence was observed in the control cells (see “Labeling of exosomes” in Materials and Metods) (Figure 20 E). Thus, exosome uptake increases over time and their localization into the nanotubes suggests an involvement of these structures in functional exosome movement.

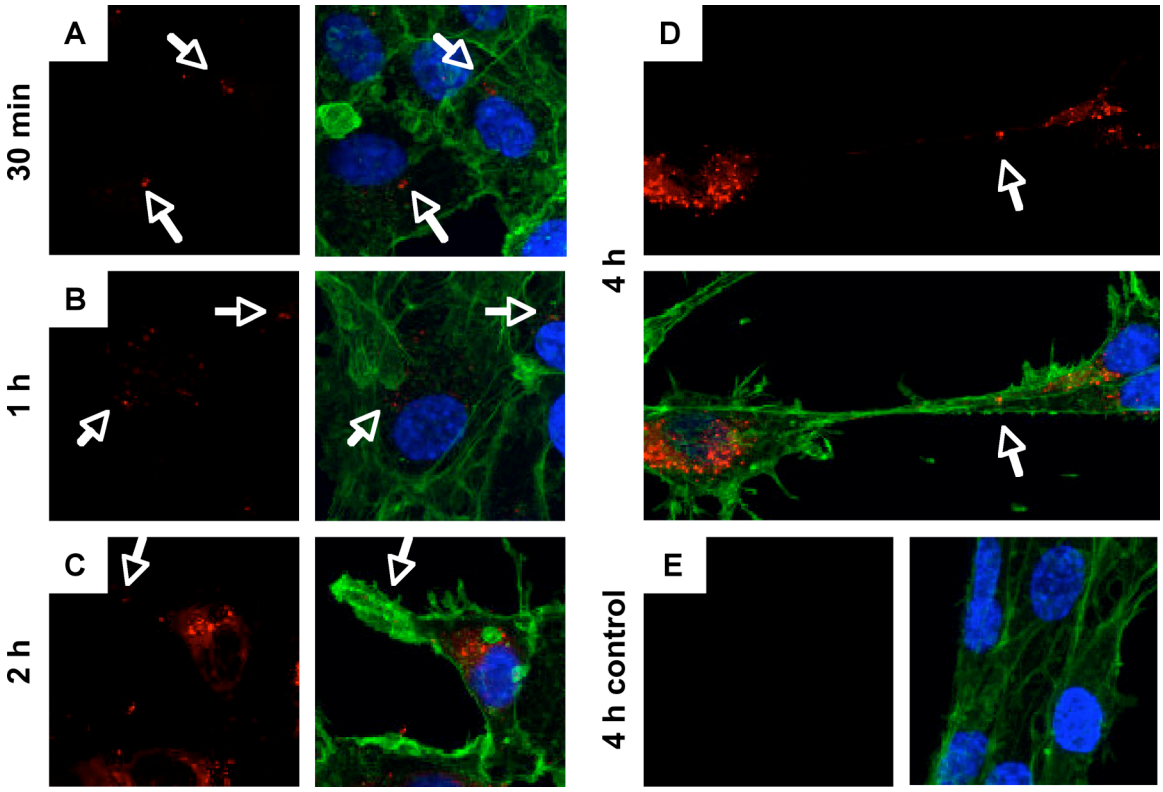

Figure 20: Time dependent uptake and localization of exosomes in HUVEC cells during differentiation. At the time of plating on Matrigel exosomes labeled with PKH26 (red) were added to the HUVEC cells and incubated for 30 min (A), 1 h (B), 2 h (C), and 4 h (D). As control a suspension of PKH26-labeled exosomes were filtered (as described in Materials and Methods) and the flowthrough was incubated with the HUVECs (E). After the incubation the cells were fixed and stained for the actin cytoskeleton (green), and the nuclei (DAPI). Arrows indicate exosome localization at the different time points of tube formation.

Exosomes localize inside nanotubes

To examine nanotube structure and exosome localization inside these structures, HUVECs were incubatedwith PKH26-labeled exosomes on Matrigel to allow nanotube formation. Then HUVECs were then fixed and stained for actin and α-tubulin. As shown in Figure 21 nanotubes connecting HUVECs contained both microtubules and actin (Figure 21B and C). Immunostaining of nanotubes and confocal analysis confirmed exosome presence within cell-to-cell connections (Figure 21A).

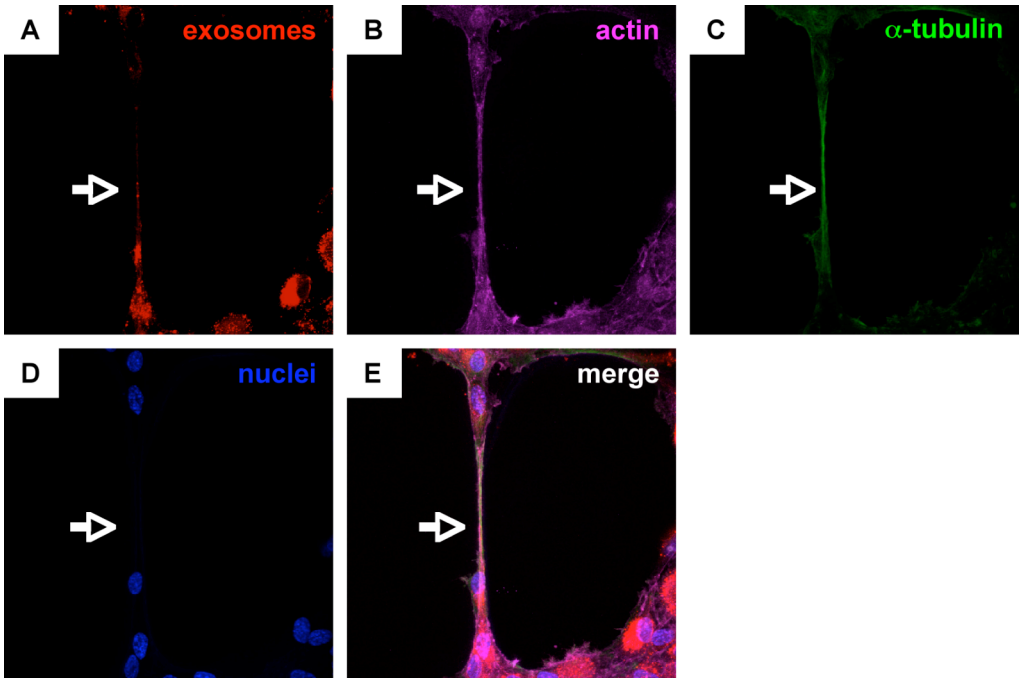

Figure 21. Exosomes localize inside nanotube structures. HUVEC cells incubated with PKH26-labeled exosomes (A) on Matrigel reorganized and sent out pseudopods that extended into nanotubes containing both F-actin (B) and microtubules (C). Nuclei were stained with DAPI (D). Merged image (E) shows the localization of exosomes at level of the nanotube.

Exosome localization inside the nanotubes was further confirmed through a 3D reconstruction of the confocal images by surface rendering using the Imaris software (Figure 22). A projection of the Z-plans showed in Figure 21E was used to create a 3D volume rendered image. Contrast, brightness and opacity of the

image were adjusted to optimize the volume rendering. Then, for each channel a surface was created, setting the threshold in order to reduce the background fluorescence.

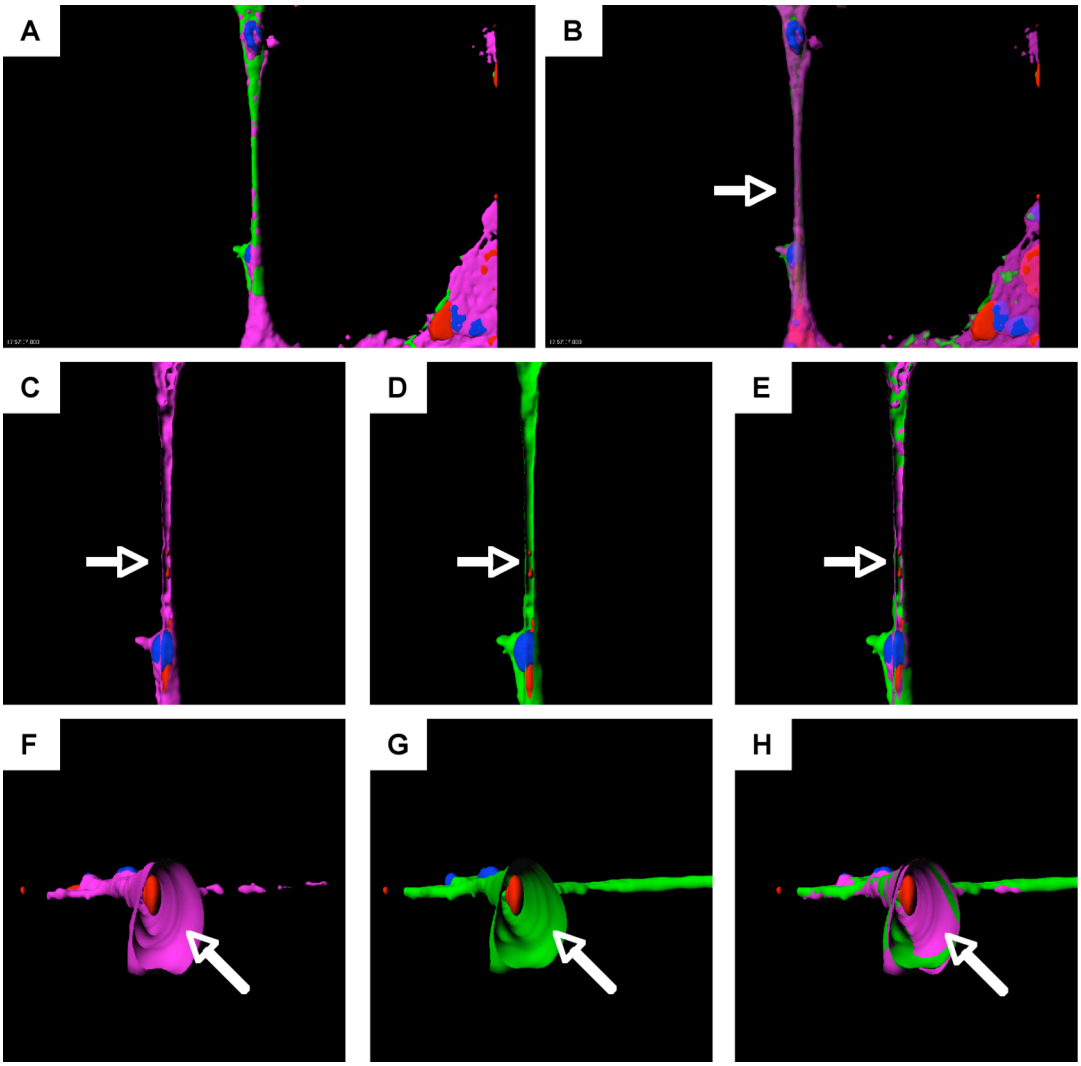

Figure 22. Three-dimensional reconstruction of nanotubes. A) Surface rendering of two HUVEC cells carrying exosomes (red) connected by nanotube. HUVECs were stained for actin (pink), tubulin (green) and nuclei (blue). B) Semi-transparency of the pink and the green (B), and sections of the nanotube (C-H) show that exosome localize inside the nanotube.

This procedure allowed to obtain a 3D image of the nanotubes, shown in Figure 22A. Semi-transparency of actin and tubulin, and sections of the 3D image confirmed that exosomes were transported inside the nanutubes (Figure 22B-H). This approach allowed examination of the actin and tubulin network within the

nanotube structure. They were found in a loose network without clear organization (Fiugure 22E and H).

Exosome are transferred cell-to-cell by nanotube formation

To examine the possibility of cell-to-cell transfer of exosomes, it was examined exosome localization during tube formation using a mixed cell suspension composed of two different populations of HUVECs.

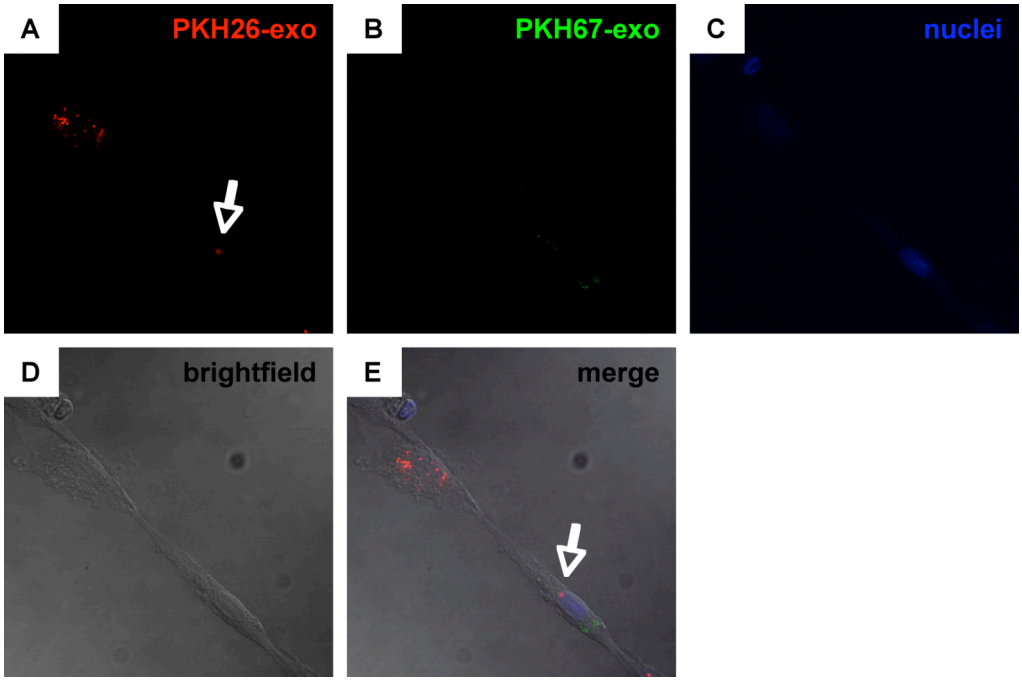

Figure 23. Exosomes are transferred cell to cell. HUVECs carrying PKH26-stained exosomes (A, red) were mixed with HUVECs carrying PKH67-stained exosomes (B, green) and plated on Matrigel for 4 h. After the incubation, cells were fixed and DAPI stained for nucleai (C). Tube forming cells show the presence of both green and red exosomes inside the same cell (arrows)

The first population of cells was preincubated with PKH26-stained red fluorescent exosomes, while the second population was preincubated with PKH67-stained, green fluorescent, exosomes. They were mixed and plated on Matrigel to form tubes. Four hours later, the tubular network showed HUVECs containing both red and green exosomes (arrows, Figure 23). A subset of cells, those involved in the tubular network, contained colocalized red and green exosomes (Figure 24E).

The arrows in Figure 24 indicate cells containing red exosomes colocalized internally with green exosomes. These data suggest a cell-cell transfer and that the green and red exosomes colocalize to the same subcellular organelle.

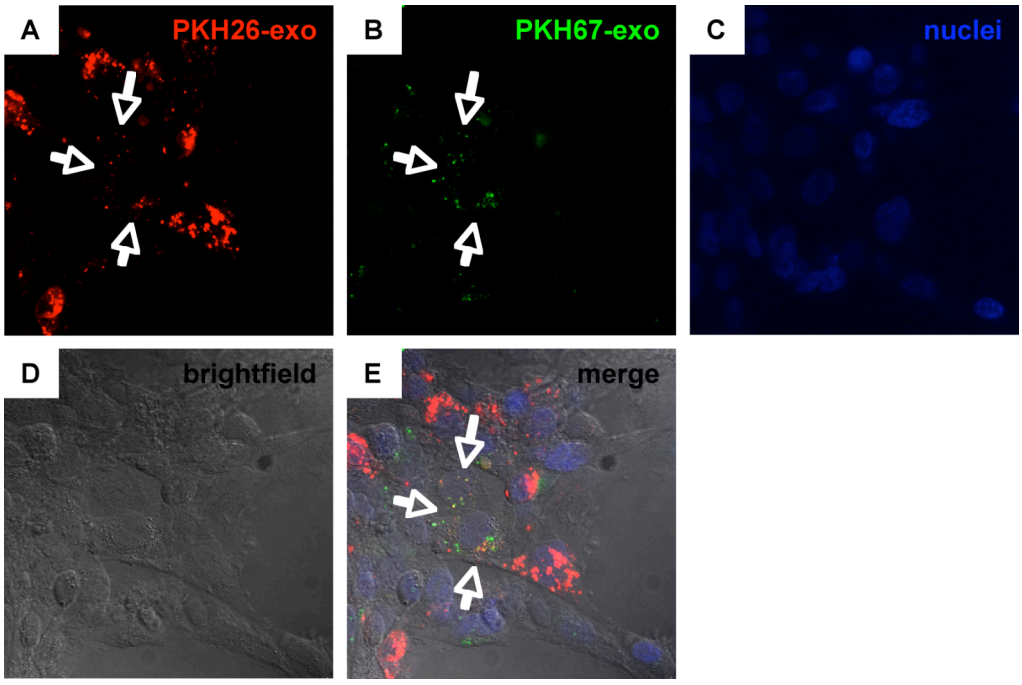

Figure 24. Colocalization of exosomes after cell-to-cell transfer. The tube network formed by HUVECs positive for both PKH26 (A) exosomes and PKH67 (B) exosomes displayed cells in which some of the red exosomes colocalized with the green exosomes (arrows).

To finally demonstrate exosome transfer through nanotubes and characterize the exosome movement, time-lapse video microscopy was performed. This enabled to track exosome movement over time. It was observed that exosomes in the perinuclear area showed mostly a vibratory movement; whereas, those inside the nanotubes moved straight from one cell to the other. It was possible also to detect both unidirectional movement in some nanotubes and bidirectional movement in other (Figure 25A-D). Overall, these experiments demonstrate that HUVECs can internalize exosomes, and transfer them to neighboring cells through extended nanotube structures.

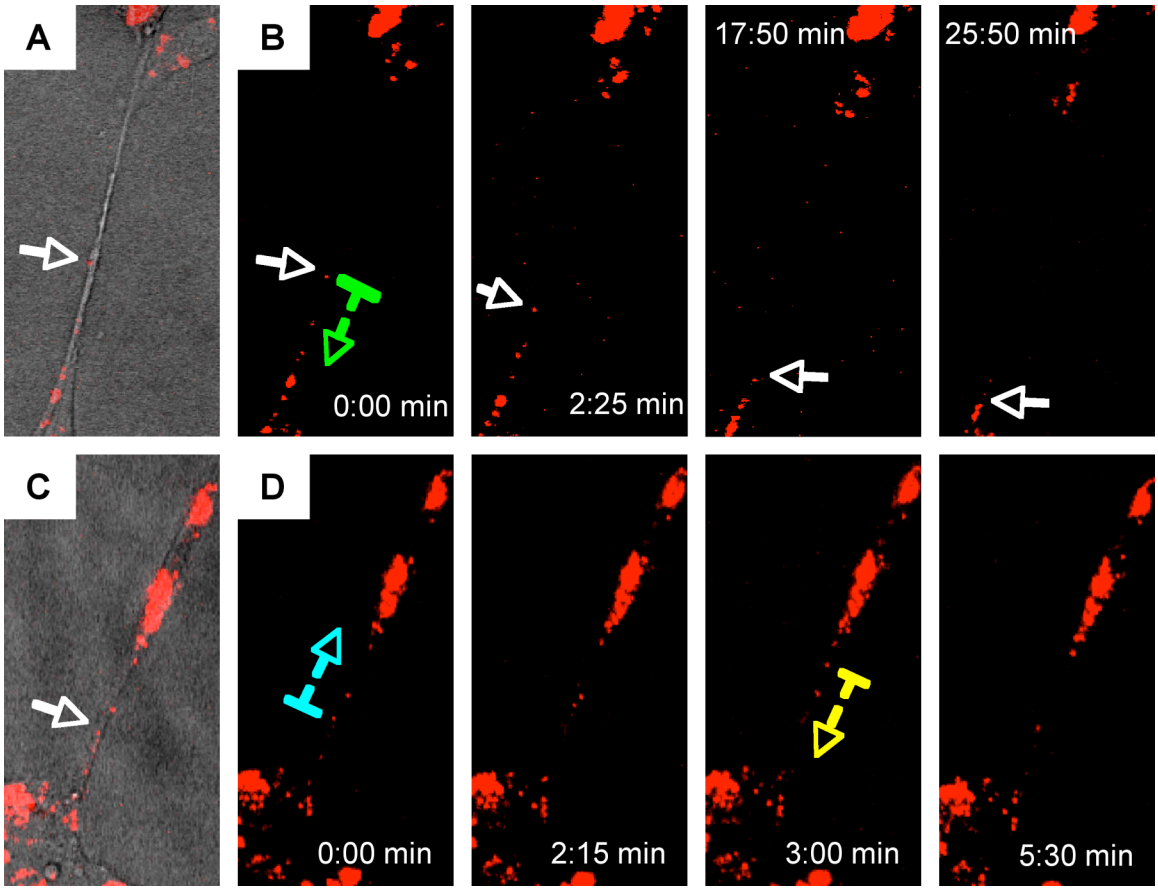

Figure 25. Exosomes move along nanotubes. HUVECs were incubated with PKH26-labelled exosomes and analyzed by fluorescent time lapse videomicroscopy. A and C) Brightfield view of HUVECs carrying exosomes (arrows) connected by nanotubes. B and D) Selected frames of a video sequence showing unidirectional (B) or bidirectional (D) transfer of PKH26 exosomes (dotted arrows indicate direction of movement).

Imatinib affect CML tumor cells but not tumor microenvironment

Imatinib mesylate is a selective inhibitor of ABL protein tyrosine kinase activity, with inhibitory activity against the BCR/ABL proto-oncogene (265, 266). It has been shown recently that imatinib-treated CML patients have a reduced plasma VEGF concentration (263). This finding suggests that imatinib may have a potential role in modulation of bone marrow angiogenesis. To determine whether imatinib is able to reduce exosome release and pro-angiogenic effects, K562 CML cells were treated with non-toxic dose of imatinib and exosomes isolated

from these cells evaluated for angiogenic effects. The XTT cell proliferation assay was performed on K562 cells using different concentrations of imatinib in order to establish the dose that doesn't have toxic effects. After 24 h of imatinib treatment, K562 cells proliferation was reduced of 20% (Figure 26A). A dramatic decrease of the proliferation was seen after 48 h with a 66% reduction in cell proliferation at the dose of 1 μM imatinib (Figure 26B).

Next, exosomes were isolated from K562 with or without 0.125 μM of imatinib treatment for 24 h. This concentration of imatinib was chosen because had a little effect on proliferation of K562, with a cells viability >99% calculated by trypan blue exclusion test, as well as to reduce the possibility of presence of apoptotic bodies in the conditioned medium of K562. The preliminary data show that K562 cells still release exosomes when treated with 0.125 μM imatinib since we were able to recover vesicles expressing the exosomal markers CD81 and Tsg101 (Figure 26C). The quantity of released exosomes was determined by measurement of total amount of protein in the exosome preparation pellet. The amount of secreted exosomes was reduced by 58% in the imatinib-treated cells. The next question was to evaluate the functional ability of exosomes released by imatinib-treated cells (IM-exosomes). HUVECs were plated on Matrigel in low growth factor conditions, as in Figure 18, in the presence of K562 IM-exosomes and tube formation was measured after 6 h of incubation. As shown in figure 26E IM-exosomes induced formation of tubular structure by HUVECs, with a 2 fold of increase in the total tube length at the dose of 10 μg/ml. These results suggest that imatinib regulates exosome secretion process but does not change exosome angiogenic activity.

Next it was evaluated the effect of imatinib directly on HUVEC uptake and response to exosomes from untreated K562 cells. First, the effect of imatinib on HUVECs viability was evaluated. An XTT cell proliferation assay was performed treating HUVECs with increasing concentrations of imatinib (range: 0.1-10 μM) for 24 and 48 h (Figure 27).

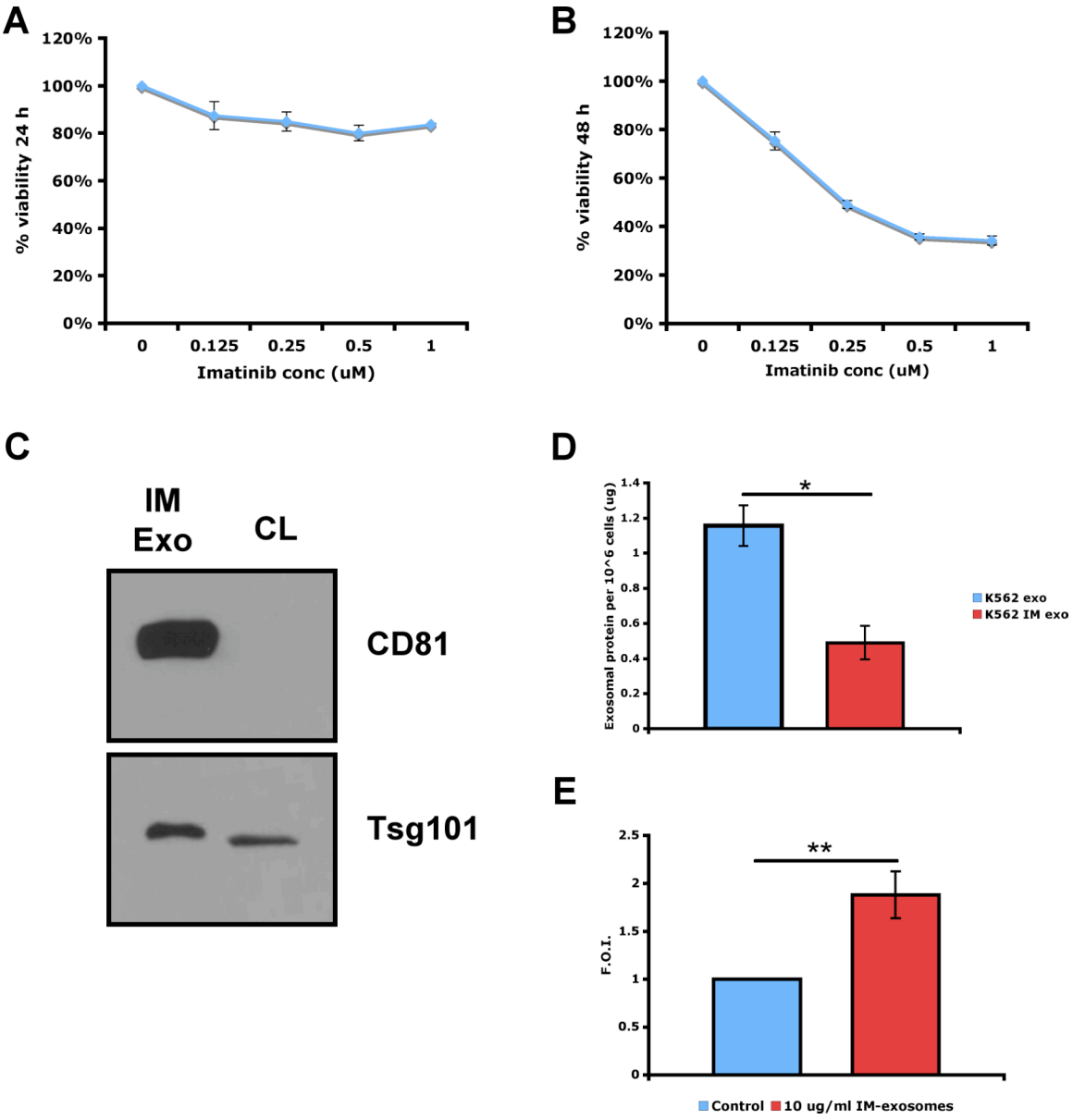

Figure 26. Imatinib affects exosome release but not exosome function. XTT cell proliferation assay of K562 treated for (A) 24 h and (B) 48 h, with increasing concentrations of imatinib (0.125-1 μM). C) IM treatment does not alter characteristic exosomal protein expression. Equal amount of exosome proteins and IM-treated K562 cell lysate (CL) were analyzed for exosomal markers CD81 and Tsg101. D) Total amount of proteins in the exosomal pellet purified from K562 control cells and K562 treated with the non-toxic dose of imatinib 0.125 μM (IM exo) for 24 h (*p = 0.0018). E) Quantitative analysis of cumulative HUVEC tube length shows that IM exosomes promote tube formation (**p < 0.05).

No toxic effects of imatinib were seen after 24 h of incubation (Figure 27A), and only a 20% of reduction in HUVEC proliferation was demonstrated at the highest tested concentration (10 μM) at 48 h (Figure 27B).

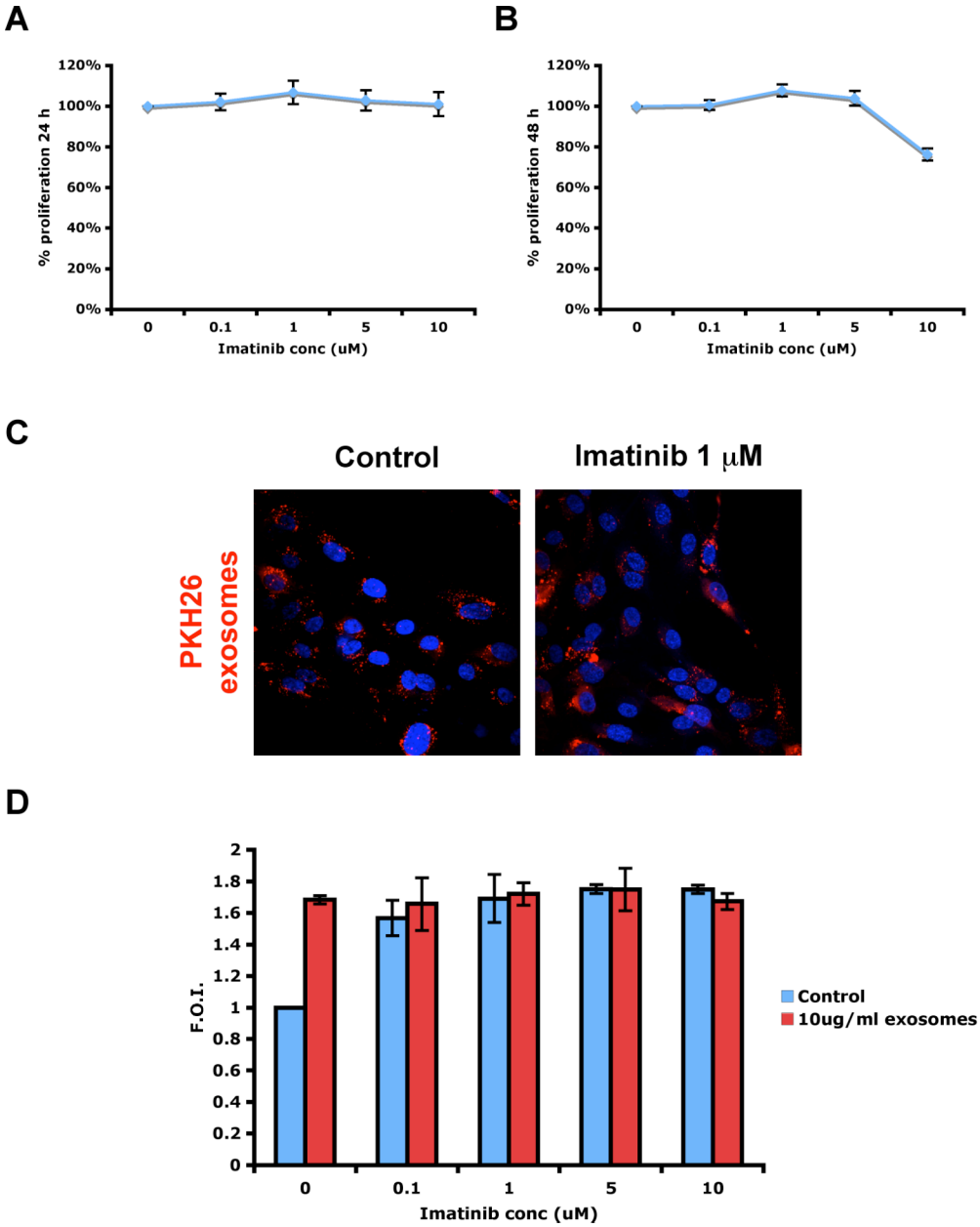

Figure 27. Imatinib does not affect exosome uptake or tube formation of HUVECs at non-toxic concentrations. XTT cell proliferation assay of HUVECs treated with increasing concentrations of imatinib (0.1-10 μM) for (A) 24 h and (B) 48 h shows that imatinib has limited activity against HUVEC cells. C) HUVECs were incubated on Matrigel for 4 h with PKH26-labeled exosomes (red) and with or without 1 μM imatinib. After incubation cells were fixed and stained for nuclei (blue). D) Quantitative analysis of the total tube length in HUVECs plated on Matrigel and treated with increasing doses of imatinib (0.1-10 μM) and incubated with 10μg/ml of exosomes for 6 h.

Next, HUVECs were incubated on Matrigel with PKH26-labeled exosomes in presence of 1 μM imatinib, selected for its physiologic plasma concentration in patients. Even if there was variability in the exosome uptake from a cell to another, on the whole, internalization of exosomes by HUVECs was not visibly altered by imatinib. Finally, HUVECs were plated on Matrigel and incubated with 10 μg/ml of exosomes in the presence of increasing concentrations of imatinib (0.1-10 μM), and tube formation evaluated after 6 h (Figure 27D). No reduction in exosome-stimulated tube formation was seen in presence of all concentrations of imatinib tested. Moreover, imatinib treatment alone was able to stimulate tube formation in a non-concentration-dependent fashion. All together these results suggest that imatinib modulates CML cells but not tumor microenvironment.

Dasatinib regulates both CML tumor cells and tumor microenvironment

Dasatinib is a multikinase inhibitor, developed against mutant BCR/ABL and found to have substantial activity against the SRC family kinases, that is now used for the treatment of imatinib-resistant CML (91). To study the effects of dasatinib on exosome release and function, exosomes isolated from dasatinib-treated K562 cells were quantified and their angiogenic effects on HUVECs evaluated *in vitro*. A dose-finding assay was done to determine the non-toxic dose for subsequent use. Dasatinib induced a 20% decrease in cell proliferation of K562 cells at the concentrations 1 and 5 nM after 24 h of treatment (Figure 28A). Treatment with dasatinib for 48 h more substantially reduced cell proliferation with a 69% decrease of vitality (Figure 28B). Exosome were isolated from K562 cells treated with the relatively non-toxic concentration of 0.1 nM dasatinib, and exosome identity was confirmed by immunoblot for the exosomal markers CD81 and Tsg101 (Figure 28D). Isolation of exosomes from K562 cells teated with 0.1 nM dasatinib yielded a 56% of reduction in exosome release compared to the untreated cells (Figure 28C). The angiogenic potential of exosomes isolated from dasatinib-treated K562 cells was tested next. HUVECs

were plated on Matrigel and incubated with 10 μg/ml of dasatinib-K562 exosomes. As shown in Figure 28E, dasatinib exosomes were still able to induce tubular differentiation with an increase of 2 fold in the total tube length.

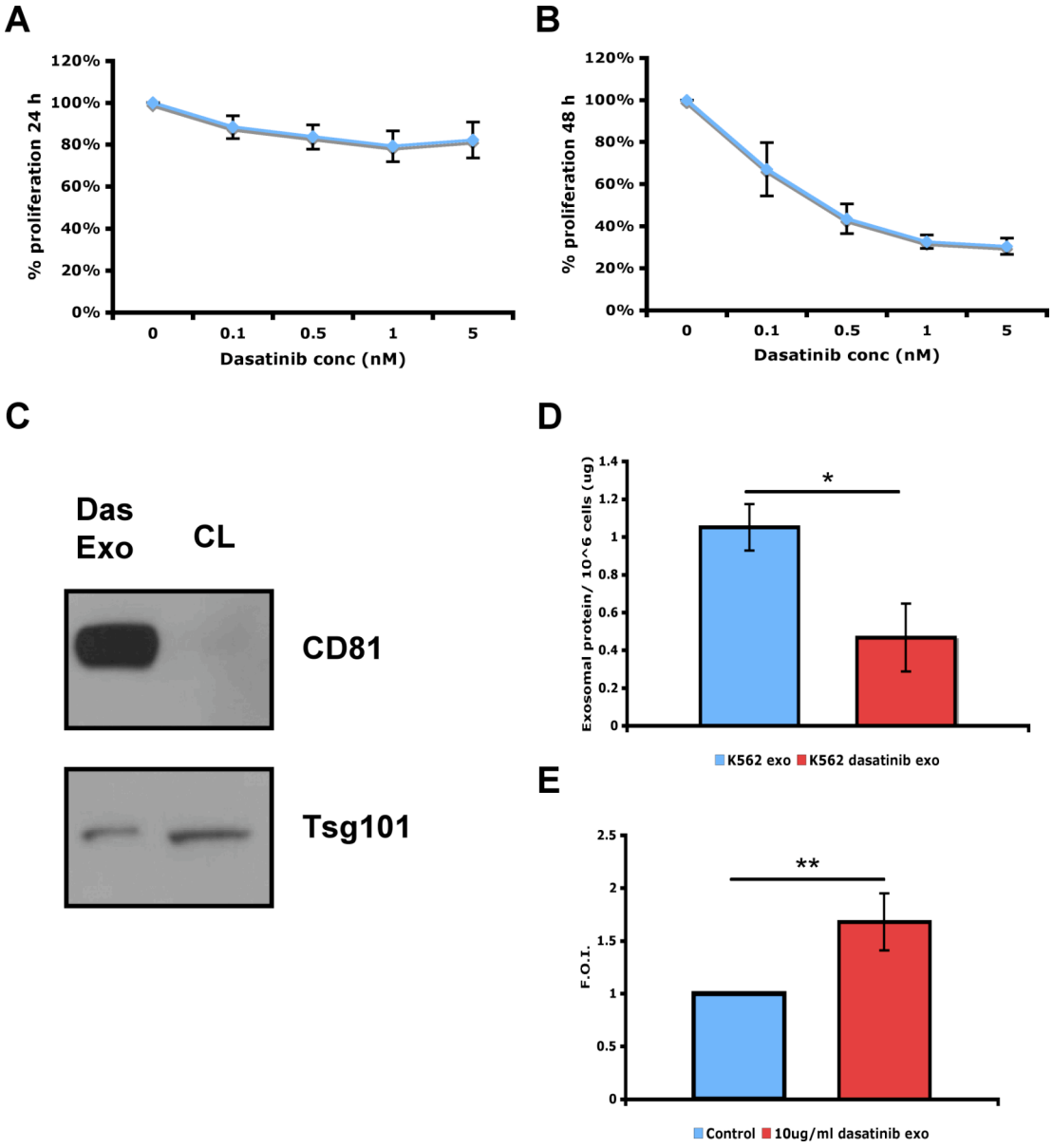

Figure 28. Dasatinib affect exosome release but not exosome function. XTT cell proliferation assay on K562 treated for (A) 24 h and (B) 48 h with increasing doses of dasatinib (0.1-100 nM). C) Dasatinib treatment does not alter characteristic exosomal protein expression. Equal amount of exosome proteins and dasatinib-treated K562 cell lysate (CL) were analyzed for exosomal markers CD81 and Tsg101. D) Total amount of proteins in the exosomal pellet purified from K562 control cells and K562 treated with the non-toxic dose of dasatinib 0.1 nM (dasatinib exo) for 24 h (*p = 0.01). E) Quantitative analysis of total tube length shows that dasatinib exosomes promote tube formation (**p < 0.05).

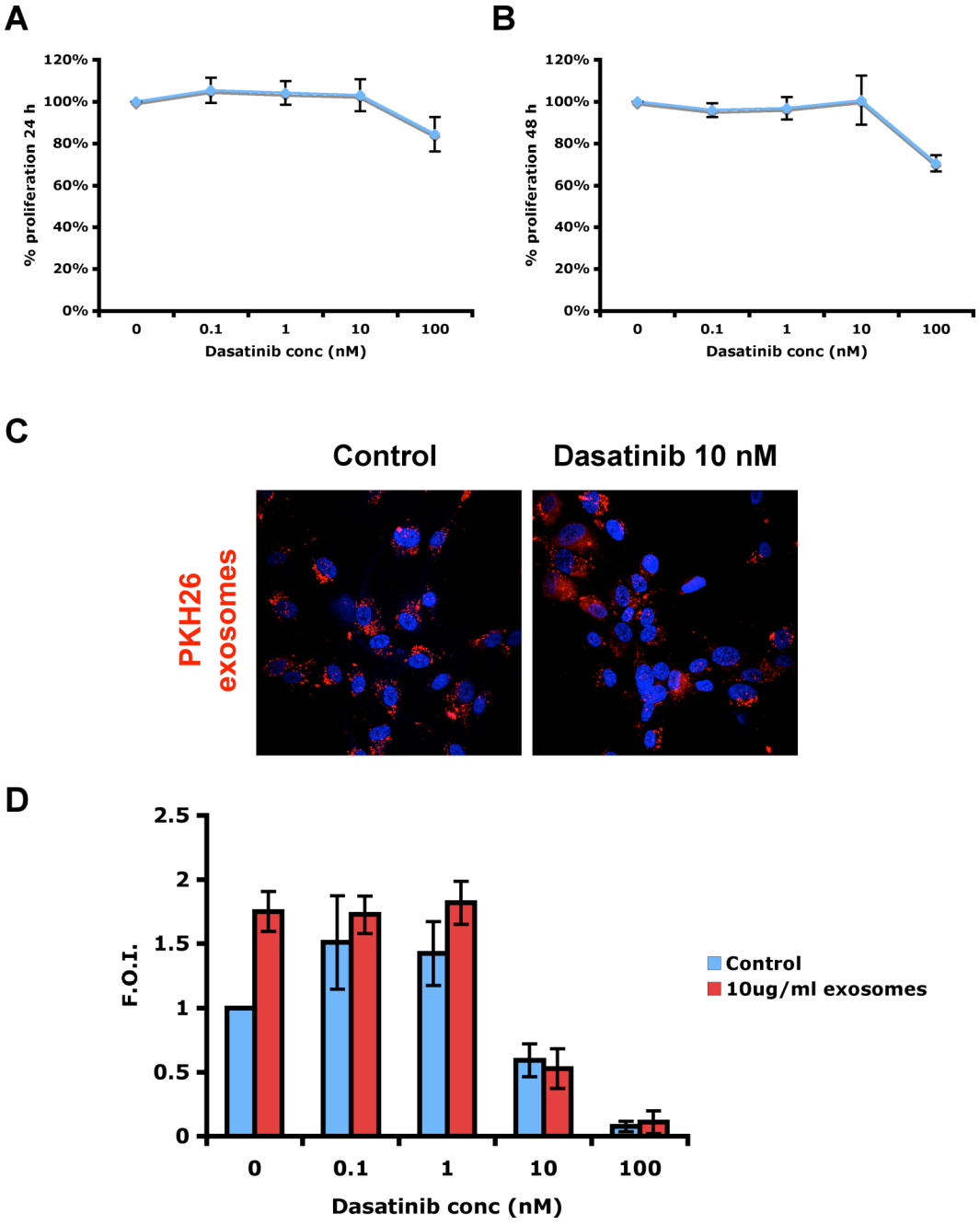

Figure 29. Dasatinib does not affect exosome uptake but blocks exosome-induced tube formation by HUVECs. A) XTT cell proliferation assay on HUVECs treated with increasing doses of dasatinib (0.1-100 nM) for 24 h and (B) 48 h shows that dasatinib does not have a toxic effect. C) HUVECs were incubated on Matrigel for 4 h with PKH26-labeled exosomes (red) and treated or not with 10 nM of dasatinib. After incubation cells were fixed and stained for nuclei (blue). D) Quantitative analysis of the total tube length in HUVECs plated on Matrigel and treated with increasing doses of dasatinib (0.1-100 nM) and incubated with 10μg/ml of exosomes for 6 h.

Again, the direct effect on HUVEC cells of the small molecule inhibitor was tested. To analyze the effect of dasatinib on HUVECs, XTT cell proliferation assay was performed on HUVECs treated with increasing concentrations of dasatinib (0.1-100 nM). Dasatinib caused a minimal toxic effect on HUVECs, with only a 20% reduction in cell proliferation after 24 h (Figure 29A) and 30% after 48 h (Figure 29B) with the highest concentration used (100nM). The effect of dasatinib on HUVEC exosome uptake was then tested. HUVECs were plated on Matrigel in presence of 10 nM of dasatinib and incubated for 4 h with PKH26-labeled K562 exosomes. As shown in Figure 29C, no differences in exosome uptake were seen in HUVECs treated with or without dasatinib.

Finally, the effect of dasatinib on exosome-induced tube formation was analyzed. HUVECs were plated on Matrigel and incubated with K562 exosomes in presence of increasing concentrations of dasatinib (0.1-100 nM) or vehicle (DMSO). Low concentrations of dasatinib (0.1 and 1 nM) did not affect HUVEC response to exosomes (Figure 29D). On the contrary, treatment with higher concentrations of dasatinib (10 and 100 nM) inhibited tube formation equally and in dose dependent manner in HUVECs plated in low grow factor medium (control) and those stimulated with exosomes (Figure 29D). These results suggest that dasatinib is able to block both tumor cell function and, unlike imatinib, tumor-associated angiogenesis. This occurs, at least in part, through the inhibition of exosome effects.

Exosomes stimulate HUVECs through the activation of Src signaling

Dasatinib differs from imatinib in its ability to recognize multiple conformations of BCR/ABL, and also for its inhibitory activity against the Src family kinases (SFKs) (91). Src activity has been shown play an important role in tube formation stimulated by proangiogenic factors, such as VEGF and bFGF (267). Phoshorylation of Tyr416 in the kinase domain of Src is required for catalytic activity (268). The previous results suggest that HUVEC stimulation by exosomes could be directly correlated with the activation of the Src signaling. To assess this

hypothesis, HUVECs were incubated with exosomes, allowed to adhere to Matrigel for 30 min, and then Src activation analyzed by immunofluorescence. This incubation time was chosen based on the observation that the first hour of incubation with exosomes was important to obtain the maximum stimulatory response by HUVECs (Figure 19B). Figure 30 shows that HUVECs treated with 10 μg/ml of K562 exosomes showed a higher fluorescence intensity of phosphorylated Src compared to the untreated control, with an increased Src localization at points of membrane contact (Figure 30 arrows). Dasatinib blocked the Src phosphorylation both in control and exosome-stimulated cells with loss of membrane Src staining. In contrast, imatinib treatment did not alter exosome effect, but resulted in a small increase in total fluorescence in control cells (Figure 30).

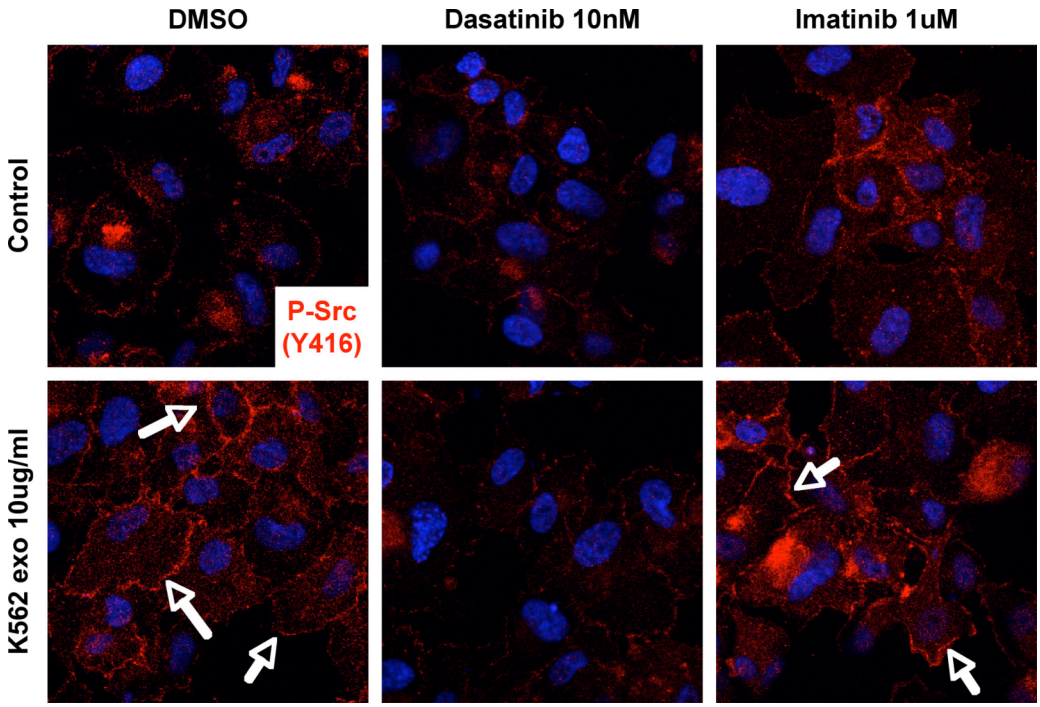

Figure 30. Exosomes stimulate Src phosphorylation in HUVECs. Semiconfluent HUVECs were harvested, resuspended in basal medium, and mixed with 10 μg/ml of exosomes. The cell suspension was plated on Matrigel in presence of DMSO (control), dasatinib, or imatinib, and cells allowed to adhere for 30 min. After the incubation time, cells were fixed and red fluorescence labeling was performed to visualize phospho-Src. Nuclei were stained with DAPI (blue).

Next, it was investigated the effect of exosomes on focal adhesion kinase (FAK), a known substrate of Src. Activated Src phosphorylates FAK at the specific tyrosine residue Tyr861. The data indicate that exosomes induced FAK phosphorylation on Tyr861, and increased the number of focal adhesions (Figure 31, arrows). FAK activation was markedly attenuated by dasatinib treatment with associated reduction in focal adhesions. While there was little reduction in Tyr861FAK in imatininb-treated control cells, the pattern of staining was different in exosome-exposed cells. Those cells had a change in the organization and quality of stained focal adhesions compared with vehicle-treated exosome-exposed cells, but with limited loss of staining intensity. These findings suggest that Src signaling plays an important role in exosome induced tubular differentiation in endothelial cells.

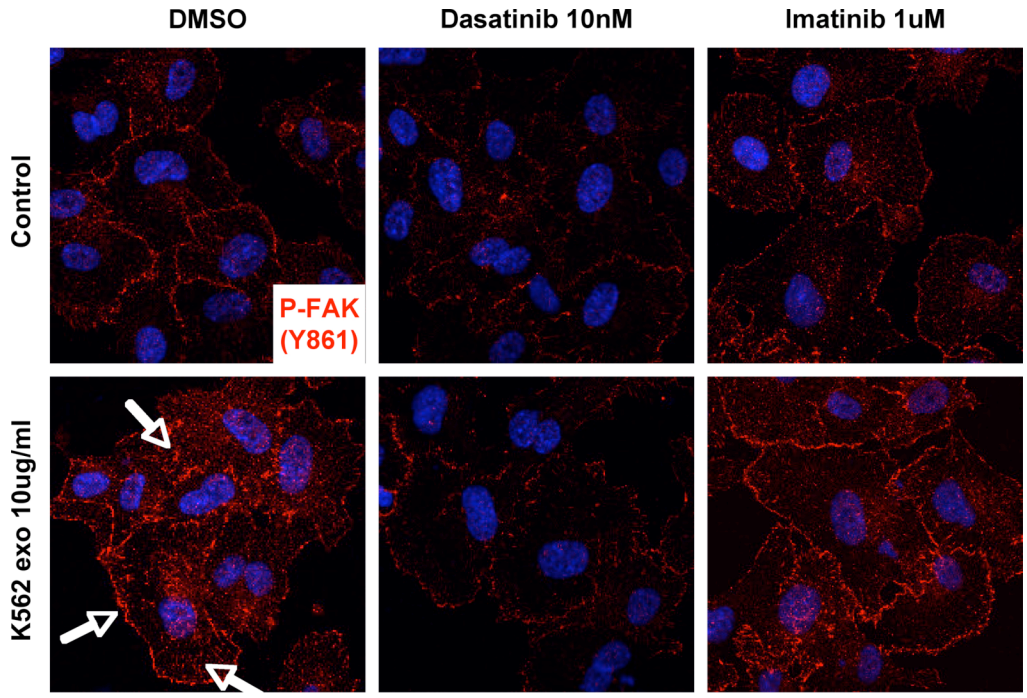

Figure 30. Exosomes activate Src signaling in HUVECs inducing selective phosphorylation of FAK. Semiconfluent HUVECs were harvested, resuspended in basal medium, and mixed with 10 μg/ml of exosomes. The cell suspension was plated on a thin layer of Matrigel in presence of DMSO (control), dasatinib, or imatinib, and cells allowed to adhere for 30 min. After the incubation time, cells were fixed and red fluorescence labeling was performed to visualize phospho-FAK (Tyr861). Nuclei were stained with DAPI (blue).

DISCUSSION

Chronic myeloid leukemia (CML) is a myeloproliferative disorder of hematopoietic stem cells that is characterized by the presence of the Philadelphia chromosome (3, 4). This chromosomal translocation results in the expression of the BCR/ABL fusion oncogene (5, 269). BCR/ABL is a constitutively activated tyrosine kinase that drives the pathogenesis of CML through the phosphorylation and activation of a broad range of downstream substrates. These are signaling proteins that play critical roles in cellular signal transduction and malignant transformation, and include RAS, PI3K and STAT5 (41, 47, 48, 62, 270). Although it is recognized that CML presents in three different clinical phases (1), little is known about the mechanism of disease progression. One hypothesis is that diverse interactions between leukemic cells and bone marrow microenvironment are important in the pathogenesis of the disease (271).

Cells may communicate through the release of soluble factors (103), cell-to-cell interaction, as well as through the release of microvesicles (MVs) (106). The most widely studied and best known types of MVs are shedding vesicles and exosomes (106). Exosomes are vesicles released by cells in response to a broad spectrum of physiologic and pathologic conditions. They can be easily distinguished from the other MVs for their characteristic cup shape, their small size, ranging between 30 and 100 nm, and the enrichment in specific proteins, such as CD63, now used as exosomal markers (108). Exosomes have been described to play an important role in modulating tumor microenvironment, and promoting tumor progression (272, 273).

Angiogenesis, the formation of new blood vessels from an existing vasculature, has been associated with grow and dissemination of solid tumors (274). It is now emerging that angiogenesis plays an important role in the pathogenesis and progression of hematological neoplasias (275). Increased vascularity is associated with a significant increase in circulation of angiogenic factors, including vascular endothelial growth factor (VEGF), fibroblast growth factor

(FGF), and hepatocyte growth factor (HGF), which are specific and potent inducers of angiogenesis (261). Moreover, increased bone marrow vascularity is more prominent in CML than in other forms of leukemia (261). However, the extent and role of exosome release during CML progression is an area of new investigation. *Our hypothesis was that exosomes released by CML cells could play a role in the stimulation of angiogenesis*.

The role of exosomes in the angiogenic process has been emerging in the last few years. It has been shown that exosomes from activated platelets induce expression of VEGF, MMP-9, interleukin-8, and HGF in lung cancer cells, and promote their adhesion to endothelial cells (276). Glioblastoma exosomes transport mRNA and proteins related to angiogenesis and promote endothelial cell proliferation *in vitro* (164). In addition, exosomes released by the D6.1A tetraspanin-transfected pancreatic cancer cell line induce endothelial tubulogenesis, a stimulation independent from the canonical angiogenic factors (277).

The study described in this thesis demonstrates that the CML cell line K562 releases exosomes into its conditioned medium. The composition of the exosome pellet obtained by differential ultracentrifugation has been confirmed by electron microscopy analysis, showing cup-shaped microvesicles ranging in size between 40 and 100 nm, and by the expression of the exosomal markers CD63, CD81, and Tsg101. It was shown here for the first time that the exosomes released by K562 CML cells induce tubular differentiation of HUVECs in an *in vitro* Matrigel assay. This could be the consequence of exosome uptake and internalization by the endothelial cells, as shown in the fluorescence tracking experiment using PHK-labeled exosomes. This finding suggests that exosomes may have an active role in CML progression through the modulation of the bone marrow microenvironment.

Exosomes released from CML cells inside the bone marrow microenvironment may serve as an alternative mechanism for the release of angiogenic factors. CML patients have been shown express higher plasma levels of VEGF, bFGF, HGF and TNF-α compared to the normal control (261). All of these factors could

be potentially packed inside exosomes. In fact, bFGF and VEGF have been shown be released by neurons and astrocytes via shedding microvesicles (278, 279). VEGF is also found in the cargo of tumor-derived microvesicles and is liberated upon disruption of the microvesicle membrane (280). It is possible that this form of VEGF release protects this and other factors from proteolytic degradation in the extracellular microenvironment. Evaluating exosome circulation and composition in the blood of CML patients would be the next step in this line of investigation. Alternatively, exosomes could be involved in the release of other factors that in combination with the angiogenic factors listed above may be responsible for overall vascularity.

CML exosomes may stimulate angiogenesis also through the delivery of mRNA to the endothelial cells. It has been shown that exosomal mRNAs can be translated inside the recipient cell (164). This suggests that tumor-derived exosomes could modify the surrounding normal cells by changing their translational profile. Microvesicles have been also shown to transfer membrane receptors to recipient cells. In this case, CML exosomes could make endothelial cells more responsive to circulating angiogenic factors. For instance, transfer of tumor-derived microvesicles containing the epidermal growth factor receptor (EGFR) into endothelial cells was shown to result in an acquisition of proangiogenic activity (281).

Next, the composition of exosomes may change during CML progression. A recent study has shown a change in angiogenic factor levels during the three clinical phases in the plasma of CML patients (282). The most significant increase of VEGF was found in patients in chronic phase, and VEGF levels decreased during the blast crisis. Instead, the highest plasma HGF concentrations were detected in patients in blast transformation (282). The discovery of a different exosome composition may add important information on how the CML cells change over time, and how this changes their interaction with the bone marrow microenvironment.

Recent studies have been focused to better understand the fate of exosomes after release into the extracellular milieu. It has been proposed that an acidic

tumor environment can promote lysis of some of the microvesicles, making intravesicular proteins available for interaction with surface receptors of the target cells (280). On the other hand, mRNA, miRNA and some angiogenic proteins, such as angiogenin, require transport inside recipient cells to exert their biological effect (283). Recent studies report that some cell lines are able to internalize exosomes (164, 284); however, little is known about mechanisms involved in that intracellular trafficking. Our observations demonstrated that exosomes moved from the cell periphery, the site of uptake, to the perinuclear region initially. This was followed by movement back towards the membrane, specifically into the reorganizing pseudopodia involved in the formation of the tube network. Then, it was showed that exosomes were shared between neighboring cells. This appears to occur through the cell-cell contact of the tunneling nanotubes.

Membrane or tunneling nanotubes (TNTs) are thin protrusions up to several micrometers long that connect cells from several cell diameters apart. They have been recently discovered as a new route of cell-to-cell communication. TNTs were originally described in cultured rat pheocromocytoma PC12 cells and immune cells (104). In PC12 cell cultures, TNTs were characterized as 50-200 nm wide actin-contained stretched tubes that provide membrane continuity between connected cells (104). Later, formation of TNT-like structures has been described in other cell types. This revealed some heterogeneity regarding formation, structure, and functional property across cell types and even within a given cell type. TNT-like bridges connecting dendritic cells appear to be the most closely related, if not identical, to TNT described in PC12 cells (285). The demonstrated intercellular transfer of triggered calcium signals and of the dye Lucifer yellow through these structures suggests membrane continuity as proposed in the TNT model (285). On the contrary, TNT-like bridges between T-cells present a similar architecture to that of PC12 TNTs and same quality of intercellular transfer, but they do not propagate calcium signals between T-cells. Furthermore, they do not permit free diffusion of fluorescent plasma membrane

proteins and a junctional border was detected at the ultrastructural level. Hence, they were classified as close-ended cellular nanotubes (286).

Besides the emerging cell-type-specific differences of TNT-like structures, evidence for different classes of bridge was also provided for a given cell type as demonstrated for macrophage (287). These cells were found be connected by thin only F-actin containing nanotubes (<0.7 μm diameter) and by thicker microtubule-containing types of cellular connections (>0.7 μm diameter). In agreement with the latter type, thicker nanotubes were also found between prostate cancer cells (288). The diversity of the TNT-like bridges may be related to different transfer mechanisms. F-actin containing bridges appear to perform a unidirectional transfer of cellular components such as organelles (104). This "one-way street" principle would be in agreement with an acto-myosin-dependent transport assuming that the F-actin fibers inside the bridges have the same polarity. In contrast, a bidirectional movement of organelles along microtubules was observed for the thick bridges between macrophages (287). Cargo has to traverse the junctional border between T-cells, which may involve exocytosis and endocytosis. We report here that exosomes internalized by HUVECs are transferred to other cells through the formation of nanotubes. The nanotubes connecting HUVECs are composed of both F-actin and microtubule. Because of their composition, these structures are thick nanotubes. Software able to perform three-dimensional reconstruction of the nanotube structure confirmed that exosomes localize inside the cytoskeletal scaffold of the nanotubes. Moreover, HUVEC nanotubes did not present junctional borders, showing a continuous cytoskeletal network. Movement of the exosomes inside the nanotubes was further confirmed by live cell imaging, showing a bidirectional transfer of exosomes.

TNTs have been reported be involved in the transfer of organelles belonging to the endosomal/lysosomal system (104). Bacteria have been shown surfing along TNT-like structures connecting macrophages (287). Moreover, transfer of mitochondria through myocytes nanotubes has been associated to the acquisition of myocyte-like phenotype in endothelial progenitor cells (289).

However, the first evidence of TNT-dependent functional connectivity was reported in myeloid cells. It was shown that calcium signals, induced in myeloid cells, were propagated via TNT to neighboring cells, where they elicited a physiological reaction (285). Evidence for the involvement of a TNT-dependent communication in immune defense arose from the detection of class I major histocompatibility complex (MHC I) in TNT between immune cells (285). This may point to the role of these bridges in a faster and more efficient antigen presentation (290). Our finding was the first to show that exosomes are transferred cell to cell using TNT-like structures. This transfer of exosomes could play an important role in propagation of exosome angiogenic information and potential amplification of exosome effects, adding a new step in the exosome trafficking after uptake. Also, this is of particular interest in the context of intercellular transfer of RNAs. In fact, it is known that mRNA and miRNA are packed inside exosomes (164). Our data, if confirmed by further experiments, could be the first evidence of cell-to-cell transfer of RNA through nanotubes. This has been demonstrated to occur through so called plasmodesmata (291), which are involved in direct cell-to-cell communication in plants, but not yet in other organisms.

In this thesis are reported also results that represent an important first step in determining whether kinase inhibitors treatment blocks CML progression at least in part by suppressing exosome modulation of the leukemia bone marrow microenvironment. First, it was evaluated the effect of imatinib on exosome release by K562 CML cells and on angiogenesis induced by those exosomes and exosomes from treated cells. Imatinib has been reported to reduce VEGF release by K562 cells (263). It is able to decrease VEGF production in patients with CML, resulting in decreased bone marrow vascularity (292). These findings led to the conclusion that imatinib regulates bone marrow angiogenesis by the regulation of VEGF production. Here, it was demonstrated that imatinib also regulates exosome release. It was found that non-toxic drug concentrations effectively reduced exosome release by 58% from K562 cells. K562 cell line has been reported not to express c-kit (263), and PDGFR inhibitors did not affect cell

functions (293), so the decreased exosome release observed should be related to the BCR/ABL tyrosine kinase inhibitor activity of imatinib. It was also showed that exosomes released by K562 cells treated with imatinib maintained their ability to stimulate tubular differentiation by endothelial cells on Matrigel. This suggests that imatinib interferes with the mechanisms involved in exosome secretion but doesn't change exosome composition.

It was then studied the effect of imatinib on endothelial cells and on their ability to respond to exosome stimulation. It was found that treatment of HUVECs with imatinib for 48 h did not have toxic effects, even with concentrations above physiologically attainable plasma concentrations. This is in accordance with a previous report that describes the inability of imatinib to inhibit the normal endothelial cell function (294). Imatinib also did not affect HUVEC internalization of exosomes. Moreover, treatment of HUVECs plated on Matrigel with imatinib did not block exosome-stimulated tube formation. Surprisingly, imatinib itself induced increased tube formation at all the concentrations tested. This could be due to a response of the endothelial cells to the presence of the inhibitor resulting in activation of other pathways that cause stimulation of tubular differentiation.

Dasatinib is a kinase inhibitor that has been shown be an effective therapeutic for imatinib-resistant CML. Dasatinib, in addition to inhibition of the fusion oncogene BCR/ABL, inhibits Src family kinases (SFKs), c-kit, PDGFR, and EphA2 (91, 93, 295, 296). SFKs comprise a subset of non-receptor protein tyrosine kinases that includes c-Src, Fyn, Yes, Lyn, Lck, Hck, Blk, Fgr, and Yrk (268). Other than their ability to promote tumor growth and metastasis (268), SFKs coordinate multiple signaling pathways involved in regulating endothelial cell function, making SFKs targets for antiangiogenic therapy (297). A recent study reports that dasatinib suppresses tumor growth *in vivo* by inhibiting the recruitment and function of endothelial and myeloid cells, and SFK signaling in these cell types. Moreover, it is reported that dasatinib treatment inhibits HUVEC cell migration in response to VEGF and bFGF (267).

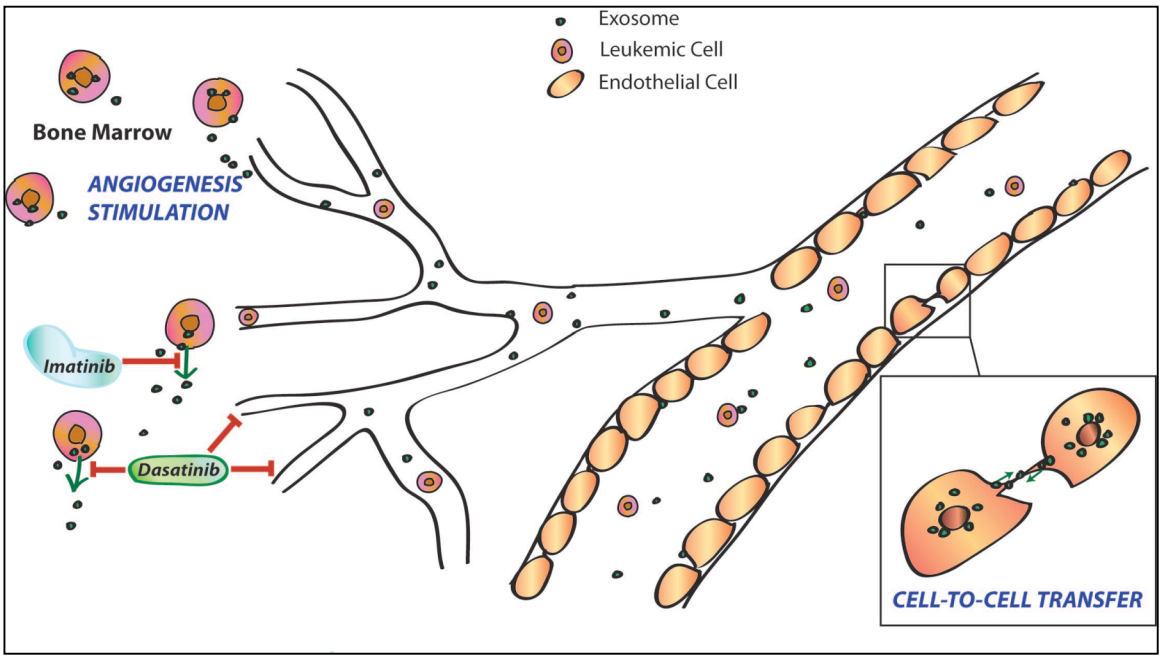

Figure 32. Proposed model of CML exosomes activity inside the bone marrow microenvironment. Exosomes released by CML cells stimulate increase in bone marrow vascularity. This is due, at least in part, to exosome internalization by endothelial cells and exosome trafficking through nanotubular structures. Exosome effects are modulated by imatinib through the inhibition of exosome release, and by dasatinib blocking both exosome release and angiogenesis stimulation.

Our findings show that dasatinib, like imatinib, is able to reduce exosome release from K562 CML cells. This was expected, since dasatinib targets many of the same protein kinases inhibited by imatinib. Exosomes isolated from dasatinib treated K562 cells were still able to induce tube formation *in vitro*. However, in contrast to imatinib treatment, dasatinib exposure blocked tubular differentiation in HUVECs incubated with exosomes. This inhibition was not correlated to impaired exosome internalization. These results suggest that targeting SFKs is important for endothelial cell activation by CML exosomes. The above-mentioned finding was supported by data showing that exosome treatment increased phospho-c-Src levels, and that dasatinib inhibited c-Src activation stimulated by exosomes.

The activation of c-Src as a consequence of exosome treatment is an important finding because Src can modulate angiogenesis in different ways. Src has been shown control expression of angiogenic growth factor and cytokines by regulating

their gene expression (297). Src can induce up regulation of VEGF or IL-8 expression (297, 298). Repression of Src down regulates the expression of these two factors resulting in decreased tumor vascular formation *in vivo* and *in vitro* (299, 300). Src can also elicit signaling in endothelial cells. Src can activate FAK, a protein that is involved in the control of cell motility and invasion (301). Here, it was showed that exosome treatment stimulated FAK phosphorylation at the site known to be phosphorylated by Src kinase (268). The levels of phosphorylation and the number of focal adhesions were reduced by dasatinib treatment. This indicates that dasatinib regulates FAK activity by selective inhibition of c-Src. This thesis suggests that dasatinib may also be active against CML because of its activity against c-Src, indicating Src as an important kinase for therapeutic intervention in CML. It has been recently reported that the c-Src inhibitor AZM475271 is able to inhibit tumor growth and metastasis of human pancreatic cancer in part for its anti-angiogenic activity (302). These new treatment could be proposed in association with imatinib to yield a more effective response against CML-associated angiogenesis. Alternatively, this compound could be administered in association with other drugs, especially in the case of resistance to the imatinib treatment.

In conclusion, this thesis shows for the first time that exosomes released by CML cells stimulate vascular cytoskeletal reorganization. We have characterized the uptake and relocalization of exosomes in activated endothelial cells, and demonstrated for the first time cell-to-cell exosome transfer. We showed that imatinib reduce exosome secretion and dasatinib targets both CML cells and endothelial cell response to CML exosome stimulation. Overall, this study suggests exosomes as a new target for CML therapy.

REFERENCES

1. Savage DG, Szydlo RM, Goldman JM. Clinical features at diagnosis in 430 patients with chronic myeloid leukaemia seen at a referral centre over a 16-year period. Br J Haematol 1997;96(1):111-116.
2. Kantarjian HM, Keating MJ, Talpaz M, Walters RS, Smith TL, Cork A, McCredie KB, Freireich EJ. Chronic myelogenous leukemia in blast crisis. Analysis of 242 patients. Am J Med 1987;83(3):445-454.
3. Nowell PC, Hungerford D.A. A minute chromosome in human chronic granulocytic leukemia. Science 1960;132:1497-1499.
4. Rowley JD. A new consistent chromosomal abnormality in chronic myelogenous leukemia identified by quinacrine fluorescence and Giemsa staining. Nature 1973;243:290-293.
5. Shtivelman E, Lifshitz B, Gale RP, Roe BA, Canaani E. Alternative splicing of RNAs transcribed from the human abl gene and from the bcr-abl fused gene. Cell 1986;47(2):277-284.
6. Pasternak G, Hochhaus A, Schultheis B, Hehlmann R. Chronic myelogenous leukemia: molecular and cellular aspects. J Cancer Res Clin Oncol 1998;124(12):643-660.
7. Melo JV. The diversity of BCR-ABL fusion proteins and their relationship to leukemia phenotype. Blood 1996;88(7):2375-2384.
8. Saglio G, Pane F, Martinelli G, Guerrasio A. BCR/ABL transcripts and leukemia phenotype: an unsolved puzzle. Leuk Lymphoma 1997;26(3-4):281-286.
9. Chissoe SL, Bodenteich A, Wang YF, Wang YP, Burian D, Clifton SW, Crabtree J, Freeman A, Iyer K, Jian L, et al. Sequence and analysis of the human ABL gene, the BCR gene, and regions involved in the Philadelphia chromosomal translocation. Genomics 1995;27(1):67-82.
10. McWhirter JR, Galasso DL, Wang JY. A coiled-coil oligomerization domain of Bcr is essential for the transforming function of Bcr-Abl oncoproteins. Mol Cell Biol 1993;13(12):7587-7595.
11. Groffen J, Stephenson JR, Heisterkamp N, de Klein A, Bartram CR, Grosveld G. Philadelphia chromosomal breakpoints are clustered within a limited region, bcr, on chromosome 22. Cell 1984;36(1):93-99.
12. Heisterkamp N, Stam K, Groffen J, de Klein A, Grosveld G. Structural organization of the bcr gene and its role in the Ph' translocation. Nature 1985;315(6022):758-761.
13. Shtivelman E, Lifshitz B, Gale RP, Canaani E. Fused transcript of abl and bcr genes in chronic myelogenous leukaemia. Nature 1985;315(6020):550-554.
14. Chan LC, Karhi KK, Rayter SI, Heisterkamp N, Eridani S, Powles R, Lawler SD, Groffen J, Foulkes JG, Greaves MF, et al. A novel abl protein expressed in Philadelphia chromosome positive acute lymphoblastic leukaemia. Nature 1987;325(6105):635-637.

15. Fainstein E, Marcelle C, Rosner A, Canaani E, Gale RP, Dreazen O, Smith SD, Croce CM. A new fused transcript in Philadelphia chromosome positive acute lymphocytic leukaemia. Nature 1987;330(6146):386-388.
16. Lugo TG, Pendergast AM, Muller AJ, Witte ON. Tyrosine kinase activity and transformation potency of bcr-abl oncogene products. Science 1990;247(4946):1079-1082.
17. Saglio G, Guerrasio A, Rosso C, Zaccaria A, Tassinari A, Serra A, Rege-Cambrin G, Mazza U, Gavosto F. New type of Bcr/Abl junction in Philadelphia chromosome-positive chronic myelogenous leukemia. Blood 1990;76(9):1819-1824.
18. Pane F, Frigeri F, Sindona M, Luciano L, Ferrara F, Cimino R, Meloni G, Saglio G, Salvatore F, Rotoli B. Neutrophilic-chronic myeloid leukemia: a distinct disease with a specific molecular marker (BCR/ABL with C3/A2 junction). Blood 1996;88(7):2410-2414.
19. Pendergast AM. The Abl family kinases: mechanisms of regulation and signaling. Adv Cancer Res 2002;85:51-100.
20. Scheijen B, Griffin JD. Tyrosine kinase oncogenes in normal hematopoiesis and hematological disease. Oncogene 2002;21(21):3314-3333.
21. Puil L, Liu J, Gish G, Mbamalu G, Bowtell D, Pelicci PG, Arlinghaus R, Pawson T. Bcr-Abl oncoproteins bind directly to activators of the Ras signalling pathway. EMBO J 1994;13(4):764-773.
22. McWhirter JR, Wang JY. An actin-binding function contributes to transformation by the Bcr-Abl oncoprotein of Philadelphia chromosome-positive human leukemias. EMBO J 1993;12(4):1533-1546.
23. Wen ST, Jackson PK, Van Etten RA. The cytostatic function of c-Abl is controlled by multiple nuclear localization signals and requires the p53 and Rb tumor suppressor gene products. EMBO J 1996;15(7):1583-1595.
24. Taagepera S, McDonald D, Loeb JE, Whitaker LL, McElroy AK, Wang JY, Hope TJ. Nuclear-cytoplasmic shuttling of C-ABL tyrosine kinase. Proc Natl Acad Sci U S A 1998;95(13):7457-7462.
25. Welch PJ, Wang JY. A C-terminal protein-binding domain in the retinoblastoma protein regulates nuclear c-Abl tyrosine kinase in the cell cycle. Cell 1993;75(4):779-790.
26. Baskaran R, Wood LD, Whitaker LL, Canman CE, Morgan SE, Xu Y, Barlow C, Baltimore D, Wynshaw-Boris A, Kastan MB, Wang JY. Ataxia telangiectasia mutant protein activates c-Abl tyrosine kinase in response to ionizing radiation. Nature 1997;387(6632):516-519.
27. Furstoss O, Dorey K, Simon V, Barila D, Superti-Furga G, Roche S. c-Abl is an effector of Src for growth factor-induced c-myc expression and DNA synthesis. EMBO J 2002;21(4):514-524.
28. Plattner R, Irvin BJ, Guo S, Blackburn K, Kazlauskas A, Abraham RT, York JD, Pendergast AM. A new link between the c-Abl tyrosine kinase and phosphoinositide signalling through PLC-gamma1. Nat Cell Biol 2003;5(4):309-319.

29. Plattner R, Koleske AJ, Kazlauskas A, Pendergast AM. Bidirectional signaling links the Abelson kinases to the platelet-derived growth factor receptor. Mol Cell Biol 2004;24(6):2573-2583.
30. Sawyers CL, McLaughlin J, Goga A, Havlik M, Witte O. The nuclear tyrosine kinase c-Abl negatively regulates cell growth. Cell 1994;77(1):121-131.
31. Wang JY. Regulation of cell death by the Abl tyrosine kinase. Oncogene 2000;19(49):5643-5650.
32. Barila D, Mangano R, Gonfloni S, Kretzschmar J, Moro M, Bohmann D, Superti-Furga G. A nuclear tyrosine phosphorylation circuit: c-Jun as an activator and substrate of c-Abl and JNK. EMBO J 2000;19(2):273-281.
33. Deininger MW, Druker BJ. Specific targeted therapy of chronic myelogenous leukemia with imatinib. Pharmacol Rev 2003;55(3):401-423.
34. Laurent E, Talpaz M, Kantarjian H, Kurzrock R. The BCR gene and philadelphia chromosome-positive leukemogenesis. Cancer Res 2001;61(6):2343-2355.
35. Maru Y, Witte ON. The BCR gene encodes a novel serine/threonine kinase activity within a single exon. Cell 1991;67(3):459-468.
36. Pendergast AM, Muller AJ, Havlik MH, Maru Y, Witte ON. BCR sequences essential for transformation by the BCR-ABL oncogene bind to the ABL SH2 regulatory domain in a non-phosphotyrosine-dependent manner. Cell 1991;66(1):161-171.
37. He Y, Wertheim JA, Xu L, Miller JP, Karnell FG, Choi JK, Ren R, Pear WS. The coiled-coil domain and Tyr177 of bcr are required to induce a murine chronic myelogenous leukemia-like disease by bcr/abl. Blood 2002;99(8):2957-2968.
38. Konopka JB, Witte ON. Detection of c-abl tyrosine kinase activity in vitro permits direct comparison of normal and altered abl gene products. Mol Cell Biol 1985;5(11):3116-3123.
39. McWhirter JR, Wang JY. Activation of tyrosinase kinase and microfilament-binding functions of c-abl by bcr sequences in bcr/abl fusion proteins. Mol Cell Biol 1991;11(3):1553-1565.
40. Cortez D, Kadlec L, Pendergast AM. Structural and signaling requirements for BCR-ABL-mediated transformation and inhibition of apoptosis. Mol Cell Biol 1995;15(10):5531-5541.
41. Goga A, McLaughlin J, Afar DE, Saffran DC, Witte ON. Alternative signals to RAS for hematopoietic transformation by the BCR-ABL oncogene. Cell 1995;82(6):981-988.
42. Sattler M, Mohi MG, Pride YB, Quinnan LR, Malouf NA, Podar K, Gesbert F, Iwasaki H, Li S, Van Etten RA, Gu H, Griffin JD, Neel BG. Critical role for Gab2 in transformation by BCR/ABL. Cancer Cell 2002;1(5):479-492.
43. Sawyers CL, McLaughlin J, Witte ON. Genetic requirement for Ras in the transformation of fibroblasts and hematopoietic cells by the Bcr-Abl oncogene. J Exp Med 1995;181(1):307-313.
44. Skorski T, Kanakaraj P, Ku DH, Nieborowska-Skorska M, Canaani E, Zon G, Perussia B, Calabretta B. Negative regulation of p120GAP GTPase promoting

activity by p210bcr/abl: implication for RAS-dependent Philadelphia chromosome positive cell growth. J Exp Med 1994;179(6):1855-1865.
45. Peters DG, Hoover RR, Gerlach MJ, Koh EY, Zhang H, Choe K, Kirschmeier P, Bishop WR, Daley GQ. Activity of the farnesyl protein transferase inhibitor SCH66336 against BCR/ABL-induced murine leukemia and primary cells from patients with chronic myeloid leukemia. Blood 2001;97(5):1404-1412.
46. Calabretta B, Perrotti D. The biology of CML blast crisis. Blood 2004;103(11):4010-4022.
47. Varticovski L, Daley GQ, Jackson P, Baltimore D, Cantley LC. Activation of phosphatidylinositol 3-kinase in cells expressing abl oncogene variants. Mol Cell Biol 1991;11(2):1107-1113.
48. Skorski T, Kanakaraj P, Nieborowska-Skorska M, Ratajczak MZ, Wen SC, Zon G, Gewirtz AM, Perussia B, Calabretta B. Phosphatidylinositol-3 kinase activity is regulated by BCR/ABL and is required for the growth of Philadelphia chromosome-positive cells. Blood 1995;86(2):726-736.
49. Jain SK, Susa M, Keeler ML, Carlesso N, Druker B, Varticovski L. PI 3-kinase activation in BCR/abl-transformed hematopoietic cells does not require interaction of p85 SH2 domains with p210 BCR/abl. Blood 1996;88(5):1542-1550.
50. Jain SK, Langdon WY, Varticovski L. Tyrosine phosphorylation of p120cbl in BCR/abl transformed hematopoietic cells mediates enhanced association with phosphatidylinositol 3-kinase. Oncogene 1997;14(18):2217-2228.
51. Skorski T, Bellacosa A, Nieborowska-Skorska M, Majewski M, Martinez R, Choi JK, Trotta R, Wlodarski P, Perrotti D, Chan TO, Wasik MA, Tsichlis PN, Calabretta B. Transformation of hematopoietic cells by BCR/ABL requires activation of a PI-3k/Akt-dependent pathway. EMBO J 1997;16(20):6151-6161.
52. Vivanco I, Sawyers CL. The phosphatidylinositol 3-Kinase AKT pathway in human cancer. Nat Rev Cancer 2002;2(7):489-501.
53. Datta SR, Dudek H, Tao X, Masters S, Fu H, Gotoh Y, Greenberg ME. Akt phosphorylation of BAD couples survival signals to the cell-intrinsic death machinery. Cell 1997;91(2):231-241.
54. Salomoni P, Condorelli F, Sweeney SM, Calabretta B. Versatility of BCR/ABL-expressing leukemic cells in circumventing proapoptotic BAD effects. Blood 2000;96(2):676-684.
55. Mayo LD, Donner DB. A phosphatidylinositol 3-kinase/Akt pathway promotes translocation of Mdm2 from the cytoplasm to the nucleus. Proc Natl Acad Sci U S A 2001;98(20):11598-11603.
56. Zhou BP, Liao Y, Xia W, Zou Y, Spohn B, Hung MC. HER-2/neu induces p53 ubiquitination via Akt-mediated MDM2 phosphorylation. Nat Cell Biol 2001;3(11):973-982.
57. Ozes ON, Mayo LD, Gustin JA, Pfeffer SR, Pfeffer LM, Donner DB. NF-kappaB activation by tumour necrosis factor requires the Akt serine-threonine kinase. Nature 1999;401(6748):82-85.
58. Silverman N, Maniatis T. NF-kappaB signaling pathways in mammalian and insect innate immunity. Genes Dev 2001;15(18):2321-2342.

59. Reuther JY, Reuther GW, Cortez D, Pendergast AM, Baldwin AS, Jr. A requirement for NF-kappaB activation in Bcr-Abl-mediated transformation. Genes Dev 1998;12(7):968-981.
60. Ghaffari S, Jagani Z, Kitidis C, Lodish HF, Khosravi-Far R. Cytokines and BCR-ABL mediate suppression of TRAIL-induced apoptosis through inhibition of forkhead FOXO3a transcription factor. Proc Natl Acad Sci U S A 2003;100(11):6523-6528.
61. Komatsu N, Watanabe T, Uchida M, Mori M, Kirito K, Kikuchi S, Liu Q, Tauchi T, Miyazawa K, Endo H, Nagai T, Ozawa K. A member of Forkhead transcription factor FKHRL1 is a downstream effector of STI571-induced cell cycle arrest in BCR-ABL-expressing cells. J Biol Chem 2003;278(8):6411-6419.
62. Shuai K, Halpern J, ten Hoeve J, Rao X, Sawyers CL. Constitutive activation of STAT5 by the BCR-ABL oncogene in chronic myelogenous leukemia. Oncogene 1996;13(2):247-254.
63. Ilaria RL, Jr., Van Etten RA. P210 and P190(BCR/ABL) induce the tyrosine phosphorylation and DNA binding activity of multiple specific STAT family members. J Biol Chem 1996;271(49):31704-31710.
64. Carlesso N, Frank DA, Griffin JD. Tyrosyl phosphorylation and DNA binding activity of signal transducers and activators of transcription (STAT) proteins in hematopoietic cell lines transformed by Bcr/Abl. J Exp Med 1996;183(3):811-820.
65. Frank DA, Varticovski L. BCR/abl leads to the constitutive activation of Stat proteins, and shares an epitope with tyrosine phosphorylated Stats. Leukemia 1996;10(11):1724-1730.
66. Klejman A, Schreiner SJ, Nieborowska-Skorska M, Slupianek A, Wilson M, Smithgall TE, Skorski T. The Src family kinase Hck couples BCR/ABL to STAT5 activation in myeloid leukemia cells. EMBO J 2002;21(21):5766-5774.
67. Horita M, Andreu EJ, Benito A, Arbona C, Sanz C, Benet I, Prosper F, Fernandez-Luna JL. Blockade of the Bcr-Abl kinase activity induces apoptosis of chronic myelogenous leukemia cells by suppressing signal transducer and activator of transcription 5-dependent expression of Bcl-xL. J Exp Med 2000;191(6):977-984.
68. Salgia R, Li JL, Lo SH, Brunkhorst B, Kansas GS, Sobhany ES, Sun Y, Pisick E, Hallek M, Ernst T, et al. Molecular cloning of human paxillin, a focal adhesion protein phosphorylated by P210BCR/ABL. J Biol Chem 1995;270(10):5039-5047.
69. Salgia R, Brunkhorst B, Pisick E, Li JL, Lo SH, Chen LB, Griffin JD. Increased tyrosine phosphorylation of focal adhesion proteins in myeloid cell lines expressing p210BCR/ABL. Oncogene 1995;11(6):1149-1155.
70. Bhatia R, McGlave PB, Dewald GW, Blazar BR, Verfaillie CM. Abnormal function of the bone marrow microenvironment in chronic myelogenous leukemia: role of malignant stromal macrophages. Blood 1995;85(12):3636-3645.
71. Upadhyaya G, Guba SC, Sih SA, Feinberg AP, Talpaz M, Kantarjian HM, Deisseroth AB, Emerson SG. Interferon-alpha restores the deficient expression of the cytoadhesion molecule lymphocyte function antigen-3 by chronic myelogenous leukemia progenitor cells. J Clin Invest 1991;88(6):2131-2136.

72. Daley GQ, Van Etten RA, Baltimore D. Induction of chronic myelogenous leukemia in mice by the P210bcr/abl gene of the Philadelphia chromosome. Science 1990;247(4944):824-830.
73. Huse M, Kuriyan J. The conformational plasticity of protein kinases. Cell 2002;109(3):275-282.
74. Druker BJ, Guilhot F, O'Brien SG, Gathmann I, Kantarjian H, Gattermann N, Deininger MW, Silver RT, Goldman JM, Stone RM, Cervantes F, Hochhaus A, Powell BL, Gabrilove JL, Rousselot P*, et al.* Five-year follow-up of patients receiving imatinib for chronic myeloid leukemia. N Engl J Med 2006;355(23):2408-2417.
75. Hochhaus A, Erben P, Ernst T, Mueller MC. Resistance to targeted therapy in chronic myelogenous leukemia. Semin Hematol 2007;44(1 Suppl 1):S15-24.
76. Litzow MR. Imatinib resistance: obstacles and opportunities. Arch Pathol Lab Med 2006;130(5):669-679.
77. O'Hare T, Eide CA, Deininger MW. Bcr-Abl kinase domain mutations, drug resistance, and the road to a cure for chronic myeloid leukemia. Blood 2007;110(7):2242-2249.
78. Shah NP, Nicoll JM, Nagar B, Gorre ME, Paquette RL, Kuriyan J, Sawyers CL. Multiple BCR-ABL kinase domain mutations confer polyclonal resistance to the tyrosine kinase inhibitor imatinib (STI571) in chronic phase and blast crisis chronic myeloid leukemia. Cancer Cell 2002;2(2):117-125.
79. Gorre ME, Mohammed M, Ellwood K, Hsu N, Paquette R, Rao PN, Sawyers CL. Clinical resistance to STI-571 cancer therapy caused by BCR-ABL gene mutation or amplification. Science 2001;293(5531):876-880.
80. Lowenberg B. Minimal residual disease in chronic myeloid leukemia. N Engl J Med 2003;349(15):1399-1401.
81. Corbin AS, La Rosee P, Stoffregen EP, Druker BJ, Deininger MW. Several Bcr-Abl kinase domain mutants associated with imatinib mesylate resistance remain sensitive to imatinib. Blood 2003;101(11):4611-4614.
82. Gambacorti-Passerini CB, Gunby RH, Piazza R, Galietta A, Rostagno R, Scapozza L. Molecular mechanisms of resistance to imatinib in Philadelphia-chromosome-positive leukaemias. Lancet Oncol 2003;4(2):75-85.
83. Nagar B, Bornmann WG, Pellicena P, Schindler T, Veach DR, Miller WT, Clarkson B, Kuriyan J. Crystal structures of the kinase domain of c-Abl in complex with the small molecule inhibitors PD173955 and imatinib (STI-571). Cancer Res 2002;62(15):4236-4243.
84. Hantschel O, Nagar B, Guettler S, Kretzschmar J, Dorey K, Kuriyan J, Superti-Furga G. A myristoyl/phosphotyrosine switch regulates c-Abl. Cell 2003;112(6):845-857.
85. Azam M, Latek RR, Daley GQ. Mechanisms of autoinhibition and STI-571/imatinib resistance revealed by mutagenesis of BCR-ABL. Cell 2003;112(6):831-843.
86. O'Hare T, Walters DK, Stoffregen EP, Jia T, Manley PW, Mestan J, Cowan-Jacob SW, Lee FY, Heinrich MC, Deininger MW, Druker BJ. In vitro activity of Bcr-Abl inhibitors AMN107 and BMS-354825 against clinically relevant

imatinib-resistant Abl kinase domain mutants. Cancer Res 2005;65(11):4500-4505.
87. Hochhaus A, Kreil S, Corbin AS, La Rosee P, Muller MC, Lahaye T, Hanfstein B, Schoch C, Cross NC, Berger U, Gschaidmeier H, Druker BJ, Hehlmann R. Molecular and chromosomal mechanisms of resistance to imatinib (STI571) therapy. Leukemia 2002;16(11):2190-2196.
88. Donato NJ, Wu JY, Stapley J, Gallick G, Lin H, Arlinghaus R, Talpaz M. BCR-ABL independence and LYN kinase overexpression in chronic myelogenous leukemia cells selected for resistance to STI571. Blood 2003;101(2):690-698.
89. Dai Y, Rahmani M, Corey SJ, Dent P, Grant S. A Bcr/Abl-independent, Lyn-dependent form of imatinib mesylate (STI-571) resistance is associated with altered expression of Bcl-2. J Biol Chem 2004;279(33):34227-34239.
90. Thomas J, Wang L, Clark RE, Pirmohamed M. Active transport of imatinib into and out of cells: implications for drug resistance. Blood 2004;104(12):3739-3745.
91. Lombardo LJ, Lee FY, Chen P, Norris D, Barrish JC, Behnia K, Castaneda S, Cornelius LA, Das J, Doweyko AM, Fairchild C, Hunt JT, Inigo I, Johnston K, Kamath A*, et al.* Discovery of N-(2-chloro-6-methyl- phenyl)-2-(6-(4-(2-hydroxyethyl)- piperazin-1-yl)-2-methylpyrimidin-4- ylamino)thiazole-5-carboxamide (BMS-354825), a dual Src/Abl kinase inhibitor with potent antitumor activity in preclinical assays. J Med Chem 2004;47(27):6658-6661.
92. Talpaz M, Shah NP, Kantarjian H, Donato N, Nicoll J, Paquette R, Cortes J, O'Brien S, Nicaise C, Bleickardt E, Blackwood-Chirchir MA, Iyer V, Chen TT, Huang F, Decillis AP*, et al.* Dasatinib in imatinib-resistant Philadelphia chromosome-positive leukemias. N Engl J Med 2006;354(24):2531-2541.
93. Shah NP, Tran C, Lee FY, Chen P, Norris D, Sawyers CL. Overriding imatinib resistance with a novel ABL kinase inhibitor. Science 2004;305(5682):399-401.
94. Weisberg E, Manley PW, Breitenstein W, Bruggen J, Cowan-Jacob SW, Ray A, Huntly B, Fabbro D, Fendrich G, Hall-Meyers E, Kung AL, Mestan J, Daley GQ, Callahan L, Catley L*, et al.* Characterization of AMN107, a selective inhibitor of native and mutant Bcr-Abl. Cancer Cell 2005;7(2):129-141.
95. Weisberg E, Manley P, Mestan J, Cowan-Jacob S, Ray A, Griffin JD. AMN107 (nilotinib): a novel and selective inhibitor of BCR-ABL. Br J Cancer 2006;94(12):1765-1769.
96. Quintas-Cardama A, Kantarjian H, Cortes J. Flying under the radar: the new wave of BCR-ABL inhibitors. Nat Rev Drug Discov 2007;6(10):834-848.
97. Kohn EC, Liotta LA. L651582: a novel antiproliferative and antimetastasis agent. J Natl Cancer Inst 1990;82(1):54-60.
98. Kohn EC, Sandeen MA, Liotta LA. In vivo efficacy of a novel inhibitor of selected signal transduction pathways including calcium, arachidonate, and inositol phosphates. Cancer Res 1992;52(11):3208-3212.
99. Alessandro R, Masiero L, Liotta LA, Kohn EC. The role of calcium in the regulation of invasion and angiogenesis. In Vivo 1996;10(2):153-160.

100. Guo L, Li ZS, Wang HL, Ye CY, Zhang DC. Carboxyamido-triazole inhibits proliferation of human breast cancer cells via G(2)/M cell cycle arrest and apoptosis. Eur J Pharmacol 2006;538(1-3):15-22.
101. Kohn EC, Alessandro R, Spoonster J, Wersto RP, Liotta LA. Angiogenesis: role of calcium-mediated signal transduction. Proc Natl Acad Sci U S A 1995;92(5):1307-1311.
102. Alessandro R, Fontana S, Giordano M, Corrado C, Colomba P, Flugy AM, Santoro A, Kohn EC, De Leo G. Effects of carboxyamidotriazole on in vitro models of imatinib-resistant chronic myeloid leukemia. J Cell Physiol 2008;215(1):111-121.
103. Majka M, Janowska-Wieczorek A, Ratajczak J, Ehrenman K, Pietrzkowski Z, Kowalska MA, Gewirtz AM, Emerson SG, Ratajczak MZ. Numerous growth factors, cytokines, and chemokines are secreted by human CD34(+) cells, myeloblasts, erythroblasts, and megakaryoblasts and regulate normal hematopoiesis in an autocrine/paracrine manner. Blood 2001;97(10):3075-3085.
104. Rustom A, Saffrich R, Markovic I, Walther P, Gerdes HH. Nanotubular highways for intercellular organelle transport. Science 2004;303(5660):1007-1010.
105. Heijnen HF, Schiel AE, Fijnheer R, Geuze HJ, Sixma JJ. Activated platelets release two types of membrane vesicles: microvesicles by surface shedding and exosomes derived from exocytosis of multivesicular bodies and alpha-granules. Blood 1999;94(11):3791-3799.
106. Camussi G, Deregibus MC, Bruno S, Cantaluppi V, Biancone L. Exosomes/microvesicles as a mechanism of cell-to-cell communication. Kidney Int.
107. Cocucci E, Racchetti G, Rupnik M, Meldolesi J. The regulated exocytosis of enlargeosomes is mediated by a SNARE machinery that includes VAMP4. J Cell Sci 2008;121(Pt 18):2983-2991.
108. Thery C, Zitvogel L, Amigorena S. Exosomes: composition, biogenesis and function. Nat Rev Immunol 2002;2(8):569-579.
109. Huber V, Fais S, Iero M, Lugini L, Canese P, Squarcina P, Zaccheddu A, Colone M, Arancia G, Gentile M, Seregni E, Valenti R, Ballabio G, Belli F, Leo E*, et al.* Human colorectal cancer cells induce T-cell death through release of proapoptotic microvesicles: role in immune escape. Gastroenterology 2005;128(7):1796-1804.
110. Andreola G, Rivoltini L, Castelli C, Huber V, Perego P, Deho P, Squarcina P, Accornero P, Lozupone F, Lugini L, Stringaro A, Molinari A, Arancia G, Gentile M, Parmiani G*, et al.* Induction of lymphocyte apoptosis by tumor cell secretion of FasL-bearing microvesicles. J Exp Med 2002;195(10):1303-1316.
111. Monleon I, Martinez-Lorenzo MJ, Monteagudo L, Lasierra P, Taules M, Iturralde M, Pineiro A, Larrad L, Alava MA, Naval J, Anel A. Differential secretion of Fas ligand- or APO2 ligand/TNF-related apoptosis-inducing ligand-carrying microvesicles during activation-induced death of human T cells. J Immunol 2001;167(12):6736-6744.

112. Poutsiaka DD, Schroder EW, Taylor DD, Levy EM, Black PH. Membrane vesicles shed by murine melanoma cells selectively inhibit the expression of Ia antigen by macrophages. J Immunol 1985;134(1):138-144.
113. Taylor DD, Gercel-Taylor C. Tumour-derived exosomes and their role in cancer-associated T-cell signalling defects. Br J Cancer 2005;92(2):305-311.
114. Mathivanan S, Ji H, Simpson RJ. Exosomes: extracellular organelles important in intercellular communication. J Proteomics;73(10):1907-1920.
115. Mathivanan S, Lim JW, Tauro BJ, Ji H, Moritz RL, Simpson RJ. Proteomics analysis of A33 immunoaffinity-purified exosomes released from the human colon tumor cell line LIM1215 reveals a tissue-specific protein signature. Mol Cell Proteomics;9(2):197-208.
116. Srivastava P. Interaction of heat shock proteins with peptides and antigen presenting cells: chaperoning of the innate and adaptive immune responses. Annu Rev Immunol 2002;20:395-425.
117. Savina A, Fader CM, Damiani MT, Colombo MI. Rab11 promotes docking and fusion of multivesicular bodies in a calcium-dependent manner. Traffic 2005;6(2):131-143.
118. Ostrowski M, Carmo NB, Krumeich S, Fanget I, Raposo G, Savina A, Moita CF, Schauer K, Hume AN, Freitas RP, Goud B, Benaroch P, Hacohen N, Fukuda M, Desnos C*, et al.* Rab27a and Rab27b control different steps of the exosome secretion pathway. Nat Cell Biol;12(1):19-30; sup pp 11-13.
119. Futter CE, White IJ. Annexins and endocytosis. Traffic 2007;8(8):951-958.
120. Zoller M. Tetraspanins: push and pull in suppressing and promoting metastasis. Nat Rev Cancer 2009;9(1):40-55.
121. Thery C, Amigorena S, Raposo G, Clayton A. Isolation and characterization of exosomes from cell culture supernatants and biological fluids. Curr Protoc Cell Biol 2006;Chapter 3:Unit 3 22.
122. Johnstone RM, Adam M, Hammond JR, Orr L, Turbide C. Vesicle formation during reticulocyte maturation. Association of plasma membrane activities with released vesicles (exosomes). J Biol Chem 1987;262(19):9412-9420.
123. Denzer K, van Eijk M, Kleijmeer MJ, Jakobson E, de Groot C, Geuze HJ. Follicular dendritic cells carry MHC class II-expressing microvesicles at their surface. J Immunol 2000;165(3):1259-1265.
124. Mobius W, Ohno-Iwashita Y, van Donselaar EG, Oorschot VM, Shimada Y, Fujimoto T, Heijnen HF, Geuze HJ, Slot JW. Immunoelectron microscopic localization of cholesterol using biotinylated and non-cytolytic perfringolysin O. J Histochem Cytochem 2002;50(1):43-55.
125. Saksena S, Sun J, Chu T, Emr SD. ESCRTing proteins in the endocytic pathway. Trends Biochem Sci 2007;32(12):561-573.
126. Williams RL, Urbe S. The emerging shape of the ESCRT machinery. Nat Rev Mol Cell Biol 2007;8(5):355-368.
127. Pisitkun T, Shen RF, Knepper MA. Identification and proteomic profiling of exosomes in human urine. Proc Natl Acad Sci U S A 2004;101(36):13368-13373.
128. Hurley JH. ESCRT complexes and the biogenesis of multivesicular bodies. Curr Opin Cell Biol 2008;20(1):4-11.

129. Babst M. A protein's final ESCRT. Traffic 2005;6(1):2-9.
130. Trajkovic K, Hsu C, Chiantia S, Rajendran L, Wenzel D, Wieland F, Schwille P, Brugger B, Simons M. Ceramide triggers budding of exosome vesicles into multivesicular endosomes. Science 2008;319(5867):1244-1247.
131. Fang Y, Wu N, Gan X, Yan W, Morrell JC, Gould SJ. Higher-order oligomerization targets plasma membrane proteins and HIV gag to exosomes. PLoS Biol 2007;5(6):e158.
132. Zhang F, Sun S, Feng D, Zhao WL, Sui SF. A novel strategy for the invasive toxin: hijacking exosome-mediated intercellular trafficking. Traffic 2009;10(4):411-424.
133. Bianco F, Perrotta C, Novellino L, Francolini M, Riganti L, Menna E, Saglietti L, Schuchman EH, Furlan R, Clementi E, Matteoli M, Verderio C. Acid sphingomyelinase activity triggers microparticle release from glial cells. EMBO J 2009;28(8):1043-1054.
134. Goni FM, Alonso A. Biophysics of sphingolipids I. Membrane properties of sphingosine, ceramides and other simple sphingolipids. Biochim Biophys Acta 2006;1758(12):1902-1921.
135. Vidal M, Mangeat P, Hoekstra D. Aggregation reroutes molecules from a recycling to a vesicle-mediated secretion pathway during reticulocyte maturation. J Cell Sci 1997;110 (Pt 16):1867-1877.
136. Muntasell A, Berger AC, Roche PA. T cell-induced secretion of MHC class II-peptide complexes on B cell exosomes. EMBO J 2007;26(19):4263-4272.
137. Baumgart T, Hess ST, Webb WW. Imaging coexisting fluid domains in biomembrane models coupling curvature and line tension. Nature 2003;425(6960):821-824.
138. Theos AC, Truschel ST, Tenza D, Hurbain I, Harper DC, Berson JF, Thomas PC, Raposo G, Marks MS. A lumenal domain-dependent pathway for sorting to intralumenal vesicles of multivesicular endosomes involved in organelle morphogenesis. Dev Cell 2006;10(3):343-354.
139. van Niel G, Porto-Carreiro I, Simoes S, Raposo G. Exosomes: a common pathway for a specialized function. J Biochem 2006;140(1):13-21.
140. Andrews NW, Chakrabarti S. There's more to life than neurotransmission: the regulation of exocytosis by synaptotagmin VII. Trends Cell Biol 2005;15(11):626-631.
141. Savina A, Furlan M, Vidal M, Colombo MI. Exosome release is regulated by a calcium-dependent mechanism in K562 cells. J Biol Chem 2003;278(22):20083-20090.
142. Stoeck A, Keller S, Riedle S, Sanderson MP, Runz S, Le Naour F, Gutwein P, Ludwig A, Rubinstein E, Altevogt P. A role for exosomes in the constitutive and stimulus-induced ectodomain cleavage of L1 and CD44. Biochem J 2006;393(Pt 3):609-618.
143. Valadi H, Ekstrom K, Bossios A, Sjostrand M, Lee JJ, Lotvall JO. Exosome-mediated transfer of mRNAs and microRNAs is a novel mechanism of genetic exchange between cells. Nat Cell Biol 2007;9(6):654-659.
144. Raposo G, Tenza D, Mecheri S, Peronet R, Bonnerot C, Desaymard C. Accumulation of major histocompatibility complex class II molecules in mast cell

secretory granules and their release upon degranulation. Mol Biol Cell 1997;8(12):2631-2645.
145. Faure J, Lachenal G, Court M, Hirrlinger J, Chatellard-Causse C, Blot B, Grange J, Schoehn G, Goldberg Y, Boyer V, Kirchhoff F, Raposo G, Garin J, Sadoul R. Exosomes are released by cultured cortical neurones. Mol Cell Neurosci 2006;31(4):642-648.
146. Yu X, Harris SL, Levine AJ. The regulation of exosome secretion: a novel function of the p53 protein. Cancer Res 2006;66(9):4795-4801.
147. Losche W, Scholz T, Temmler U, Oberle V, Claus RA. Platelet-derived microvesicles transfer tissue factor to monocytes but not to neutrophils. Platelets 2004;15(2):109-115.
148. Gasser O, Hess C, Miot S, Deon C, Sanchez JC, Schifferli JA. Characterisation and properties of ectosomes released by human polymorphonuclear neutrophils. Exp Cell Res 2003;285(2):243-257.
149. Eken C, Gasser O, Zenhaeusern G, Oehri I, Hess C, Schifferli JA. Polymorphonuclear neutrophil-derived ectosomes interfere with the maturation of monocyte-derived dendritic cells. J Immunol 2008;180(2):817-824.
150. Pluskota E, Woody NM, Szpak D, Ballantyne CM, Soloviev DA, Simon DI, Plow EF. Expression, activation, and function of integrin alphaMbeta2 (Mac-1) on neutrophil-derived microparticles. Blood 2008;112(6):2327-2335.
151. Gasser O, Schifferli JA. Activated polymorphonuclear neutrophils disseminate anti-inflammatory microparticles by ectocytosis. Blood 2004;104(8):2543-2548.
152. Ratajczak J, Wysoczynski M, Hayek F, Janowska-Wieczorek A, Ratajczak MZ. Membrane-derived microvesicles: important and underappreciated mediators of cell-to-cell communication. Leukemia 2006;20(9):1487-1495.
153. Zwaal RF, Comfurius P, Bevers EM. Scott syndrome, a bleeding disorder caused by defective scrambling of membrane phospholipids. Biochim Biophys Acta 2004;1636(2-3):119-128.
154. Polgar J, Matuskova J, Wagner DD. The P-selectin, tissue factor, coagulation triad. J Thromb Haemost 2005;3(8):1590-1596.
155. Andrews RK, Berndt MC. Platelet physiology and thrombosis. Thromb Res 2004;114(5-6):447-453.
156. Quah BJ, Barlow VP, McPhun V, Matthaei KI, Hulett MD, Parish CR. Bystander B cells rapidly acquire antigen receptors from activated B cells by membrane transfer. Proc Natl Acad Sci U S A 2008;105(11):4259-4264.
157. Barry OP, Pratico D, Savani RC, FitzGerald GA. Modulation of monocyte-endothelial cell interactions by platelet microparticles. J Clin Invest 1998;102(1):136-144.
158. Janowska-Wieczorek A, Majka M, Kijowski J, Baj-Krzyworzeka M, Reca R, Turner AR, Ratajczak J, Emerson SG, Kowalska MA, Ratajczak MZ. Platelet-derived microparticles bind to hematopoietic stem/progenitor cells and enhance their engraftment. Blood 2001;98(10):3143-3149.
159. Kim JW, Wieckowski E, Taylor DD, Reichert TE, Watkins S, Whiteside TL. Fas ligand-positive membranous vesicles isolated from sera of patients with oral

cancer induce apoptosis of activated T lymphocytes. Clin Cancer Res 2005;11(3):1010-1020.
160. Al-Nedawi K, Meehan B, Micallef J, Lhotak V, May L, Guha A, Rak J. Intercellular transfer of the oncogenic receptor EGFRvIII by microvesicles derived from tumour cells. Nat Cell Biol 2008;10(5):619-624.
161. Sarkar A, Mitra S, Mehta S, Raices R, Wewers MD. Monocyte derived microvesicles deliver a cell death message via encapsulated caspase-1. PLoS One 2009;4(9):e7140.
162. Fackler OT, Peterlin BM. Endocytic entry of HIV-1. Curr Biol 2000;10(16):1005-1008.
163. Fevrier B, Vilette D, Archer F, Loew D, Faigle W, Vidal M, Laude H, Raposo G. Cells release prions in association with exosomes. Proc Natl Acad Sci U S A 2004;101(26):9683-9688.
164. Skog J, Wurdinger T, van Rijn S, Meijer DH, Gainche L, Sena-Esteves M, Curry WT, Jr., Carter BS, Krichevsky AM, Breakefield XO. Glioblastoma microvesicles transport RNA and proteins that promote tumour growth and provide diagnostic biomarkers. Nat Cell Biol 2008;10(12):1470-1476.
165. Hunter MP, Ismail N, Zhang X, Aguda BD, Lee EJ, Yu L, Xiao T, Schafer J, Lee ML, Schmittgen TD, Nana-Sinkam SP, Jarjoura D, Marsh CB. Detection of microRNA expression in human peripheral blood microvesicles. PLoS One 2008;3(11):e3694.
166. Deregibus MC, Cantaluppi V, Calogero R, Lo Iacono M, Tetta C, Biancone L, Bruno S, Bussolati B, Camussi G. Endothelial progenitor cell derived microvesicles activate an angiogenic program in endothelial cells by a horizontal transfer of mRNA. Blood 2007;110(7):2440-2448.
167. Baj-Krzyworzeka M, Szatanek R, Weglarczyk K, Baran J, Urbanowicz B, Branski P, Ratajczak MZ, Zembala M. Tumour-derived microvesicles carry several surface determinants and mRNA of tumour cells and transfer some of these determinants to monocytes. Cancer Immunol Immunother 2006;55(7):808-818.
168. Wolfers J, Lozier A, Raposo G, Regnault A, Thery C, Masurier C, Flament C, Pouzieux S, Faure F, Tursz T, Angevin E, Amigorena S, Zitvogel L. Tumor-derived exosomes are a source of shared tumor rejection antigens for CTL cross-priming. Nat Med 2001;7(3):297-303.
169. Andre F, Schartz NE, Movassagh M, Flament C, Pautier P, Morice P, Pomel C, Lhomme C, Escudier B, Le Chevalier T, Tursz T, Amigorena S, Raposo G, Angevin E, Zitvogel L. Malignant effusions and immunogenic tumour-derived exosomes. Lancet 2002;360(9329):295-305.
170. Luketic L, Delanghe J, Sobol PT, Yang P, Frotten E, Mossman KL, Gauldie J, Bramson J, Wan Y. Antigen presentation by exosomes released from peptide-pulsed dendritic cells is not suppressed by the presence of active CTL. J Immunol 2007;179(8):5024-5032.
171. Admyre C, Johansson SM, Paulie S, Gabrielsson S. Direct exosome stimulation of peripheral human T cells detected by ELISPOT. Eur J Immunol 2006;36(7):1772-1781.

172. Utsugi-Kobukai S, Fujimaki H, Hotta C, Nakazawa M, Minami M. MHC class I-mediated exogenous antigen presentation by exosomes secreted from immature and mature bone marrow derived dendritic cells. Immunol Lett 2003;89(2-3):125-131.
173. Hsu DH, Paz P, Villaflor G, Rivas A, Mehta-Damani A, Angevin E, Zitvogel L, Le Pecq JB. Exosomes as a tumor vaccine: enhancing potency through direct loading of antigenic peptides. J Immunother 2003;26(5):440-450.
174. Chaput N, Schartz NE, Andre F, Taieb J, Novault S, Bonnaventure P, Aubert N, Bernard J, Lemonnier F, Merad M, Adema G, Adams M, Ferrantini M, Carpentier AF, Escudier B*, et al.* Exosomes as potent cell-free peptide-based vaccine. II. Exosomes in CpG adjuvants efficiently prime naive Tc1 lymphocytes leading to tumor rejection. J Immunol 2004;172(4):2137-2146.
175. Raposo G, Nijman HW, Stoorvogel W, Liejendekker R, Harding CV, Melief CJ, Geuze HJ. B lymphocytes secrete antigen-presenting vesicles. J Exp Med 1996;183(3):1161-1172.
176. Thery C, Regnault A, Garin J, Wolfers J, Zitvogel L, Ricciardi-Castagnoli P, Raposo G, Amigorena S. Molecular characterization of dendritic cell-derived exosomes. Selective accumulation of the heat shock protein hsc73. J Cell Biol 1999;147(3):599-610.
177. Segura E, Nicco C, Lombard B, Veron P, Raposo G, Batteux F, Amigorena S, Thery C. ICAM-1 on exosomes from mature dendritic cells is critical for efficient naive T-cell priming. Blood 2005;106(1):216-223.
178. Thery C, Duban L, Segura E, Veron P, Lantz O, Amigorena S. Indirect activation of naive CD4+ T cells by dendritic cell-derived exosomes. Nat Immunol 2002;3(12):1156-1162.
179. Ryan GB, Majno G. Acute inflammation. A review. Am J Pathol 1977;86(1):183-276.
180. Koppler B, Cohen C, Schlondorff D, Mack M. Differential mechanisms of microparticle transfer toB cells and monocytes: anti-inflammatory propertiesof microparticles. Eur J Immunol 2006;36(3):648-660.
181. Distler JH, Pisetsky DS, Huber LC, Kalden JR, Gay S, Distler O. Microparticles as regulators of inflammation: novel players of cellular crosstalk in the rheumatic diseases. Arthritis Rheum 2005;52(11):3337-3348.
182. Kim HK, Song KS, Park YS, Kang YH, Lee YJ, Lee KR, Ryu KW, Bae JM, Kim S. Elevated levels of circulating platelet microparticles, VEGF, IL-6 and RANTES in patients with gastric cancer: possible role of a metastasis predictor. Eur J Cancer 2003;39(2):184-191.
183. Ginestra A, La Placa MD, Saladino F, Cassara D, Nagase H, Vittorelli ML. The amount and proteolytic content of vesicles shed by human cancer cell lines correlates with their in vitro invasiveness. Anticancer Res 1998;18(5A):3433-3437.
184. Gutwein P, Mechtersheimer S, Riedle S, Stoeck A, Gast D, Joumaa S, Zentgraf H, Fogel M, Altevogt DP. ADAM10-mediated cleavage of L1 adhesion molecule at the cell surface and in released membrane vesicles. FASEB J 2003;17(2):292-294.

185. Millimaggi D, Festuccia C, Angelucci A, D'Ascenzo S, Rucci N, Flati S, Bologna M, Teti A, Pavan A, Dolo V. Osteoblast-conditioned media stimulate membrane vesicle shedding in prostate cancer cells. Int J Oncol 2006;28(4):909-914.
186. Giusti I, D'Ascenzo S, Millimaggi D, Taraboletti G, Carta G, Franceschini N, Pavan A, Dolo V. Cathepsin B mediates the pH-dependent proinvasive activity of tumor-shed microvesicles. Neoplasia 2008;10(5):481-488.
187. Taraboletti G, D'Ascenzo S, Borsotti P, Giavazzi R, Pavan A, Dolo V. Shedding of the matrix metalloproteinases MMP-2, MMP-9, and MT1-MMP as membrane vesicle-associated components by endothelial cells. Am J Pathol 2002;160(2):673-680.
188. Albanese J, Meterissian S, Kontogiannea M, Dubreuil C, Hand A, Sorba S, Dainiak N. Biologically active Fas antigen and its cognate ligand are expressed on plasma membrane-derived extracellular vesicles. Blood 1998;91(10):3862-3874.
189. Szajnik M, Czystowska M, Szczepanski MJ, Mandapathil M, Whiteside TL. Tumor-derived microvesicles induce, expand and up-regulate biological activities of human regulatory T cells (Treg). PLoS One;5(7):e11469.
190. Shedden K, Xie XT, Chandaroy P, Chang YT, Rosania GR. Expulsion of small molecules in vesicles shed by cancer cells: association with gene expression and chemosensitivity profiles. Cancer Res 2003;63(15):4331-4337.
191. Folkman J, Shing Y. Angiogenesis. J Biol Chem 1992;267(16):10931-10934.
192. Hanahan D, Weinberg RA. The hallmarks of cancer. Cell 2000;100(1):57-70.
193. Kerbel RS. Tumor angiogenesis: past, present and the near future. Carcinogenesis 2000;21(3):505-515.
194. Moses MA. The regulation of neovascularization of matrix metalloproteinases and their inhibitors. Stem Cells 1997;15(3):180-189.
195. Hirschi KK, D'Amore PA. Pericytes in the microvasculature. Cardiovasc Res 1996;32(4):687-698.
196. Grant DS, Kleinman HK. Regulation of capillary formation by laminin and other components of the extracellular matrix. EXS 1997;79:317-333.
197. Ferrara N. Vascular endothelial growth factor: molecular and biological aspects. Curr Top Microbiol Immunol 1999;237:1-30.
198. Ogawa S, Oku A, Sawano A, Yamaguchi S, Yazaki Y, Shibuya M. A novel type of vascular endothelial growth factor, VEGF-E (NZ-7 VEGF), preferentially utilizes KDR/Flk-1 receptor and carries a potent mitotic activity without heparin-binding domain. J Biol Chem 1998;273(47):31273-31282.
199. Eriksson U, Alitalo K. Structure, expression and receptor-binding properties of novel vascular endothelial growth factors. Curr Top Microbiol Immunol 1999;237:41-57.
200. Persico MG, Vincenti V, DiPalma T. Structure, expression and receptor-binding properties of placenta growth factor (PlGF). Curr Top Microbiol Immunol 1999;237:31-40.

201. Meyer M, Clauss M, Lepple-Wienhues A, Waltenberger J, Augustin HG, Ziche M, Lanz C, Buttner M, Rziha HJ, Dehio C. A novel vascular endothelial growth factor encoded by Orf virus, VEGF-E, mediates angiogenesis via signalling through VEGFR-2 (KDR) but not VEGFR-1 (Flt-1) receptor tyrosine kinases. EMBO J 1999;18(2):363-374.
202. Houck KA, Ferrara N, Winer J, Cachianes G, Li B, Leung DW. The vascular endothelial growth factor family: identification of a fourth molecular species and characterization of alternative splicing of RNA. Mol Endocrinol 1991;5(12):1806-1814.
203. Houck KA, Leung DW, Rowland AM, Winer J, Ferrara N. Dual regulation of vascular endothelial growth factor bioavailability by genetic and proteolytic mechanisms. J Biol Chem 1992;267(36):26031-26037.
204. Tischer E, Mitchell R, Hartman T, Silva M, Gospodarowicz D, Fiddes JC, Abraham JA. The human gene for vascular endothelial growth factor. Multiple protein forms are encoded through alternative exon splicing. J Biol Chem 1991;266(18):11947-11954.
205. Dumont DJ, Fong GH, Puri MC, Gradwohl G, Alitalo K, Breitman ML. Vascularization of the mouse embryo: a study of flk-1, tek, tie, and vascular endothelial growth factor expression during development. Dev Dyn 1995;203(1):80-92.
206. Berse B, Brown LF, Van de Water L, Dvorak HF, Senger DR. Vascular permeability factor (vascular endothelial growth factor) gene is expressed differentially in normal tissues, macrophages, and tumors. Mol Biol Cell 1992;3(2):211-220.
207. Damert A, Machein M, Breier G, Fujita MQ, Hanahan D, Risau W, Plate KH. Up-regulation of vascular endothelial growth factor expression in a rat glioma is conferred by two distinct hypoxia-driven mechanisms. Cancer Res 1997;57(17):3860-3864.
208. Shibuya M, Ito N, Claesson-Welsh L. Structure and function of vascular endothelial growth factor receptor-1 and -2. Curr Top Microbiol Immunol 1999;237:59-83.
209. Korpelainen EI, Alitalo K. Signaling angiogenesis and lymphangiogenesis. Curr Opin Cell Biol 1998;10(2):159-164.
210. Heldin CH. Dimerization of cell surface receptors in signal transduction. Cell 1995;80(2):213-223.
211. Cunningham SA, Arrate MP, Brock TA, Waxham MN. Interactions of FLT-1 and KDR with phospholipase C gamma: identification of the phosphotyrosine binding sites. Biochem Biophys Res Commun 1997;240(3):635-639.
212. Sawano A, Takahashi T, Yamaguchi S, Shibuya M. The phosphorylated 1169-tyrosine containing region of flt-1 kinase (VEGFR-1) is a major binding site for PLCgamma. Biochem Biophys Res Commun 1997;238(2):487-491.
213. Dougher-Vermazen M, Hulmes JD, Bohlen P, Terman BI. Biological activity and phosphorylation sites of the bacterially expressed cytosolic domain of the KDR VEGF-receptor. Biochem Biophys Res Commun 1994;205(1):728-738.
214. Ito N, Wernstedt C, Engstrom U, Claesson-Welsh L. Identification of vascular endothelial growth factor receptor-1 tyrosine phosphorylation sites and

binding of SH2 domain-containing molecules. J Biol Chem 1998;273(36):23410-23418.
215. Takahashi T, Ueno H, Shibuya M. VEGF activates protein kinase C-dependent, but Ras-independent Raf-MEK-MAP kinase pathway for DNA synthesis in primary endothelial cells. Oncogene 1999;18(13):2221-2230.
216. Schonwasser DC, Marais RM, Marshall CJ, Parker PJ. Activation of the mitogen-activated protein kinase/extracellular signal-regulated kinase pathway by conventional, novel, and atypical protein kinase C isotypes. Mol Cell Biol 1998;18(2):790-798.
217. Rousseau S, Houle F, Landry J, Huot J. p38 MAP kinase activation by vascular endothelial growth factor mediates actin reorganization and cell migration in human endothelial cells. Oncogene 1997;15(18):2169-2177.
218. Matsumoto T, Claesson-Welsh L. VEGF receptor signal transduction. Sci STKE 2001;2001(112):re21.
219. Nishimura T, Utsunomiya Y, Hoshikawa M, Ohuchi H, Itoh N. Structure and expression of a novel human FGF, FGF-19, expressed in the fetal brain. Biochim Biophys Acta 1999;1444(1):148-151.
220. Spivak-Kroizman T, Lemmon MA, Dikic I, Ladbury JE, Pinchasi D, Huang J, Jaye M, Crumley G, Schlessinger J, Lax I. Heparin-induced oligomerization of FGF molecules is responsible for FGF receptor dimerization, activation, and cell proliferation. Cell 1994;79(6):1015-1024.
221. Friesel RE, Maciag T. Molecular mechanisms of angiogenesis: fibroblast growth factor signal transduction. FASEB J 1995;9(10):919-925.
222. Partanen J, Vainikka S, Korhonen J, Armstrong E, Alitalo K. Diverse receptors for fibroblast growth factors. Prog Growth Factor Res 1992;4(1):69-83.
223. Peters KG, Werner S, Chen G, Williams LT. Two FGF receptor genes are differentially expressed in epithelial and mesenchymal tissues during limb formation and organogenesis in the mouse. Development 1992;114(1):233-243.
224. Kanda S, Landgren E, Ljungstrom M, Claesson-Welsh L. Fibroblast growth factor receptor 1-induced differentiation of endothelial cell line established from tsA58 large T transgenic mice. Cell Growth Differ 1996;7(3):383-395.
225. Bastaki M, Nelli EE, Dell'Era P, Rusnati M, Molinari-Tosatti MP, Parolini S, Auerbach R, Ruco LP, Possati L, Presta M. Basic fibroblast growth factor-induced angiogenic phenotype in mouse endothelium. A study of aortic and microvascular endothelial cell lines. Arterioscler Thromb Vasc Biol 1997;17(3):454-464.
226. Kan M, Wang F, Xu J, Crabb JW, Hou J, McKeehan WL. An essential heparin-binding domain in the fibroblast growth factor receptor kinase. Science 1993;259(5103):1918-1921.
227. Guimond S, Maccarana M, Olwin BB, Lindahl U, Rapraeger AC. Activating and inhibitory heparin sequences for FGF-2 (basic FGF). Distinct requirements for FGF-1, FGF-2, and FGF-4. J Biol Chem 1993;268(32):23906-23914.
228. Mohammadi M, Dikic I, Sorokin A, Burgess WH, Jaye M, Schlessinger J. Identification of six novel autophosphorylation sites on fibroblast growth factor receptor 1 and elucidation of their importance in receptor activation and signal transduction. Mol Cell Biol 1996;16(3):977-989.

229. Klint P, Claesson-Welsh L. Signal transduction by fibroblast growth factor receptors. Front Biosci 1999;4:D165-177.
230. Su N, Du X, Chen L. FGF signaling: its role in bone development and human skeleton diseases. Front Biosci 2008;13:2842-2865.
231. Folkman J. Role of angiogenesis in tumor growth and metastasis. Semin Oncol 2002;29(6 Suppl 16):15-18.
232. Carmeliet P, Jain RK. Angiogenesis in cancer and other diseases. Nature 2000;407(6801):249-257.
233. Voss MJ, Niggemann B, Zanker KS, Entschladen F. Tumour reactions to hypoxia. Curr Mol Med;10(4):381-386.
234. Baish JW, Jain RK. Fractals and cancer. Cancer Res 2000;60(14):3683-3688.
235. Helmlinger G, Yuan F, Dellian M, Jain RK. Interstitial pH and pO2 gradients in solid tumors in vivo: high-resolution measurements reveal a lack of correlation. Nat Med 1997;3(2):177-182.
236. Giaccia AJ. Hypoxic Stress Proteins: Survival of the Fittest. Semin Radiat Oncol 1996;6(1):46-58.
237. Hobbs SK, Monsky WL, Yuan F, Roberts WG, Griffith L, Torchilin VP, Jain RK. Regulation of transport pathways in tumor vessels: role of tumor type and microenvironment. Proc Natl Acad Sci U S A 1998;95(8):4607-4612.
238. Hashizume H, Baluk P, Morikawa S, McLean JW, Thurston G, Roberge S, Jain RK, McDonald DM. Openings between defective endothelial cells explain tumor vessel leakiness. Am J Pathol 2000;156(4):1363-1380.
239. Dvorak HF, Nagy JA, Feng D, Brown LF, Dvorak AM. Vascular permeability factor/vascular endothelial growth factor and the significance of microvascular hyperpermeability in angiogenesis. Curr Top Microbiol Immunol 1999;237:97-132.
240. Jain RK, Koenig GC, Dellian M, Fukumura D, Munn LL, Melder RJ. Leukocyte-endothelial adhesion and angiogenesis in tumors. Cancer Metastasis Rev 1996;15(2):195-204.
241. Kleinman HK, Martin GR. Matrigel: basement membrane matrix with biological activity. Semin Cancer Biol 2005;15(5):378-386.
242. Kalluri R. Basement membranes: structure, assembly and role in tumour angiogenesis. Nat Rev Cancer 2003;3(6):422-433.
243. Hallmann R, Horn N, Selg M, Wendler O, Pausch F, Sorokin LM. Expression and function of laminins in the embryonic and mature vasculature. Physiol Rev 2005;85(3):979-1000.
244. Kubota Y, Kleinman HK, Martin GR, Lawley TJ. Role of laminin and basement membrane in the morphological differentiation of human endothelial cells into capillary-like structures. J Cell Biol 1988;107(4):1589-1598.
245. Marneros AG, Olsen BR. The role of collagen-derived proteolytic fragments in angiogenesis. Matrix Biol 2001;20(5-6):337-345.
246. Sanz L, Alvarez-Vallina L. The extracellular matrix: a new turn-of-the-screw for anti-angiogenic strategies. Trends Mol Med 2003;9(6):256-262.
247. Rundhaug JE. Matrix metalloproteinases and angiogenesis. J Cell Mol Med 2005;9(2):267-285.

248. Segev A, Nili N, Strauss BH. The role of perlecan in arterial injury and angiogenesis. Cardiovasc Res 2004;63(4):603-610.
249. Scheele S, Nystrom A, Durbeej M, Talts JF, Ekblom M, Ekblom P. Laminin isoforms in development and disease. J Mol Med 2007;85(8):825-836.
250. Miner JH. Laminins and their roles in mammals. Microsc Res Tech 2008;71(5):349-356.
251. de Vega S, Iwamoto T, Yamada Y. Fibulins: multiple roles in matrix structures and tissue functions. Cell Mol Life Sci 2009;66(11-12):1890-1902.
252. Auerbach R, Lewis R, Shinners B, Kubai L, Akhtar N. Angiogenesis assays: a critical overview. Clin Chem 2003;49(1):32-40.
253. Browning AC, Dua HS, Amoaku WM. The effects of growth factors on the proliferation and in vitro angiogenesis of human macular inner choroidal endothelial cells. Br J Ophthalmol 2008;92(7):1003-1008.
254. Benelli R, Albini A. In vitro models of angiogenesis: the use of Matrigel. Int J Biol Markers 1999;14(4):243-246.
255. Albini A, Benelli R. The chemoinvasion assay: a method to assess tumor and endothelial cell invasion and its modulation. Nat Protoc 2007;2(3):504-511.
256. Koh W, Stratman AN, Sacharidou A, Davis GE. In vitro three dimensional collagen matrix models of endothelial lumen formation during vasculogenesis and angiogenesis. Methods Enzymol 2008;443:83-101.
257. Grove AD, Prabhu VV, Young BL, Lee FC, Kulpa V, Munson PJ, Kohn EC. Both protein activation and gene expression are involved in early vascular tube formation in vitro. Clin Cancer Res 2002;8(9):3019-3026.
258. Folkman J. Tumor angiogenesis: therapeutic implications. N Engl J Med 1971;285(21):1182-1186.
259. Folkman J. Angiogenesis in cancer, vascular, rheumatoid and other disease. Nat Med 1995;1(1):27-31.
260. Ellis LM, Fidler IJ. Angiogenesis and metastasis. Eur J Cancer 1996;32A(14):2451-2460.
261. Aguayo A, Kantarjian H, Manshouri T, Gidel C, Estey E, Thomas D, Koller C, Estrov Z, O'Brien S, Keating M, Freireich E, Albitar M. Angiogenesis in acute and chronic leukemias and myelodysplastic syndromes. Blood 2000;96(6):2240-2245.
262. Bellamy WT, Richter L, Frutiger Y, Grogan TM. Expression of vascular endothelial growth factor and its receptors in hematopoietic malignancies. Cancer Res 1999;59(3):728-733.
263. Legros L, Bourcier C, Jacquel A, Mahon FX, Cassuto JP, Auberger P, Pages G. Imatinib mesylate (STI571) decreases the vascular endothelial growth factor plasma concentration in patients with chronic myeloid leukemia. Blood 2004;104(2):495-501.
264. Li L, Zhang R, Fang ZY, Chen JN, Zhu ZL. Suppression of vascular endothelial growth factor (VEGF) expression by targeting the Bcr-Abl oncogene and protein tyrosine kinase activity in Bcr-Abl-positive leukaemia cells. J Int Med Res 2009;37(2):426-437.

265. Schindler T, Bornmann W, Pellicena P, Miller WT, Clarkson B, Kuriyan J. Structural mechanism for STI-571 inhibition of abelson tyrosine kinase. Science 2000;289(5486):1938-1942.
266. Druker BJ, Tamura S, Buchdunger E, Ohno S, Segal GM, Fanning S, Zimmermann J, Lydon NB. Effects of a selective inhibitor of the Abl tyrosine kinase on the growth of Bcr-Abl positive cells. Nat Med 1996;2(5):561-566.
267. Liang W, Kujawski M, Wu J, Lu J, Herrmann A, Loera S, Yen Y, Lee F, Yu H, Wen W, Jove R. Antitumor activity of targeting SRC kinases in endothelial and myeloid cell compartments of the tumor microenvironment. Clin Cancer Res;16(3):924-935.
268. Thomas SM, Brugge JS. Cellular functions regulated by Src family kinases. Annu Rev Cell Dev Biol 1997;13:513-609.
269. Ben-Neriah Y, Daley GQ, Mes-Masson AM, Witte ON, Baltimore D. The chronic myelogenous leukemia-specific P210 protein is the product of the bcr/abl hybrid gene. Science 1986;233(4760):212-214.
270. Laneuville P, Sun G, Timm M, Vekemans M. Clonal evolution in a myeloid cell line transformed to interleukin-3 independent growth by retroviral transduction and expression of p210bcr/abl. Blood 1992;80(7):1788-1797.
271. Gordon MY, Dowding CR, Riley GP, Goldman JM, Greaves MF. Altered adhesive interactions with marrow stroma of haematopoietic progenitor cells in chronic myeloid leukaemia. Nature 1987;328(6128):342-344.
272. Liu C, Yu S, Zinn K, Wang J, Zhang L, Jia Y, Kappes JC, Barnes S, Kimberly RP, Grizzle WE, Zhang HG. Murine mammary carcinoma exosomes promote tumor growth by suppression of NK cell function. J Immunol 2006;176(3):1375-1385.
273. Clayton A, Mitchell JP, Court J, Mason MD, Tabi Z. Human tumor-derived exosomes selectively impair lymphocyte responses to interleukin-2. Cancer Res 2007;67(15):7458-7466.
274. Cines DB, Pollak ES, Buck CA, Loscalzo J, Zimmerman GA, McEver RP, Pober JS, Wick TM, Konkle BA, Schwartz BS, Barnathan ES, McCrae KR, Hug BA, Schmidt AM, Stern DM. Endothelial cells in physiology and in the pathophysiology of vascular disorders. Blood 1998;91(10):3527-3561.
275. Ayala F, Dewar R, Kieran M, Kalluri R. Contribution of bone microenvironment to leukemogenesis and leukemia progression. Leukemia 2009;23(12):2233-2241.
276. Janowska-Wieczorek A, Wysoczynski M, Kijowski J, Marquez-Curtis L, Machalinski B, Ratajczak J, Ratajczak MZ. Microvesicles derived from activated platelets induce metastasis and angiogenesis in lung cancer. Int J Cancer 2005;113(5):752-760.
277. Gesierich S, Berezovskiy I, Ryschich E, Zoller M. Systemic induction of the angiogenesis switch by the tetraspanin D6.1A/CO-029. Cancer Res 2006;66(14):7083-7094.
278. Schiera G, Proia P, Alberti C, Mineo M, Savettieri G, Di Liegro I. Neurons produce FGF2 and VEGF and secrete them at least in part by shedding extracellular vesicles. J Cell Mol Med 2007;11(6):1384-1394.

279. Proia P, Schiera G, Mineo M, Ingrassia AM, Santoro G, Savettieri G, Di Liegro I. Astrocytes shed extracellular vesicles that contain fibroblast growth factor-2 and vascular endothelial growth factor. Int J Mol Med 2008;21(1):63-67.
280. Taraboletti G, D'Ascenzo S, Giusti I, Marchetti D, Borsotti P, Millimaggi D, Giavazzi R, Pavan A, Dolo V. Bioavailability of VEGF in tumor-shed vesicles depends on vesicle burst induced by acidic pH. Neoplasia 2006;8(2):96-103.
281. Al-Nedawi K, Meehan B, Kerbel RS, Allison AC, Rak J. Endothelial expression of autocrine VEGF upon the uptake of tumor-derived microvesicles containing oncogenic EGFR. Proc Natl Acad Sci U S A 2009;106(10):3794-3799.
282. Zhelyazkova AG, Tonchev AB, Kolova P, Ivanova L, Gercheva L. Prognostic significance of hepatocyte growth factor and microvessel bone marrow density in patients with chronic myeloid leukaemia. Scand J Clin Lab Invest 2008;68(6):492-500.
283. Xu ZP, Tsuji T, Riordan JF, Hu GF. Identification and characterization of an angiogenin-binding DNA sequence that stimulates luciferase reporter gene expression. Biochemistry 2003;42(1):121-128.
284. Feng D, Zhao WL, Ye YY, Bai XC, Liu RQ, Chang LF, Zhou Q, Sui SF. Cellular internalization of exosomes occurs through phagocytosis. Traffic;11(5):675-687.
285. Watkins SC, Salter RD. Functional connectivity between immune cells mediated by tunneling nanotubules. Immunity 2005;23(3):309-318.
286. Sowinski S, Jolly C, Berninghausen O, Purbhoo MA, Chauveau A, Kohler K, Oddos S, Eissmann P, Brodsky FM, Hopkins C, Onfelt B, Sattentau Q, Davis DM. Membrane nanotubes physically connect T cells over long distances presenting a novel route for HIV-1 transmission. Nat Cell Biol 2008;10(2):211-219.
287. Onfelt B, Nedvetzki S, Benninger RK, Purbhoo MA, Sowinski S, Hume AN, Seabra MC, Neil MA, French PM, Davis DM. Structurally distinct membrane nanotubes between human macrophages support long-distance vesicular traffic or surfing of bacteria. J Immunol 2006;177(12):8476-8483.
288. Vidulescu C, Clejan S, O'Connor K C. Vesicle traffic through intercellular bridges in DU 145 human prostate cancer cells. J Cell Mol Med 2004;8(3):388-396.
289. Koyanagi M, Brandes RP, Haendeler J, Zeiher AM, Dimmeler S. Cell-to-cell connection of endothelial progenitor cells with cardiac myocytes by nanotubes: a novel mechanism for cell fate changes? Circ Res 2005;96(10):1039-1041.
290. Groothuis TA, Griekspoor AC, Neijssen JJ, Herberts CA, Neefjes JJ. MHC class I alleles and their exploration of the antigen-processing machinery. Immunol Rev 2005;207:60-76.
291. Lucas WJ, Bouche-Pillon S, Jackson DP, Nguyen L, Baker L, Ding B, Hake S. Selective trafficking of KNOTTED1 homeodomain protein and its mRNA through plasmodesmata. Science 1995;270(5244):1980-1983.
292. Kvasnicka HM, Thiele J, Staib P, Schmitt-Graeff A, Griesshammer M, Klose J, Engels K, Kriener S. Reversal of bone marrow angiogenesis in chronic

myeloid leukemia following imatinib mesylate (STI571) therapy. Blood 2004;103(9):3549-3551.
293. Lierman E, Folens C, Stover EH, Mentens N, Van Miegroet H, Scheers W, Boogaerts M, Vandenberghe P, Marynen P, Cools J. Sorafenib is a potent inhibitor of FIP1L1-PDGFRalpha and the imatinib-resistant FIP1L1-PDGFRalpha T674I mutant. Blood 2006;108(4):1374-1376.
294. Venalis P, Maurer B, Akhmetshina A, Busch N, Dees C, Sturzl M, Zwerina J, Jungel A, Gay S, Schett G, Distler O, Distler JH. Lack of inhibitory effects of the anti-fibrotic drug imatinib on endothelial cell functions in vitro and in vivo. J Cell Mol Med 2009;13(10):4185-4191.
295. Schittenhelm MM, Shiraga S, Schroeder A, Corbin AS, Griffith D, Lee FY, Bokemeyer C, Deininger MW, Druker BJ, Heinrich MC. Dasatinib (BMS-354825), a dual SRC/ABL kinase inhibitor, inhibits the kinase activity of wild-type, juxtamembrane, and activation loop mutant KIT isoforms associated with human malignancies. Cancer Res 2006;66(1):473-481.
296. Huang F, Reeves K, Han X, Fairchild C, Platero S, Wong TW, Lee F, Shaw P, Clark E. Identification of candidate molecular markers predicting sensitivity in solid tumors to dasatinib: rationale for patient selection. Cancer Res 2007;67(5):2226-2238.
297. Kanda S, Miyata Y, Kanetake H, Smithgall TE. Non-receptor protein-tyrosine kinases as molecular targets for antiangiogenic therapy (Review). Int J Mol Med 2007;20(1):113-121.
298. Mukhopadhyay D, Tsiokas L, Sukhatme VP. Wild-type p53 and v-Src exert opposing influences on human vascular endothelial growth factor gene expression. Cancer Res 1995;55(24):6161-6165.
299. Eliceiri BP, Puente XS, Hood JD, Stupack DG, Schlaepfer DD, Huang XZ, Sheppard D, Cheresh DA. Src-mediated coupling of focal adhesion kinase to integrin alpha(v)beta5 in vascular endothelial growth factor signaling. J Cell Biol 2002;157(1):149-160.
300. Trevino JG, Summy JM, Gray MJ, Nilsson MB, Lesslie DP, Baker CH, Gallick GE. Expression and activity of SRC regulate interleukin-8 expression in pancreatic adenocarcinoma cells: implications for angiogenesis. Cancer Res 2005;65(16):7214-7222.
301. Lesslie DP, Summy JM, Parikh NU, Fan F, Trevino JG, Sawyer TK, Metcalf CA, Shakespeare WC, Hicklin DJ, Ellis LM, Gallick GE. Vascular endothelial growth factor receptor-1 mediates migration of human colorectal carcinoma cells by activation of Src family kinases. Br J Cancer 2006;94(11):1710-1717.
302. Ischenko I, Guba M, Yezhelyev M, Papyan A, Schmid G, Green T, Fennell M, Jauch KW, Bruns CJ. Effect of Src kinase inhibition on metastasis and tumor angiogenesis in human pancreatic cancer. Angiogenesis 2007;10(3):167-182.